THE EFFECTS OF SINGLE PULSE AND REPETITIVE (CUMULATIVE) NEODYMIUM AND FREQUENCY-DOUBLED NEODYMIUM LASER IRRADIATIONS ON PRIOR LIGHT- AND DARK-ADAPTED MONKEY RETINAS

FINAL REPORT

BESSIE BORWEIN

DECEMBER 1990

Supported by

U.S. ARMY MEDICAL RESEARCH AND DEVELOPMENT COMMAND
Fort Detrick, Frederick, Maryland 21702-5012

Contract No. DAMD17-83-G-9539
DAMD17-85-G-5023

The University of Western Ontario
London, Ontario, Canada N6A 5C1

DISCLAIMER NOTICE

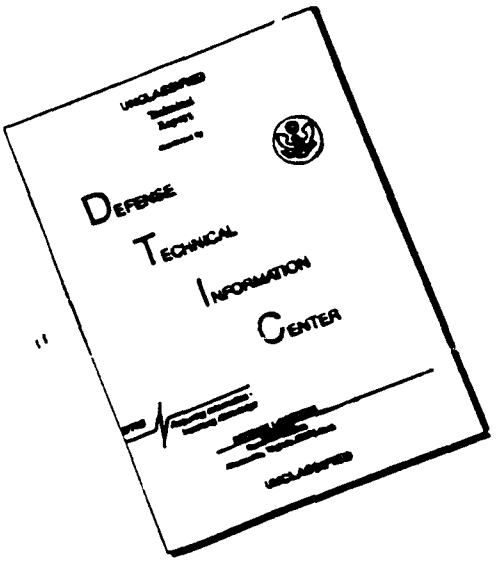

THIS DOCUMENT IS BEST QUALITY AVAILABLE. THE COPY FURNISHED TO DTIC CONTAINED A SIGNIFICANT NUMBER OF PAGES WHICH DO NOT REPRODUCE LEGIBLY.

SECURITY CLASSIFICATION OF THIS PAGE

REPORT DOCUMENTATION PAGE

Form Approved
OMB No. 0704-0188

1a. REPORT SECURITY CLASSIFICATION Unclassified	1b. RESTRICTIVE MARKINGS
2a. SECURITY CLASSIFICATION AUTHORITY	3. DISTRIBUTION/AVAILABILITY OF REPORT Approved for public release; distribution unlimited
2b. DECLASSIFICATION/DOWNGRADING SCHEDULE	
4. PERFORMING ORGANIZATION REPORT NUMBER(S)	5. MONITORING ORGANIZATION REPORT NUMBER(S)
6a. NAME OF PERFORMING ORGANIZATION The University of Western Ontario 6b. OFFICE SYMBOL (If applicable)	7a. NAME OF MONITORING ORGANIZATION
6c. ADDRESS (City, State, and ZIP Code) London, Ontario, Canada N6A 5C1	7b. ADDRESS (City, State, and ZIP Code)
8a. NAME OF FUNDING/SPONSORING ORGANIZATION U.S. Army Medical Research & Development Command 8b. OFFICE SYMBOL (If applicable)	9. PROCUREMENT INSTRUMENT IDENTIFICATION NUMBER DAMD17-83-G-9539 and DAMD17-85-G-5023
8c. ADDRESS (City, State, and ZIP Code) Fort Detrick Frederick, Maryland 21702-5012	10. SOURCE OF FUNDING NUMBERS PROGRAM ELEMENT NO. 61102A; PROJECT NO. 3M1-61102BS10; TASK NO. CF; WORK UNIT ACCESSION NO. DA307940

11. TITLE (Include Security Classification)
(U) The Effects of Single and Repetitive (Cumulative) Neodymium and Frequency-doubled Neodymium Laser Irradiations on Prior Light and Dark-Adapted Monkey Retinas

12. PERSONAL AUTHOR(S)
Bessie Borwein

13a. TYPE OF REPORT	13b. TIME COVERED	14. DATE OF REPORT (Year, Month, Day)	15. PAGE COUNT
Final	FROM 6/16/83 TO 3/15/87	1990 December	

16. SUPPLEMENTARY NOTATION

17. COSATI CODES			18. SUBJECT TERMS (Continue on reverse if necessary and identify by block number)
FIELD	GROUP	SUB-GROUP	RA 3; Laser Bioeffects; Morphology
20	05		
06	18		

19. ABSTRACT (Continue on reverse if necessary and identify by block number)

20. DISTRIBUTION/AVAILABILITY OF ABSTRACT ☐ UNCLASSIFIED/UNLIMITED ☒ SAME AS RPT. ☐ DTIC USERS	21. ABSTRACT SECURITY CLASSIFICATION Unclassified
22a. NAME OF RESPONSIBLE INDIVIDUAL Mary Frances Bostian	22b. TELEPHONE (Include Area Code) 301-663-7325
	22c. OFFICE SYMBOL SGRD-RMI-S

DD Form 1473, JUN 86 Previous editions are obsolete. SECURITY CLASSIFICATION OF THIS PAGE

19. ABSTRACT

The project evaluated, morphologically, mainly by electron microscopy, the changes effected one hour and 24 hours post-exposure in Macaca mulatta (old animals) and M. fascicularis (young animals), and up to 25 days in rabbits by a Q-switched pulsed neodymium-YAG λ1064 nm laser (and also frequency-doubled λ 532 nm)(output energy $\geq$ 100 J/pulse; max. pulse rate frequency 20 pulses/sec.). An ophthalmologist prior-examined all eyes.

The laser "burns" were inserted in deeply anaesthetized animals, in the macula (mainly) of the monkeys and just below the visual streak in the rabbits, in light-adapted and dark-adapted conditions and in the morning and afternoon. Markers were at threshold and experimental lesions were subthreshold at intraocular energy 115-150 μJ, with estimated spot sizes 25-50 μ diameter at the retina.

Each lesion affects a distinctly circumscribed group of cells in the RPE and associated outer segments (OS). There is a gradation of damage within a lesion from the most severe centrally to the least severe peripherally.

There is suggestive, but not definite, information in the lesions that prior dark-adaptation makes the monkey retina (but not the rabbit retina) slightly more vulnerable to laser damage. λ 532 nm creates greater damage than does λ1064 nm. The wavelength differences makes a greater difference to the lesion size and severity than does any other parameter. Lesions inserted in the morning and afternoon showed no differences.

The earliest and most consistent indicators of laser-induced alterations are in the RPE and these are in: (i) the more uneven apical RPE border; (ii) the apical microvilli (AMV) (retractions into the cell, reductions, fragmentation, loss); (iii) the basal infolds (swelling, reduction, loss); the melanin granules (MG) (withdrawal from the AMV, loss); (iv) the hypopigmentation of the RPE cell. In lesion centres, RPE cells may be reduced in height or absent.

In the rabbit lesion areas, the normally scalloped border of the apical RPE becomes exaggerated and club-like, and pillar-like expansions extend into the subretinal space (SRS). These expansions of RPE pinch off and separate from the basal RPE and become macrophage-like scavengers in the SRS. Many similar macrophage-like bodies are seen in the SRS in the monkey following laser irradiation.

The basal RPE retains its basic morphological integrity better than does the apical RPE. Affected RPE cells develop three distinct strata and RPE itself may become multi-layered.

Sometimes in the small lesions, the RPE lifts off Bruch's membrane (BM) and the neighbouring RPE cells send out "tongues" which very rapidly cover the bare spot on BM.

The laser light triggers a sudden burst of OS shedding and phagosomes lie alongside the apical RPE border and some of the phagosomes are unusually large. In the lesions, shed packets of OS discs often line the apical RPE as a continuous border. Very large phagosomes containing OS discs were more often seen in the one day old lesions; in those pre-exposed to constant light (for 26 hrs); in the superior quadrant and in the λ 532 nm lesions. RPE cells 3-8 cells distant from the lesion margin contain unusually large phagosomes. It seems that damage changes as a result of the laser impact are circumscribed but nearby RPE cells respond to the laser flash by a burst of disc shedding.

Bubble-like cystic spaces were seen in the outer retina, in the SRS and within the RPE.

OS are more readily disrupted in their proximal parts and whorled arrangements of discs are frequent near the OS-inner segment (IS) border in the controls in the older monkeys, as well as in lesions.

Most often in the subthreshold lesions there is no obvious pyknosis or necrosis in the photoreceptor (PR) nuclei, but some Henle fibres show pyknosis. The inner retinal layers are little or not affected. Bruch's membrane is not breached. Very small electron dense particles appear in the basal RPE, BM, and in the CC. BM may contain a few cells.

Choroidal changes include: endothelial swelling and thickening, reduction of fenestrations, congestion in the choriocapillaris (CC), "ghost" cell outlines in the lumen of the CC; necrotic changes in melanocytes with vacuolization and fragmentation of some MG which may also show "halos". Many of these changes are also age-related.

Very similar types of alterations are seen in all subthreshold lesions. Despite similar energy input and spot sizes, no two lesions are identical.

Some regions and organelles show greater resistance to changes in response to laser irradiations: RPE junctional complexes; the ciliary connective; striated rootlets; outer limiting membrane; BM; the cone nuclei compared to the rod nuclei; IS compared to OS; nasal quadrants compared to temporal quadrants and inferior quadrants compared to superior quadrants.

TABLE OF CONTENTS

FOREWORD

This project evaluated morphologically the microscopic changes effected by a Q-switched, pulsed, Neodymium-YAG (Nd-YAG) laser λ 1064 nm (and also frequency-doubled λ 532 nm), on the retina and choroid of rabbits and monkeys.

This Nd-YAG laser emits in the near-infra-red (λ 1064 nm) which the primate eye cannot see and for which there is no blink reflex. These lasers are being used increasingly in diverse ways. It is a dangerous laser for eye damage, classed as a high risk (Class IV) laser. There are very specific controls for its use.

Most of the pulsed Neodymium laser radiation is absorbed in the anterior parts of the eye, but the retina is the site of injury because is absorbs much more radiant energy per volume of tissue than other parts of the eye. Almost all the Nd-YAG laser spots studied were too small to be detected ophthalmologically (with the exception of marker burns) and many could not be seen even under the dissecting microscope. Lesions were located with the help of detailed mapping strategies at the time of laser irradiation, but not all the lesions could be found.

The assessment of damage levels is important to the general data bank of information used for the establishment of laser safety standards, the permissable exposure limits, the design of protective eyewear, and an understanding of the bio-effects of this specific laser on the ultrastructural changes in the photoreceptors, pigment epithelium, Bruch's membrane, the outer retina in general and the choroid. The very small changes in the laser lesions aid in understanding the effects of light on the retina and choroidal cells at the ultrastructural level.

All the research was conducted in accordance with the "Guide to the Care and Use of Laboratory Animals" (U.S. Department of Health and Human Services, NIH Publication No. 85-23, revised 1985) and the Guidelines and Standards set by the Canadian Council on Animal Care (1985) and the University of Western Ontario Council on Animal Care, from which prior approval is required before experimentation can commence. The monkeys were visited frequently with fruit and vegetable treats, in addition to the fastidious care provided by the staff of the Animal Care facility.

INTRODUCTION

The lesions evaluated by light microscopy (LM) and transmission electron microscopy (TEM) the microscopic changes effected by a Q-switched pulsed Neodymium-YAG (Nd-YAG) laser on the retina mainly but also the choroid of:

(1) rabbit retina, below the visual streak
(2) Macaca mulatta (old animals) and M. fascicularis (young animals)
  (a) in the macula mainly
  (b) in the perimacula (in the temporal, nasal, superior and inferior parts)
  (c) when light-adapted, in the morning and in the afternoon
  (d) when dark-adapted (DA) first thing in the morning and in the afternoon. The periods of DA were 3 1/2 hours, and overnight.
  (e) after constant light for 26 hours
  (f) in single laser exposures
  (g) with dose-fractionated exposures
  (h) at 1064 nmλ and frequency doubled at 532 nm λ
  (i) at threshold and at subthreshold (not ophthalmoscopically visible 1 hour after exposure)

The animals were euthanised at 1 hour and at 24 hours post-exposure. The lesions were assessed and compared to each other and to control areas of the same retina about 10 cells distant from the outermost edge in the pigment epithelium of the laser lesion.

Marker lesions were always inserted and to aid in the location of the lesions retinal maps were made and fundus photographs taken.

The project involved work in several areas:

(1) The design and building de nova of a laser laboratory to house Laser Photonics Laser Model Y QL-102D S/N, pulsed Neodymium-YAG (1064 nm) and frequency-doubled (532 nm); maximum pulse rate frequency 20/sec; output power 15 milliwatts at 532 nm, 45 milliwatts at 1064 nm; output energy $\geq$ 100 J/pulse; pulse width 15 nsec. This specific laser was selected after considerable consultation with Mr. Jack Lund at LAIR, the Presidio, San Francisco.

The laser had to be returned twice, airfreight, to Laser Photonics in Florida. In the first case, the key starter switch did not operate, and that was repaired under warranty. On the return journey, the coolant at the back of the power supply leaked onto the electronics and it had to be returned again. It had been inadequately packed. This took a very long time, many months.

(2) The initial promise of space was made at the time of the submission of the proposal. By the time the proposal was granted, departmental conditions had changed and the room initially allocated was no longer available. It took some time to locate and negotiate the acquisition of another room.

(3) A technician who was a biomedical engineering graduate student was employed part-time to help assemble the laser lab and all the required optics; design an animal holder for the monkeys; and learn the detailed operation of the laser. The animal holder was designed and built at the University of Western Ontario. There was a considerable hold-up while a search was undertaken to locate a continuous motor rather than a stepped motor.

(4) The technician, Dev Sainani, had a training visit to LAIR with Jack Lund.

(5) Preliminary experiments were undertaken with rabbits.

(6) Jack Lund paid a visit to the lab for purposes of inspection and assisting with the first monkey experiment. He was very pleased with what he found. The animal holder is excellent, and has since been modified to hold monkeys, rabbits, squirrels (or other animals with laterally placed eyes).

(7) The Province of Ontario and the University Safety Section inspected the lab for safety compliances and were very complimentary.

(8) The TopCon camera, which the project inherited from earlier laser work undertaken by Dr. Bill McGowan, had to be sent away to Quebec City for overhauling and cleaning. All the above created unavoidable delays.

The lighting conditions in the Animal House rooms was cyclic, 12 hours at 75-125 foot candles (equivalent to 8.07 - 13.45 lux) and 12 hours of darkness.

Energy was reduced or attenuated by the use of four neutral density filters placed either singly or collectively in the beam path.

Radiometric detectors were used to measure reference and target energies when calibrating the laser.

Reference energy was obtained by splitting a part of the beam with a pellicle beamsplitter.

A radio of target to reference energy was used to calculate Q target for the animal based on Q reference during the actual exposure of the animal to the laser's light.

Beam diameter may be varied by dipping the central gaussian shape of the beam by passing it through orifice plates. These plates have orifices varying from 15/1000 of an inch up to 4 mm.

The estimated energy levels on the retina are between 6-15 μJ. The laser, on a few occasions, became unpredictably unstable (and had to be dismantled and cleaned) and this accounts for some of the low output energies recorded. Retinal spot size depends on the momentary state of refraction of the eye.

METHODS

1. Irradiations were performed according to the attached chart.

2. Marker lesions were placed around the macula in a 3 row grid pattern and the experimental lesions were aligned with this grid pattern within the macula. The lesions were also marked on hand-drawn maps, and polaroid pictures taken.

3. The total number of animals involved was:
   (i) six rabbits
   (ii) five Rhesus female monkeys (M. mulatta) acquired from a gynaecological-endocrine experiment, and were all "mature", probably old. Exact age unknown.
   (iii) four young cynomolgus monkeys (M. fascicularis)

4. All animals were examined for clear media and normal fundi before every experiment by Drs. Werner Cadera or Christopher Canny, Ophthalmologists of the Dept. of Ophthalmology at the University of Western Ontario. All the eyes appeared normal by funduscopic examination except for one which had two haemorrhage spots in the peripheral retina, which Jack Lund assured us was not unusual. All the animals were weighed.

5. All the eyes were photographed in a TopCon TRC-F Fundus camera at the start of every experiment and after each batch of lesions were inserted.

6. The monkeys were sedated with Ketamine and then anaesthetized intramuscularly with Rogarsetic (Ketamine) (10 mg/kg body weight) and Xylazine (Rompun) (1 mg/kg body weight). The anaesthetized animal was placed on an incontinent pad on the holder, taped into position, and covered with a prewarmed electrical water-blanket. Rabbits were sedated with the same mixture of Rogarsetic and Rompun (10:1) at about the same dosage but the injections were made intraperitoneally. There was constant monitoring for depth of anaesthesia and additional anaesthesia was administered when necessary.

7. Monkey pupils were dilated with a few drops each of phenyltrope (0.8% tropicamide, 5% phenylephrine hydrochloride and 1% cyclogyl (cyclopentolate hydrochloride) and taped shut for a short while to prevent corneal drying. After untaping the eyes, the eyelids were retracted with a paediatric speculum and the cornea irrigated frequently, manually, with sterile physiological saline, from a fine, long pipette-syringe. Rabbit pupils were dilated with midriacyl (tropicamide 1%) and all other procedures for the laser experiments were carried out as for the monkeys.

8. The laser lesions were of two kinds in both the rabbit eyes (below the visual streak) and in the macula and immediate paramacular of the Macaca eye:
   (a) Markers were inserted intra-ocular energy ± 250-275 μ J as threshold lesions. Most of these were just barely visible in the camera at insertion time and at dissection.

(b) Experimental lesions: rarely and barely visible in the camera and hardly ever visible at dissection (subthreshold lesions). Some became more visible after 24 hours.
- Intra-ocular energy - 115-150 μ J
- Estimated spot sizes 25 - 50 μ at the retina.

Although energy input and spot size were kept constant, no two lesions were identical. This might be associated with the variations in local pigmentation in the RPE. A few created bleeding, most did not.

9. For dark adaptation experiments: A light-excluding curtain was made to create a protected entrance to the laser room which happened to have a door inset within an alcove. Within the alcove the curtain was fixed in such a way that full-length Velcro could secure a light-proof ante-chamber to the laser lab. For dark adaptation, the animals were transported to the laser room in their large cages and kept under red light only. The TopCon camera was fitted with a red filter. All the lights on the system were protected with devices that fitted thimble-like. When the light had to be turned on for essential work on the laser, the cages were temporarily and briefly enclosed in the same light-proof material as the curtains.
The laser lab was equipped with 3 Kodak Wratten Red lights for the dark adaptation experiments which were conducted under red light in a light-proofed room.
The lesions were allowed to mature in the dark for one hour post-exposure. The unexposed eye was closed and covered with light-proof material taped over the anaesthetized animals.

10. The lesions in rabbits were allowed to mature 1 day, 4 days, 1 week, 2 weeks and 25 days. In the monkeys, lesions were allowed to mature for 1 hour or 24 hours.

11. Intracardiac injection of euthanyl overdose was used for euthanasia in sedated, anaesthetized animals.

12. The eye was enucleated, excess tissue trimmed from the sclera, immediately incised at the limbus with a very sharp blade and plunged into the fixative (2.5% glutaraldehyde, 0.8% paraformaldehyde in 0.1 M phosphate buffer, pH 7.3 - 7.4). At ten minute intervals, to allow for a degree of tissue hardening in the fixative, the anterior potions of the eye (cornea and lens) were successively dissected away, and then the vitreous was carefully cut away. After a total fixation time of 1 1/2 hours, the eye cup was dissected in fixative under a Zeiss dissecting microscope, with flexible fibre optic light arms (non-heating). Fixation was continued in vials for a total of 3 hours at room temperature. Tissues were rinsed in buffered 5% sucrose. Buffered 1% OsO_4 was used for postfixation for 1 1/2 hours at 4°C. The tissues were dehydrated in graded alcohols, stained en bloc with uranyl acetate and embedded in Spurr. Samples were also taken for Scanning Electron Microscopy (SEM), critical point dried and gold coated. Thick (.5 μm and 1 μm) sections for light microscopy were cut with glass knives and stained with warm 1% toluidine blue in 0.5% sodium borate, de-stained if necessary with methanol, and examined in a Wild light microscope. There was a very careful and methodical search through the retinal blocks by serial sectioning with glass knives in the damage zones. Despite this, it was not possible to locate all the lesions that were inserted. It seems that some laser exposures failed to create enough damage to be recognized or that such small zones of damage were missed as only a few cells were involved. Once the very subtle changes that indicated the approach to, or the actual

presence of a lesion, thin sections were cut. Such subtle changes in the smaller lesions were generally: slight perturbations in the apical surface of the pigment epithelial cells (RPE), a change in the staining of the RPE cell (usually hypopigmentation but also hyperpigmentation), signs of vacuolation in the RPE or in the subretinal space, change in thickness of the RPE layer. In the larger lesions these were also: pyknotic RPE nuclei; pyknotic photoreceptor nuclei; pyknotic Henle fibres.

13. Grey or light gold sections (about 80 nm) were cut on a Reichert OMU2 Ultramicrotome with a Diatome diamond knife and post-stained with uranyl acetate and lead citrate.

14. (a) The sections were viewed with a JEOL CX-100 11 electron microscope operated at 60 kv, fitted with a rotary specimen holder, which facilitated the photography for montages.

14. (b) Pictures were taken on KODAK Electron Microscope Plate Film 4489 (3 1/4 x 4 inch plates) and developed in Kodak D-19 (2:1 dilution) developer. Prints were made using Ilford Ilfobrom black-and-white photographic paper.

15. Every lesion was matched with a piece of control retinal tissue about 10 - 15 cells distant from the lesion edge, in the retinal pigment epithelium.

16. Light Microscopy and Lesion Measurement. Toluidine blue-stained 0.75 - 1.0 μm sections through the centres of the laser lesions were examined in the Zeiss light microscope. The limits of laser damage were clear at the edges of the limit of pigment epithelial cell changes. The longest segments of damaged RPE were assumed to be the centre of the lesions. Sections containing the largest lesion diameters for each lesion were chosen for direct measurement under the light microscope. A stage micrometer was used to calibrate the ocular scale for each objective.

The planapo oil-immersion 40 x objective was chosen as the most accurate and accommodating lens for making the measurements. Estimates were made of the demarcation points of the lesion edges, in the RPE, as this tissue yielded the broadest area of damage. Measurements were made from edge to edge of the lesion. Ocular-unit-distances were translated to micrometers and tabulated.

Photographs were taken of each lesion area at various magnification on a Kodak 35 mm Panatomic-X film. Negatives were developed in Kodak Microdol X. Prints were made at a photo-enlargement of 3 x on Ilford Ilfobrom photographic paper.

DETAILS OF THE LASER USED

1-4 SYSTEM SPECIFICATIONS

Specifications for Laser Photonics Model YQL-102D Pulsed Nd:YAG Laser are provided in the following table.

TRANSMITTER

Wavelength primary	1064 microns
frequency doubled	.532 microns
Output energy	= 100 millijoules/pulse @ 1.06 microns = 20 millijoules/pulse @ .532 microns
Pulse rate frequency	20 pulses/second maximum. 15, 10, 5 and 1 pps switch selectable. Push button single shot. Externally triggerable to 20 pps with 5 volt TTL signal.
Pulse width	20 nanoseconds, nominal @ 1.06 microns
Beam divergence	less than 2 milliradians
Beam diameter	0.20 inches
Beam shape is Gaussian	
Cooling	Internal, closed cycle liquid to air heat exchanger
Transmitter dimensions	5" x 4" x 19"
Transmitter weight	11 pounds

The laser emits both wavelengths simultaneously. The 1064λ or 532λ was selected by the use of appropriate filters.

POWER SUPPLY

Input power requirements	110 volts ac, 60 hz, single phase, 10 amps peak
Size	8" high by 18" wide by 19 3/4" deep
Weight	55 pounds

RESULTS

The detailed results are presented in accompanying figures and figure legends, tables, and the comments that follow.

General Comments

The normal rabbit RPE has a markedly scalloped apical border (Figs. 13, 16,17), while that of the normal primate RPE is hardly scalloped at all. The basal infolds of the RPE are more prominent in the rabbit (Fig. 17). The rabbit RPE cell contains one or two very large lipid globules (Figs. 2, 11), while in the monkey retinas, if present at all, the lipid vesicles are seen isolated (Figs. 32, 158), or as grouped (Figs. 23, 56, 87, 110, 155), small lipid droplets, and these are more frequent and abundant in the older retinas Figs. 43, 64).

In the lased rabbit retina, the RPE shows a few different modes of response:

(1) A damaged RPE cell may detach entirely from Bruch's membrane, and narrow tongue-like portions of neighbouring RPE cells (lightly damaged or undamaged) extend along the denuded part of Bruch's membrane to close the gap (Fig. 3).

(2) Apical portions of the RPE may detach to leave the basal RPE in place (Fig. 15).

(3) More often the humping of the apical RPE becomes very exaggerated, and pillar-like or club-like expansions of the RPE cell extend into the subretinal space (Figs. 11 and 14), and these pinch off to separate from the basal RPE (Fig. 12). Between these RPE extensions, the RPE is reduced in height. In all three cases these RPE cells or cell portions become rounded off as independent unattached cells in the subretinal space and appear to act as macrophages, laden with RPE-derived organelles such as melanin granules, lipofuscin granules, residual bodies, and outer segment disks in packets (Fig. 6).

After exposure of the monkey retina to laser irradiation, these macrophage-like cells are also seen very frequently in the subretinal space, between the remaining, damaged RPE and the outer segments. However, the monkey retina never shows the marked apical elongations seen in the rabbit RPE that precedes the extrusion of RPE cells or RPE cell apical portions after laser damage (Figs. 21, 22, 70, 169), but some slight humping may occur (Fig. 94). The RPE in the lesion centre may be much reduced in height (Fig. 34). Sometimes th RPE lifts off Bruch's membrane (Figs. 102, 127). The damaged RPE tends to become multi-layered (not multi-cellular) and co-agulated apical portions separate (Figs. 21, 147, 158, 167, 182).

Phagosomes of varying sizes containing shed outer segment disks often lie near the apical RPE border or within the apical RPE. It appears that the sudden burst of laser light triggers a shedding response in a burst that may not occur in natural conditions when the onset of the light or dark period is gradual through the period of the dawn and dusk. Phagosomes, or shed packets of outer segments disks, can be seen in RPE extrusions (Figs. 6, 15, 150, 154, 184) or at the apical RPE (Figs. 25, 31, 38, 82, 84, 86, 94, 99, 107, 118, 119, 121, 125, 134, 139, 164, 167); in or at the apical RPE (Figs. 64, 86, 152, 153, 162, 182). The unusual figures seen in Fig. 168 are probably membranes derived from outer segments. Rarely, outer segment disk packets are seen in an inner segment (Figs. 156, 171).

Drusen can be seen in Figure 49 (in an aged rhesus retina in the fovea, in a control area). Drusen were only occasionally present in monkey and not seen in the rabbit retinae.

In the monkey retina some lesions produced bubble-like spaces between the lesion in the RPE and the outer segments. These "spaces" were usually grouped but single spaces were also seen. These were never seen in the lased rabbit retinas. These spaces may be due to gas bubbles or tears in the interphotoreceptor matrix (Figs. 29, 67, 71, 78, 80, 83, 121, 127, 130, 137, 145, 151). The "bubbles" may appear to be empty of contents, or nearly so, (Figs. 29, 51, 52, 55, 59, 66), or they may contain flocculent materials (Figs. 16, 34, 50, 82, 143), and the two types may appear side by side (Fig. 104).

"Bubbles" or cystic spaces may also occur within the RPE itself, and these are presumably due to mini-explosions in the RPE or to the local production of gases, or to swellings which rend the cytoplasmic matrix (Figs. 134, 170, 173). Some of these contain fragments or electron-dense small spots (Figs. 173, 176). Small cystic spaces may also be seen basally in the RPE (Figs. 31, 53, 63, 64, 82, 85, 99, 122, 135, 136, 145, 146, 151, 173, 176, 177, 178). In the large lesions with the more severe damage (532 nm) large spaces arise which separate the RPE from Bruch's membrane (Fig. 125, and plate 46A, Fig. I). These "bubble" spaces are present whether the lesion was created after light-adaptation (Fig. 145) or after dark-adaptation (Fig. 144), in the inferior part of the macula.

Larger than usual packets of shed outer segment disks and more of these packets are found along or in the RPE in cynomolgus retinas which have been exposed to constant light for 26 hours independently of whether the exposure was to 532 nm or 1064 nm (Figs. 169,170), or the region of the retina: nasal to optic disk (Figs. 167, 168), in the temporal periphery (Figs. 162, 164), in the temporal part of the macula (Fig. 150, 169), or in the nasal periphery (Figs. 152, 153, 154). However, in the more severely affected lesions, these were seen also in dark-adapted rhesus retina, in the superior retina (Fig. 81) and in the nasal area of the fundus (Fig. 184).

Changes in the apical microvilli (AMV) and the basal infolds (BI) are the two earliest and most consistent indicators of laser-induced alterations in the RPE, and it is in the RPE that the first and most subtle changes occur.

The AMV changes take several forms in both rabbit and monkey. The AMV may be entirely absent in the central regions of the lesions, and sometimes at their edges, too (Figs. 21, 23, 80, 82, 88, 151, 165, 176); and only a few AMV fragments may remain (Fig. 94).

The AMV may retract into the RPE cell (Fig. 34). AMV tend not to be present on the RPE cells that lie freely, resembling macrophages, in the subretinal space (Figs. 15, 23, 169). AMV or remains of the AMV can be found between the extruded apical RPE and the more basal RPE attached to Bruch's membrane (Figs. 78, 119, 158, 185). Membrane figures displayed in Fig. 7 may be AMV-derived in both rabbit (Fig. 7) and monkey (Fig. 58). At the border of the lesion, an unaffected cell displays AMV, and BI, while its neighbour (altered by the laser irradiation) shows neither (Fig. 173). However, a few lesions contain RPE with AMV (Figs. 100, 109, 110, 162). Very slender AMV, which contain electron-dense spots, are seen in Figure 139, and by their positions these suggest that they are derived from fragmented melanin granules. Some AMV may be present with a tendency to clump together in groups (Fig. 54). Disrupted AMV are seen in Figures 79 and 84.

It appears that the microvilli reform on the attached RPE after the apical RPE is extruded (Figs. 15, 78, 119, 158).

RESULTS

RABBIT RETINA LASER LESIONS

The aim of these experiments was primarily to gain experience with the laser, processing the retinal lesions and assessing retinal changes before proceeding to experiments on monkey retinas. Most damage is seen in the lesion centre, and the margins always show less severe damage than the centre.

The assessments of these lesions follows:
The margins of the lesions are clearly demarcated in the retinal pigment epithelium (RPE). The greatest effect of laser irradiation is in the RPE; and the RPE lesion is saucer shaped.

In the subthreshold lesions, the damage is restricted to the outer retina and hardly ever extends beyond the outer nuclear layer and Henle fibres.

The dark-adapted retinas showed no morphological differences compared to the light-adapted retinas, nor could differences be identified between retinas exposed to laser irradiations in the mornings or afternoons.

In the centre of the lesion basal infolds are reduced or absent but reform in a few weeks.

Within the lesions the RPE becomes zoned into three areas: (1) a more-or-less intact basal area with hemidesmosomes and junctional completes apparent, but with basal infolds reduced or absent; (2) a mid-zone of dense cytoplasm and disrupted endoplasmic reticulum; and (3) an apical region of coagulated flocculent cytoplasmic matrix with apical microvilli absent, fragmented in the subretinal space, and/or retracted as layers or whorls of membranes into the body of the RPE cell.

Even in lesions extending through the full thickness of the retina (as in some of the marker burns) where the inner limiting membrane is breached, the areas in which the greatest damage is concentrated are the RPE and the outer segments.

Very large macrophage-like bodies may be present in the subretinal space. Sometimes blood is present in an unpredictable way.

There is an increased convexity (humping) of the RPE cells at the apical RPE border, which normally has a scalloped margin. This margin becomes lined by melanin granules instead of their being in their usual positions mainly in the apical microvilli. Even in the smallest lesions affecting only a few cells, the scalloping of the apical RPE border is exaggerated. This was one of the diagnostic features by which very small lesions could be identified (by light microscopy of thick sections) during the sectioning process.

The burst of laser light appears to encourage disk shedding and rather large membrane-enclosed packets of outer segment (OS) disks are present in the RPE, but are not seen in the controls. Laser damaged outer segments and inner segments lie beside apparently unaffected outer segments and inner segments.

In the centre of the maturing small lesions a clear sequence of events can be observed in the RPE from 1 day old lesions through to 4, 7 and 25 day-old lesions. The humping of the apical RPE increases. The cell becomes connected, mushroom-like, to the basal part of the RPE cell by an increasingly narrow isthmus. The apical part of this cell contains mitochondria, phagosomes and melanin granules but hardly any microvilli. A shrunken nucleus may be present. This cell separates from the basal RPE and becomes a large free cell in the subretinal space where it appears to function as a macrophage. The remaining part of the RPE cell, attached to Bruch's membrane, is much reduced in height. A few RPE cells separate off in entirety from Bruch's membrane and either degenerate or also become free cells in the subretinal space. Tongue-like extensions of the neighbouring RPE cells, in small lesions, extend to reline Bruch's membrane and they form junctional complexes where they meet. These "tongues" are devoid of melanin granules and basal infolds.

In control areas not all the OS disks are perfectly aligned. Occasional OS were seen in both peripheral regions of the lesions and in the controls in which the disks were mis-aligned, even to the extent of being arranged parallel to the long axis of the OS. Some disks within one outer segment stain more intensely and this phenomenon is more marked in the lesion areas.

The choroid often appears normal under the small lesions. In above-threshold lesions and occasionally at threshold, the choroid may show:

(1) thickening of the endothelial cells and an apparent doubling of the endothelial cell layer;

(2) reduction of fenestrations in the endothelium;

(3) reduced patency of the choriocapillaries lumen and excessive numbers of neutrophils and debris; and

(4) electron-dense osmiophilic small spots at the RPE base, in Bruch's membrane, and in the lumen of the choriocapillaris.

(5) Some choroidal cells are degenerative.

(6) In the lumen of the choriocapillaris are also membrane outlines, approximating the size and shapes of erythrocytes, and referred to in the figure legends as "ghosts".

The rabbit OS disks appear to be more resistant to laser-induced disorganization than are the disks of the primate retina.

The cellular organelles that seem to be most resistant to laser damage are:

(1) the large oil droplets of the RPE;

(2) the striated rootlet and centrioles of the inner segment;

(3) the junctional complexes of the RPE. The basal RPE is less readily damaged than is its apical cell parts; and

(4) Bruch's membrane.

The following are most vulnerable to laser damage and consistently show early changes:

(1) increased humping up of the apical RPE margin;

(2) retraction, fragmentation and/or loss of the RPE apical microvilli;

(3) the RPE basal infolds may widen, or more frequently, disappear. However, the basal infolds are more prominent and more persistent than in the monkey retina;

(4) the RPE cytoplasm becomes coagulated and flocculent;

(5) The OS disks vesiculate and/or misalign or are absent;

(6) the melanin granules withdraw from the RPE apical microvilli and they may line the apical RPE border or be absent;

(7) the photoreceptor nuclei become shrunken, show marginalized chromatin or become pyknotic and necrotic.

(8) the mitochondria of the inner segment swell; and

(9) in the more severe lesions, there are vacuolar spaces in the RPE, OS and inner segments.

MACACA RETINA

SPECIFIC COMMENTS

The extent and intensity of changes resulting from subthreshold laser irradiations varies in an unpredictable way, not correlated with energy levels or spot size, within the narrow confines of the ranges of these parameters in this study. While in all the subthreshold lesions and many of those at threshold very similar changes occur, yet for the same energy and spot sizes, no two lesions are identical. Variations are common in neighbouring photoreceptor cells and RPE cells, from normal to necrotic and all gradations between.

Each lesion affects a distinctly circumscribed group of cells within the RPE where the first identifiable changes occur. There is a gradation from severest changes in the lesion centre to less marked changes in the lesion periphery. Outer segments related to the affected RPE cells display more disruption in their proximal parts than in their distal portions abutting the RPE; while the opposite pertains to their inner segments. The subthreshold lesions tend not to create pyknosis and necrosis in the photoreceptor nuclei, but lesions resulting from greater energy exposure do. Some Henle fibres show pyknosis at angles from the lesion centre. The inner retinal layers appear to be totally unaffected. Bruch's membrane is rarely breached. The choroid closest to Bruch's membrane may be damaged. The lesions develop over one day.

THE CHOROID

The choroid may retain its normal appearance. When changes occur these are restricted to that region of the inner choroid closest to the choriocapillaris (Figs. 150, 151, 159, 163, 164).

Degenerative changes occur in the stroma with replacement of melanocytes by other cells and extracellular components (Figs. 91, 125, 159). Melanocytes may show necrotic changes, with loss of, or clumping, or fragmentation of melanin granules, or vacuolization (Fig 96). In two Rhesus monkeys in the choroidal melanocytes, many of the melanin granules were surrounded by a clear zone which was clearly delineated, forming a "halo" around one, two or three melanin granules (Fig 96; compare to Fig. 150). This "halo" effect was seen in eyes dark-adapted or light-adapted, in several regions of the fundus (including the fovea), and in the controls.

Plate 55 (Fig. 150) shows clearly the differences between the inner and outer choroid in the lesion zone, compared to the normal choroid in a control region (Plate 56A).

The endothelium alongside Bruch's membrane is normally thinner and more fenestrated than that alongside the deeper choroid. The choriocapillaris is frequently affected in the lesion area. Fenestrations may become reduced in number, or be absent. The endothelial cells may swell (Fig. 173), show vacuolization (Figs. 65, 173), show layering, become disrupted (Fig 135) and/or fragmented (Figs. 122, 129), and sufficiently destroyed so that, in some cases and places the endothelial lining is discontinuous under Bruch's membrane (Fig. 129). The choriocapillaris may be obliterated (Figs. 132, 135, 148, 149, 150, 151).

Plate 46A (IV) and Fig. 108 show degenerative changes in the choriocapillaris in control samples which, however, are only ten RPE cells distant from the lesion margin.

The lumen of the choriocapillaris may be patent and normal. It may contain many erythrocytes (Figs. 70, 71) to the extent of congesting the lumen (Figs. 86, 105, 116, 125). Many platelets may be present (Figs. 44, 94, 95). Fibrin strands and thrombi may congest and even occlude the lumen (Figs. 136, 151, 163, 164). While leukocytes are sometimes seen they are never abundant. The changes in the choriocapillaris may be slight, such as loss of endothelial fenestrations only, or extensive showing signs of degeneration (Figs. 108, 129), thrombus occlusion (Figs. 91, 150, 151, 164) or total obliteration of the lumen (Figs. 136, 148, 149).

The markers (at or above threshold) irradiated at λ 1064 nm produced more severe and more consistent changes in the choroid and in the choriocapillaris than is seen in the subthreshold lesions.

Several samples of control tissue showed a large number of erythrocytes in the choriocapillaris (Fig. 105), but most did not. However, these control samples did not show any of the severe choroidal changes seen in association with the lesions, but in Rhesus some showed choriocapillaris degeneration (Figs 46A IV, 105, 108, 116) in one animal, in both the dark-adapted left eye and in the light-adapted right eye.

Within the lumen of the choriocapillaris in both species there are often present electron-dense globules (EDG) of varying sizes. They may be larger than, the same size as, or smaller than the inclusion granules of the platelets and leukocytes (Figs. 7, 13, 14, 21, 27, 28, 32, 48, 50, 53, 54, 57, 64, 65, 72, 73, 74, 75, 78, 79, 81, 82, 86). EDG may be plentiful or sparse. These were seen whether the animal was dark- or light-adapted, in all quadrants of the retina and in the foveal samples, in the subthreshold and marker lesions, and in the controls, and in both eyes of six different animals.

EDG are also seen within Bruch's membrane (Figs. 24, 28, 48, 56, 73, 80, 81, 82, 86). In the basal RPE near Bruch's membrane (Figs. 24, 28, 32, 48, 57, 63, 72, 74, 78, 79, 82, 89) there are electron-dense spherical globules which are similar in size, shape and general appearance (see, for example, Figs. 81, 85, 89, 198). More rarely EDG are seen in the endothelium (Figs. 28, 32, 81).

In the lumen of the choriocapillaris when this is not congested, there are seen membrane-outlines whose contents resemble that of the plasma and whose size often approximates that of the erythrocytes. In order to refer to them with brevity these are called "ghost" figures. They were present in the rabbit (Fig. 14), in M. fascicularis (Fig. 37) and in M. rhesus (Figs. 50, 53, 54, 56, 57, 63, 65). A "ghost" in Figure 73 is closely associated with the endothelium. These "ghost" figures were most frequently seen in M. rhesus.

BRUCH'S MEMBRANE

The ages of the rhesus monkeys in these experiments were not known with certainty but they were all older than fourteen years. Aging changes are well known to occur in Bruch's membrane. The cynomolgus monkeys were young.

The control samples of cynomolgus monkey Bruch's membrane appeared normal (Fig. 56A). However, changes associated with laser irradiation were seen, and these resembled those described for aging primate retinae; and the extent of the changes appeared to be correlated with the severity of the lesion, greater severity elicited greater changes.

Bruch's membrane is not breached at the RPE border. Discontinuities of the endothelium of the choriocapillaris occur, and in some cases it appeared that at this surface Bruch's membrane basal lamina may be breached.

The abnormal changes seen in Bruch's membrane include:

(a) intrusion of cells into Bruch's membrane at the endothelial surface (Figs. 4, 7, 42, 86, 87, 88).

(b) Electron-dense globules (EDG) are seen within Bruch's membrane (Figs. 24, 45, 48, 56), similar to those seen in basal RPE (Figs. 25, 45, 81), endothelial cells (Fig. 28) and within the lumen of the choriocapillaris (Fig. 28).

(c) Drusen were seen but infrequently. Drusen present were associated with basement membrane material also present within and around the basal infolds of the RPE (Fig. 49). Basement membrane associated with basal infolds was also seen where there were no drusen present (Fig. 147).

(d) Non-globular electron-dense and/or dense amorphous accumulations were present (Figs. 45, 48, 54, 56, 60).

(e) Vesicles, filaments and granular material were present (Figs. 45, 47, 79, 80, 89, 109).

(f) Wide banded collagen was present (Fig. 24).

(g) A "moth-eaten" appearance (Figs. 86, 148, 153, 158, 163, 170, 176).

(h) Abundant collagen fibres and filaments (Fig. 176).

(i) Figure 149 displays extensive damage to Bruch's membrane.

(j) Vacuoles may be present, in a few cases.

These changes were seen both in association with aging and with laser irradiation damage and in all parts of the fundi examined in this study. It must be noted that there were variations in the type and extent of changes seen in different sections of the same lesion.

In certain lesions where Bruch's membrane is denuded of covering RPE cells over a very small area, cells neighbouring the denuded area extend tongues of RPE cell towards each other and very rapidly cover the denuded area and attach to each other by junctional complexes (Figs. 3, 7, 78, 178) and these 'tongues' separate Bruch's membrane from the apical co-agulated or necrotic RPE, within one day. Where the lesion is extensive this was not seen to occur.

THE RETINAL PIGMENT EPITHELIUM (RPE)

The damage created by the laser irradiations in the retinal pigment epithelium (RPE) is very localized, discreet and demarcated.

The types of changes observed are surprisingly similar whether the retinae are prior light- or dark-adapted, or whether foveal, macular, or in any the four quadrants of the perimacula (superior, inferior, nasal or temporal). However, the extent of the changes appear to be somewhat different. The extent of the changes is more dependent on the energy input, the wavelength, and spot size of the irradiation. But changes also occur that are not linked to these parameters, but to other as yet unidentified factors in the eye or retina itself.

The earliest changes by which the lesions could be identified include the following:

(1) paleness of the RPE cell **(Figs. 34, 82, 84, 85, 121) [compare with controls, Figs. 24, 72].**

(2) swelling or reduction or retraction of the apical microvilli **(Figs. 21, 34, 38, 83),** often with early retraction of the melanin granules into the RPE cell body **(Figs. 38, 71, 73, 86, 90)** or loss of melanin granules **(Fig. 153).**

(3) swelling of **(Figs. 23, 28, 84, 85, 121, 122)** reduction or disappearance of the basal infolds **(Figs. 24, 31, 32, 56, 60, 63, 82, 135, 136, 145, 148, 149, 154, 158, 168, 178, 179, 180).**

(4) reduction in height of the RPE cells **(Figs. 86, 154),** or an extension of the pale apical part of the RPE cell (swelling) **(Figs. 83, 84).**

(5) an uneven RPE apical surface **(Fig. 79).**

Phagosomes

Many montages and single electronmicrographs of lesions, and control areas, were examined for the presence or absence of obvious phagosomes, and if present whether there were only one or two, or more. There were also present (less frequently) very large phagosomes, more than twice the diameter of the rod outer segment. The observations were tabulated according to light- and dark-adaptation, previous exposure to constant light; wavelength; age of lesion; species, and quadrants of the retinae, all compared to controls.

Phagosomes were present in cynomolgus and rhesus retinae, in lesions and in control areas, at both wavelengths, in retinae dark-adapted, light-adapted and pre-exposed to constant light, and in all quadrants, but distinctly less often in the fovea. There were micrographs showing no phagosomes but these were less common.

The following observations are noted:

(1) In dark-adapted retinae only three sections showed no phagosomes whereas there were far more light-adapted sections showing no phagosomes, independently of other factors.

(2) There were more sections containing phagosomes in the superior, and in the temporal quadrants, than in the nasal and inferior quadrants.

(3) Very large phagosomes were seen more often (but not exclusively) in the one day old lesions, in those pre-exposed to constant light, and in the superior quadrants (Figs. 25, 152, 153, 162).

(4) Large numbers of what appeared to be packets of relatively normal outer segment disks were sometimes seen as if lined up at, but not inside, the apical RPE border. Packets of disarrayed and/or pyknotic disks were also seen at the RPE border (Figs. 78, 81, 150, 154, 164, 167, 178).

(5) There were no sections of λ532 nm wavelength lesions that showed no phagosomes or no disk packets at the RPE border and more λ532 nm lesions contained phagosomes. While there were λ1064 nm lesions that contained unusually large phagosomes, these were more frequent in the λ 532 nm lesions, and slightly more frequent in the superior quadrant.

(6) Whorls of membrane-material were seen in the RPE after exposure to constant light (Fig. 168).

(7) Even necrotic RPE may contain many phagosomes (Fig. 184).

TABLE 1

DETAILS OF LESIONS

ANIMAL	EXPERIMENT NUMBER	LIGHT/DARK ADAPTATION	MORNING/ AFTERNOON LASING	LESION NUMBER	LASER λ (nm)	OUTPUT Energy(μJ)	LESION SIZE (μm)	RETINAL POSITION	LESION AGE
Rabbit (Grey)	Laser 2	L.A.	afternoon	L A1	1064	15.7	180	u.v.s.	2 weeks
		L.A.	afternoon	B4	1064	31.9	204	u.v.s.	1 week
		L.A.	morning	C5	1064	x	360	u.v.s.	4 days
		L.A.		D7	1064	40.9	234	u.v.s.	1 day
	4 Z	L.A.	morning	L1-OS	1064	x	864	u.v.s.	1 day
		L.A.	morning	L2 OS	1064	x	148	u.v.s.	1 day
		L.A.	morning	L3 OS	1064	x	340	u.v.s.	1 day
		L.A.	morning	L4 OS	1064	x	648	u.v.s.	1 day
		L.A.	morning	L5 OS	1064	x	624	u.v.s.	1 day
		L.A.	afternoon	L2 OD	1064	3000	910	u.v.s.	25 days
	Nd3	D.A.	morning	LD5	1064	x	110	u.v.s.	1 day

u.v.s. = under visual streak
x = various laser energies, experimental

Table 1 ... continued

ANIMAL	EXPERIMENT NUMBER	LIGHT/DARK ADAPTATION	MORNING/ AFTERNOON LASING	LESION NUMBER	LASER λ (nm)	OUTPUT Energy(μ J)	LESION SIZE (μ m)	RETINAL POSITION	LESION AGE
M. fascicularis									
	Nd5-S1a	L.A.	morning	L3	1064	142	22	m/i	1 day
Nd5[1]	Nd5-S1b	L.A.	morning	L2	1064	148	90	fovea	1 day
YOUNG	Nd5-S1c	L.A.	morning	L4	1064	145	84	m/t	1 day
ADULT	Nd5-S2	L.A.	morning	L7	1064	133	95	p/n	1 day
MALE	Nd5-S3	L.A.	morning	L11	1064	125	90	p/t	1 day
						cumulative[2]			
Nd11	Nd11-D1	L.A.(29 hrs)	afternoon	L3	1064	305	55	m/i	1 day
YOUNG	Nd11-D1	L.A.	afternoon	L2	1064	333	80	fovea	1 day
ADULT	Nd11-D1	L.A.	afternoon	L4	1064	293	49	m/n	1 day
MALE	Nd11-D1	L.A.	afternoon	L5	1064	260	100	m/t	1 day
						single			
CONSTANT LIGHT	Nd11-S6	L.A. (2ɔ hrs)	morning	L4	1064	180	166	m/t	1 day
26 hrs.	Nd11-S2	L.A.	morning	L12	532	42	215	p/t	1 day
pre-	Nd11-S1	L.A.	morning	"S1"	532	-	240	beyond optic disc	1 day
treatment	Nd11-S3	L.A.	morning	L6	532	182	130	p/n	1 day

[1] NDS-OD retina, became severely puckered.
[2] Dose-fractioned, 3 shots, at 3 minute intervals: lesions not visible at dissection, but found in sectioning appropriate areas.

In all monkey retinae there were low level lesions that could not be located despite the aid of maps.

Table 1 ... continued

ANIMAL	EXPERIMENT NUMBER	LIGHT/DARK ADAPTATION	MORNING/ AFTERNOON LASING	LESION NUMBER	LASER λ (nm)	OUTPUT Energy(μJ)	LESION SIZE (μm)	RETINAL POSITION	LESION AGE
M. fasciculularis									
Nd12	Nd12-S1#8	D.A.	morning	L2	1064	131	180	fovea	1 day
	Nd12-S1#6	D.A.	morning	L3	532	41	130	m/i	1 day
YOUNG	Nd12-S1#2	D.A.	morning	L11	1064	163	120	p/i	1 day
ADULT	Nd12-S1#1	D.A.	morning	L12	1064	238	20	p/i	1 day
MALE	Nd12-S1#5	D.A.	morning	L"C"	532	38	241	p/i	1 day
	Nd12-S3#1	D.A.	morning	"L4C"	532	52	150	p/n	1 day
	Nd12-S3#2	D.A.	morning	L6	1064	150	195	p/n	1 day
	Nd12-S3#3	D.A.	morning	L7	1064	152	78	p/n	1 day
	Nd12-S3#5	D.A.	morning	L8	1064	221	115	p/n	1 day
	Nd12-S5#7	D.A.	morning	L13	1064	154	65	p/t	1 day

Table 1 ... continued

ANIMAL	EXPERIMENT NUMBER	LIGHT/DARK ADAPTATION	MORNING/ AFTERNOON LASING	LESION NUMBER	LASER λ (nm)	OUTPUT Energy(μJ)	LESION SIZE (μm)	RETINAL POSITION	LESION AGE
M. rhesus									
	Nd6-S1	L.A.	late a.m.	L29	1064	80	114	p/n	1 day
Nd6	Nd6-S3	L.A.	late a.m.	L25	1064	81	36	p/t	1 day
OLD	Nd6-S3	L.A.	late a.m.	L26	1064	81	24	p/t	1 day
FEMALE	Nd6-S6	L.A.	late a.m.	L12	1064	91	66	m/t	1 day
	Nd6-S6	L.A.	late a.m.	L14	1064	89	84	m/n	1 day
	Nd6-S6	L.A.	late a.m.	L17	1064	87	95	m/i/t	1 day
	Nd6-S5	L.A.	late a.m.	L23	1064	83	30	p/i	1 day
	Nd6-S6	L.A.	late a.m.	L15	1064	91	72	m/i/n	1 day
	Nd6-D4	L.A.	morning	L19	1064	139	114	p/t	1 hour
	Nd6-D1	L.A.	morning	L3	1064	134	156	p/s	1 hour
	Nd6-D5	L.A.	morning	L6	1064	133	144	fovea	1 hour
	Nd6-D5	L.A.	morning	L17	1064	138	200	m/t	1 hour
	Nd6-D5	L.A.	morning	L7	1064	133	168	m/i	1 hour
	Nd6-D5	L.A.	morning	LX	1064	130	130	near fovea	1 hour
	Nd6-D5	L.A.	morning	L12	1064	120	100	m/n	1 hour

*p/n = peripheral/nasal
p/i = peripheral/inferior
p/s = peripheral/superior
p/t = peripheral/temporal

m/i = macular/inferior
m/n = macular/nasal
m/t = macular/temporal
m/i/n = macular/inferior/nasal
m/i/t = macular/inferior/temporal

Table 1 ... continued

ANIMAL	EXPERIMENT NUMBER	LIGHT/DARK ADAPTATION	MORNING/ AFTERNOON LASING	LESION NUMBER	LASER λ (nm)	OUTPUT Energy(μJ)	LESION SIZE (μm)	RETINAL POSITION	LESION AGE
M. rhesus									
	Nd7-D4	D.A.(overnight)	morning	L11	1064	115	300	p/s	1 day
Nd7	Nd7-D3	D.A.	morning	L13	1064	106	228	p/t	1 day
OLD	Nd7-D1	D.A.	morning	L5	1064	126	108	m/t	1 day
FEMALE									
	Nd7-S13b	L.A.	afternoon	L1	1064	128	86	m/s	1 day
	Nd7-S13b	L.A.	afternoon	L2	1064	126	82	m/n	1 day
	Nd7-S1	L.A.	afternoon	L5	1064	127	60	m/n	1 day

Table 1 ... continued

ANIMAL	EXPERIMENT NUMBER	LIGHT/DARK ADAPTATION	MORNING/ AFTERNOON LASING	LESION NUMBER	LASER λ (nm)	OUTPUT Energy(μJ)	LESION SIZE (μm)	RETINAL POSITION	LESION AGE
M. rhesus									
	Nd9-D1	L.A.	morning	L5	1064	271	22	m/s	4 hours
Nd9	Nd9-D1	L.A.	morning	L6	1064	291	137	fovea	4 hours
OLD	Nd9-D1	L.A.	morning	L7	1064	302	62	m/i	4 hours
FEMALE	Nd9-D1	L.A.	morning	L8	1064	299	64	m/n	4 hours
	Nd9-D1	L.A.	morning	L9	1064	271	107	m/t	4 hours
	Nd9-D3	L.A.	morning	L14	532	44	191	p/t	4 hours
	Nd9-S1	D.A. (2 hrs)	early P.M.	L20	532	58	133	p/t	1 hour
	Nd9-S2	D.A.	early P.M.	L14	532	68	263	p/s	1 hour
	Nd9-S4	D.A.	early P.M.	L11	532	79	244	p/i	1 hour
	ND9-S5	D.A.	early P.M.	L17	532	51	35	p/n	1 hour
	Nd9-S3	D.A.	early P.M.	L9	1064	139	74	m/n	1 hour
	Nd9-S3	D.A.	early P.M.	L7	1064	142	92	m/i	1 hour
	Nd9-S3	D.A.	early P.M.	L6	1064	137	70	fovea	1 hour
	Nd9-S3	D.A.	early P.M.	L5	1064	145	78	m/s	1 hour
	Nd9-S3	D.A.	early P.M.	L8	1064	137	101	m/t	1 hour

Table 1 ... continued

ANIMAL	EXPERIMENT NUMBER	LIGHT/DARK ADAPTATION	MORNING/ AFTERNOON LASING	LESION NUMBER	LASER λ (nm)	OUTPUT Energy(μJ)	LESION SIZE (μm)	RETINAL POSITION	LESION AGE
M. rhesus									
	Nd10-D2	L.A.	morning	L11	532	166	350	m/i	1 day
Nd10	Nd10-D2	L.A.	morning	L12	532	159	137	m/n	1 day
OLD	Nd10-D2	L.A.	morning	L10	532	142	340	fovea	1 day
FEMALE	Nd10-D2	L.A.	morning	L13	532	109	88	m/t	1 day
	Nd10-D2	L.A.	morning	L9	532	157	360	m/s	1 day
	Nd10-D2	L.A.	morning	L6	1064	123	185	p/s	1 day
	Nd10-S2	D.A. (3½hrs)	afternoon	L11	532	124	360	m/i	1 day
	Nd10-S2	D.A.	afternoon	L13	532	110	68	m/n	1 day
	Nd10-S2	D.A.	afternoon	L9	532	130	205	m/s	1 day
	Nd10-D	L.A.	morning	L6	1064	123	185	s	1 day
	Nd10-D1	L.A.	morning	L8	1064	114	201	p/i	1 day
	Nd10-D3	L.A.	morning	L7	1064	130	70	p/n	1 day
	Nd10-D5	L.A.	morning	L5	1064	130	210	p/t	1 day
	Nd10-S5	D.A.	afternoon	L5	1064	207	36	p/n	1 day
	Nd10-S1	D.A.	afternoon	L8	1064	198	230	p/i	1 day
	ND10-S4	D.A.	afternoon	L7	1064	190	310	p/t	1 day

TABLE 2

SIZES OF LESIONS (AVERAGES) (nm) IN THE RPE ACCORDING TO GROUPED PARAMETERS

PARAMETER	RHESUS	CYNOMOLOGUS
λ 1064	137	159
λ 532*	202	196
F	151	117
S*	218	215
I*	212	181
T*	135	123
N*	77	116
Mac/S	174	61
Mac/I	174	130
Mac/T	109	117
Mac/N	89	-
LA a.m. λ 1064	133	76
LA p.m. λ 1064	68	71
DA a.m. λ 1064	194	110
DA p.m. λ 1064	124	-
LA λ 1064	131	147
DA λ 1064	159	176
DA a.m. λ 532*	-	207
DA p.m. λ 532*	187	-
CL pre-treatment	-	188
LA a.m. λ 532	74	-

These averages are not reliable indicators in general as they do not take association-correlations into account. However, some of the figures (*) are consonant with some general morphological observations.

THE OUTER SEGMENTS (OS)

A variety of alterations occur in the outer segments (OS) in response to the laser irradiations.

Especially in the smaller lesions where only a few RPE cells are affected, most of the OS display a normal or nearly-normal morphology (**Figures 53, 84, 85, 86**).

The regularity of disk-spacing and the uniformity of disk-staining within a single outer segment can be altered at fairly subtle levels, in OS that are not swollen (**Figures 85, 87**). These changes become more marked in more severe lesion changes (**Figures 93, 94**).

It is noted that control samples show: irregularities in disk- spacing and staining intensity within one OS (**Figures 39, 40, 76, 108, 165**); OS which contain disarrayed disks (**Figures 46, 74, 105, 107**); OS which are swollen and contain very few disks (**Figures 77, 114, 115, 131**); "thumb-print" whorls (Lawwill et al., 1973) of disks in the proximal OS, very close to its junction with the inner segment (**Figures 46, 172**). These are seen in all areas of the fundus.

The regular orientation and alignment of the OS is often changed, best displayed in light micrographs (**Figures 51, 57, 97, 98, 104**). In the smallest lesions the orientation of the OS may remain essentially unaltered even when the OS are displaced vitreally (**Figures 59, 66**). The nodules seen on the OS in **Figure 59** are OS convolutions which occur with increasing frequency with age (Marshall et al., 1979). In the more 'severe' lesions the disorientation and misalignment of the OS is marked (**Figures 81, 142, 143**).

'Thumb-print' whorls of OS disks when present in lesions are most frequent in the proximal OS (**Figure 156**), but may also be seen in the more distal OS (**Figures 78, 107, 111**). They are never seen in the distal OS in control samples.

There is a gradient in the severity of the changes seen in the OS as a result of laser irradiation:

(1) very little change, with only slight disturbance in the regularity of disk spacing, so that groups of disks become slightly separated, and/or the disks become unevenly spaced (**Figures 2, 21, 82, 93, 94, 101**).

These changes alone, however, are not a reliable morphological indicator of laser-induced change, since these changes may also be seen in the controls (**Figures 40, 76, 165**). [Small changes in RPE are a far more reliable indicator.]

(2) These changes may become more marked (**Figure 90**).

(3) Disks may be unevenly stained, or deeply stained (**Figures 21, 71**).

(4) Disks within a single OS may be disoriented slightly or considerably (**Figures 2, 23, 140, 154, 164, 167**).

(5) Disks may show gradations in the degree of their rearrangement (**Figures 93, 117, 133, 140, 146, 150, 154, 164, 167, 169, 172**).

(6) OS may swell slightly or a lot, and contain relatively few disks (**Figures 68, 84, 101, 103, 111, 117**).

(7) Vesiculation of disks is rarely seen (**Figure 133**).

(8) The changes listed above are seen in both 'same day' and 'next day' lesions. **Figures 5, 94, 111, 150** display a number of the above changes within one section.

The 'thumb-print' whorls of OS disks at the base of the OS and the re-arrangement and swelling of the OS disks seen in the control sections may be due to aging (the rhesus monkeys were old) [compare **Figure 101 control, with Figure 103 lesion**]; to the effect of close proximity to a nearby laser flash (only 10-20 cells distant from the lesion edge in the RPE); to the increased vulnerability of the aged retina to a nearby laser flash. In M. fascicularis, the 'thumb-print' whorls are seen only in lesion areas (532 nm and 1064 nm) (**Figures 21, 156, 160, 172**). In Rhesus retina these whorls are more common and seen also in controls. The 'thumb-print' whorls are seen in all regions of the fundus, within and around the macula, and in dark- and light-adapted retinae and those exposed to constant light.

Disordered OS are seen neighbouring normal or nearly-normal OS, both in controls (**Figures 107, 114**) and in lesions (**Figures 70, 71, 80, 90, 111, 117**). It is not known why within one lesion some OS are affected and others are not; why neighbouring OS should show such different reactions, within the small lesions of this study most of which could not be seen even in the dissecting microscope.

Sometimes disarrayed OS cluster at the RPE apical border (**Figures 78, 81**). Large packets of normal-looking OS disks are seen at the apical RPE border (**Figures 82, 86**), and within the RPE in the lesions (**Figures 82, 86**).

OS disks may be seen in anomalous positions, within the inner segment in a lesion (**Figure 171**); more rarely in the basal RPE near its border with Bruch's membrane (**Figure 135**).

Swollen OS are seen in all areas of the fundus in light- and dark-adapted retinae, in constant light-exposed retinae, in one hour, four hour and one day-old lesions, in both species (but less so in rabbit) and often in both the 532 and 1064 nm wavelength irradiations. The swelling of the OS appears to be a response to trauma independent of the parameters of exposure within this study.

Rabbit OS do not show as many changes in response to the laser irradiations as do the macaque retinae.

INNER SEGMENTS AND PHOTORECEPTOR NUCLEI

The inner segments (IS) are more resistant to laser-induced morphological alterations than are the outer segments and the RPE. The IS of the rabbit retina show less laser-induced reactions (Figure 9) than do the IS of the monkey retina.

In the control areas, the inner segments appear normal, with only very few exceptions (Figure 46A II).

The great majority of lesions do not show any inner segment pyknosis. Pyknosis of IS is seen predominantly in 532 nm lesions (Figures 92, 127, 130, 142), and some of these also show association with pyknotic photoreceptor nuclei.

Pyknosis and necrosis of photoreceptor nuclei is seen in the 532 nm lesions (Figures 92, 127, 128, 130, 141, 142, 166), extending to the Henle fibres (Figure 130), and to degenerating synaptic terminals, to a greater degree and more often than in the ~1064 nm lesions (Figures 30, 98, 181). One control sample (Figure 106) displays degenerating cone nuclei. Dark- and light-adaptation appear not to be a factor in this.

After exposure to laser irradiation the following inner segment changes are seen:

(1) irregularity of the IS outline, with or without swollen mitochondria creating bulges in the IS border (Figures 90, 126, 133, 160, 171, 174).

(2) swollen mitochondria which may also be lacking in or devoid of cristae (Figures 26, 90, 133, 140, 157, 174).

(3) Dark-staining mitochondria, which often contain electron-dense circular inclusions (Figures 157, 161, 174).

(4) Co-agulated and vacuolated cytoplasmic matrix (Figure 26).

(5) Electron density of the IS, including its mitochondria (Figure 126).

These many changes often may be seen in one IS, or in one section.

Necrotic IS are seen among normal or slightly affected IS (Figures 156, 160, 171).

The severest damage to the IS is most often seen in the $\succ$532 nm lesions.

Very necrotic IS (Figures 160, 161) are seen in lesions exposed to constant light for 26 hours before exposure to 532 nm laser irradiation; more so than after λ1064 nm laser irradiation after pre-exposure to constant light (Figure 157).

Dose fractionated 1064 nm irradiation after pre-exposure to constant light produced greater changes in the IS (Figure 174) than in retinae pre-exposed to constant light and then 1064 nm single-shot irradiation (Figures 156, 157).

Occasionally outer segment disks are seen within an IS after exposure to laser irradiations 532 and 1064 nm, but only after pre-exposure to constant light (Figures 156, 157, 160, 161, 171).

In a few cases the synaptic terminals display degenerative changes and/or pyknosis (Figure 98).

THE INTERPHOTORECEPTOR MATRIX (IPRM)

IPRM matrix is seen condensed around photoreceptors in some control sections (**Figures 101, 113, 114, 131**); and in some lesion sections (**Figs. 61, 69, 82, 94, 103, 111, 145**) and also around RPE apical microvilli (**Fig. 21**), whether light- or dark-adapted.

Spaces, or holes, described in the Figure legends as 'bubbles', develop in the IPRM. Some of these appear to have no contents when viewed by electron microscopy (**Figures 22, 53, 78, 80, 83, 84, 104, 134, 151**); some contain a rim of fine granular material; others contain an uneven dispersion of fine granular material (**Figures 34, 50, 54, 71, 82, 104, 109, 121, 124, 125, 145**). These 'bubbles' are clearly seen in the light micrographs (**Figures 29, 51, 52, 55, 59, 66, 67, 130, 137, 143, 144; Plate 46A I**), in both species of macaque, in both wavelength lesions, and in light- and dark-adaptation.

Spaces are also seen to develop (but more rarely) within the RPE (**Figure 182**). **Figure 173** displays spaces both in the IPRM and in the RPE.

These 'bubbles' in the subretinal space are not seen in the rabbit retina. While the 'bubbles' are seen in the macaque retinae in all conditions, they are larger and more numerous in Rhesus retinae. This suggests that the IPRM in aging eyes and in different genera of animals may have different properties. The 'bubbles' appear to be tears (breaks) in the continuity and integrity of the IPRM, and it appears that these are more readily created in the aging eye.

CONCLUSIONS

In all the subthreshold lesions and many of those barely at threshold, very similar alterations are seen to occur. Some subthreshold lesions were so small that they were not locatable.

The extent and intensity of the damage varies, and is not closely correlated with energy input or spot size within the narrow confines of the parameters used at 1064 in this study.

No two lesions are identical although lesions display many similarities.

There is a distinct border to the lesions in the retinal pigmented epithelium (RPE) and a gradation of damage in the RPE from the most severe in the lesion centre to the least severe at its periphery.

The basic types of responses elicited by Nd-Yag subthreshold lesions tend to be similar in rabbit and monkey retinas, but there are differences.

Differential vulnerabilities

Some organelles and some regions showed more persistent or better abilities to withstand the trauma of the laser irradiations:

(a) Bruch's membrane is rarely breached, although it showed alterations.

(b) The basal lamina of the RPE was more "enduring" than the basal lamina of the choriocapillaris.

(c) Junctional complexes were not disrupted morphologically in the RPE where the damage was not sufficient to obliterate or explode the cells; and they also reform very rapidly in the repair process (after one day).

(d) Mitochondria of the RPE remain as recognizable organelles, although they may show early swelling and they may elongate, especially in necrotic RPE cytoplasm. However, when the damage is extensive, the mitochondrial plasma membrane bursts.

(e) The basal RPE, although altered, retains basic integrity better than does the apical RPE, which far more often shows degenerative, necrotic changes and co-agulated cytoplasm.

(f) The ciliary connection between the inner and outer segments is not obviously disrupted even when the outer segment disks are.

(g) Striated rootlets were seen often even in considerably damaged inner segments, and sometimes in the RPE.

(h) It "takes more" to damage the inner segments than the outer segments.

(i) In the outer segments, the disks are more frequently in disarray in the proximal outer segment than in their distal portions.

(j) The outer limiting membrane is rarely altered in the range of experiments performed in this study.

(k) The rod nuclei show earlier and more severe damage-changes than do the cone nuclei.

(l) The inner retinal layers most often show no morphological alterations.

(m) Muller cells may swell but are "enduring" cells.

(n) The choriocapillaris often shows various changes but the deeper choroid is not affected.

(a) λ 532 creates greater damage than does λ 1064. The wavelength difference has a greater impact.

(b) The superior and inferior quadrants are more vulnerable to laser light damage than are the temporal and nasal quadrants.

(c) The nasal quadrant shows lesser damage than does the temporal quadrant.

(d) There is suggestive information in the lesions, in general, that prior dark-adaptation, whether in the morning or after a few hours of dark-adaptation in the afternoon, makes the retina only slightly more vulnerable to laser damage as far as lesion size is involved, if at all.

The laser irradiations used in this study were at a very low level, and the changes the laser induced in the different experiments were subtle. These comments are generalizations and variations occur within each grouping. It is clear that the ocular media affect transmission properties, and within any one retinal fundus there are unpredictable differences. There is more variability within one monkey retina than in one rabbit retina.

Despite the sizes of the lesion in the RPE, it appears that pre-exposure to constant light (26 hours) before irradiation at 532 nm creates conditions for a greater reaction to the laser irradiation than does light- or dark-adaptation.

There is a "maturation" of the development of the laser induced reactions from immediately after irradiation to one hour to 24 hours post-irradiation, but the changes are small compared to the wavelength effect (of 532 compared to 1064).

It is an interesting observation that RPE cells only 3-4 cells distant from the lesion edge, outside of the lesion, contain very large bodies with membranous contents (probably shed outer segment disks) (Figure 153) and so do RPE cells 6-8 cells distant from the lesion edge contain unusually large phagosomes (Figure 152). It seems that, while many of the changes associated with laser damage are circumscribed and contained in discretely delimited areas of the RPE, nearby RPE cells show effects of the flash of laser irradiation, in that bursts of outer segment shedding occur beyond the immediate laser-affected lesion area.

After one hour or one day the RPE shows layering. The basal RPE tends to be the least affected and remains relatively intact even when the apical RPE is necrotic. It is from the basal parts of the RPE that tongue-like projections extend along the denuded parts of Bruch's membrane to re-line it, and form junctional complexes with each other. While the normal polarity of the cell is lost, this is much more marked in later stages (e.g. seven days, Borwein, 1982) than after one hour or one day. The apical RPE tends to form a necrotic mass, or severe necrotic masses (Figures 21, 23, 78, 125, 134, 147, 151, 185). The presence of distinct membrane-enclosed phagosome-like bodies is rarely seen after only one day, whereas after 4-7 days these are regularly present (Borwein, 1982).

The RPE shows ability to recover very quickly in the small lesions described in this study.

There were many aging changes seen in the retinae of the rhesus monkeys, as displayed in control sections.

The pigment epithelium is the site of the first morphological changes seen, and it shows the most extensive changes.

When photoreceptor nuclei show pyknosis and necrosis this is much more frequent and severe in the rod nuclei than the cone nuclei.

In the majority of the lesions the photoreceptor nuclei show little or no changes. It is probable that in low level lesions the photoreceptors and RPE can recover, at least somewhat. However, the loss of melanin granules and cell height may be permanent. The choroiocapillaris recovers, but much of the debris in Bruch's membrane may remain in situ.

ABBREVIATIONS

AMV	=	apical microvilli
BI	=	basal infolds
BM	=	Bruch's membrane
CC	=	choriocapillaris
CL	=	constant light
D	=	disks
DA	=	dark-adapted
EDG	=	electron-dense globule
F	=	fovea
I	=	inferior
IO	=	intra-ocular
IPRM	=	interphotoreceptor matrix
IS	=	inner segment
L	=	lesion
LA	=	light-adapted
LC	=	lesion centre
LM	=	light microscopy/micrograph
M.	=	Macaca
MG	=	melanin granules
N	=	nasal
Nd-YAG	=	Neodymium-yttrium-aluminum-garnet laser
OS	=	outer segment
OLM	=	outer limiting membrane
PR	=	photoreceptor
RPE	=	retinal pigment epithelium
S	=	superior
T	=	temporal
TEM	=	transmission electron microscopy/micrograph
V	=	vacuole
λ	=	wavelength

TABLE 3

DETAILS OF PHOTOMICROGRAPHS

ABBREVIATIONS FOR TABLE 2

CL = Constant Light (26 hrs.)
DA = Dark-adapted
LA = Light-adapted
LM = Light micrograph
Mt = Montage
F = Fovea
Mac = Macula
N = Nasal
T = Temporal
S = Superior
I = Inferior
Mac/I, Mac/S, Mac/T, Mac/N } within macula
u.v.s. = under visual streak
λ = Wavelength
Dose F = Dose fractionated

* *

RABBIT

Plate Number	Figure Number	Retinal Position	Lesion Age	DA/LA/CL	Wavelength λ (nm)
1	1 (LM)	u.v.s.	1 day	LA	1064
	2-4	u.v.s.	1 day	LA	1064
2	5-7	u.v.s.	1 day	LA	1064
3	8-10	u.v.s.	1 day	LA	1064
4	11	u.v.s.	1 week	LA	1064
	12	u.v.s.	2 weeks	LA	1064
	13	u.v.s.	control	LA	control
5	14-15	u.v.s.	1 week	LA	1064
	16-17	u.v.s.	controls	LA	controls

Note: There is no Plate 6.

Table 2 ... continued

CYNOMOLGUS

Plate Number	Figure Number	Retinal Position	Lesion Number	Lesion Age	DA/LA/CL	Wavelength λ (nm)	Animal
7	21 (Mt)	T	L11	1 day	LA	1064	Nd5-S
8	22 (LM)	T	L11	1 day	LA	1064	Nd5-S
	23	T	L11	1 day	LA	1064	Nd5-S
	24	T	L11	1 day	LA	1064	Nd5-S
	25	T	L11	1 day	LA	1064	Nd5-S
9	26-28	N	L7	1 day	LA	1064	Nd5-S
10	29 (LM)	Mac/T	L4	1 day	LA	1064	Nd5-S
	30-32	Mac/T	L4	1 day	LA	1064	Nd5-S
11	34-36	F		1 day	LA	1064	Nd5-S
12	38	F		-	LA	control 34-36	Nd5-S
	39	N		-	LA	control 26-28	Nd5-S
	40	T		-	LA	control 21-25	Nd5-S

Table 2 ... continued

RHESUS

Plate Number	Figure Number	Retinal Position	Lesion Number	Lesion Age	DA/LA/CL	Wavelength λ (nm)	Animal
13	41-44	F	(L13)	-	LA	control	Nd6-S6
	45	Mac	(15,17)	-	LA	control	Nd6-S6
14	46-49	F	(LM)	-	LA	control	Nd6-D
15	50 (Mt)	F	L6	1 hour	LA	1064	Nd6-D
	51	F	L6	1 hour	LA	1064	Nd6-D
16	52 (LM)	S	L3	1 hour	LA	1064	Nd6-D
	53 (Mt)	S	L3	1 hour	LA	1064	Nd6-D
17	54 (Mt)	T	L19	1 hour	LA	1064	Nd6-D
18	55 (LM)	Mac/N	L12	1 hour	LA	1064	Nd6-D
	56-58	Mac/N	L12	1 hour	LA	1064	Nd6-D
19	59 (LM)	Mac/T	L17	1 hour	LA	1064	Nd6-D
	60-61	Mac/T	L17	1 hour	LA	1064	Nd6-D
20	62 (LM)	T	L19	1 hour	LA	1064	Nd6-D
	63-65	T	L19	1 hour	LA	1064	Nd6-D
21	66 (LM)	Mac/I near F	LX	1 hour	LA	1064	Nd6-D
	67 (LM)	Mac/I	L7	1 hour	LA	1064	Nd6-D
	68-69	Mac/I	L7	1 hour	LA	1064	Nd6-D
22	70-71	Mac/N I	L15	1 hour	LA	1064	Nd6-D
23	72 (Mt)	Mac/N near F	(L15)	-	LA	control	Nd7-S
24	73 (Mt)	F		-	DA	control	Nd7-D
25	74, 76	Mac/T	(L5)	-	DA	control	Nd7-D
	75	S	(L11)	-	DA	control	Nd7-D
25	77	Mac/N	(L5)	-	LA	control	Nd7-S
26	78 (Mt)	Mac/N	L5	1 day	LA	1064	Nd7-S
27	79 (Mt)	S	L1	1 day	LA	1064	Nd7-S
28	80 (Mt)	Mac/T	L5	1 day	DA	1064	Nd7-D

Table 2 ... continued

RHESUS

Plate Number	Figure Number	Retinal Position	Lesion Number	Lesion Age	DA/LA/CL	Wavelength λ (nm)	Animal
29	81 (Mt)	S	L11	1 day	DA	1064	Nd7-D
30	82 (Mt)	T	L13	1 day	DA	1064	Nd7-D
31	83 (Mt)	F	L6	4 hours	LA	1064	Nd9-D
32	84 (Mt)	Mac/T	L9	4 hours	LA	1064	Nd9-D
33	85 (Mt)	Mac/I	L7	4 hours	LA	1064	Nd9-D
34	86 (Mt)	Mac/I	L7	1 hour	DA	1064	Nd9-S
35	87-88	Mac/T	L3	1 hour	DA	1064	Nd9-S
36	89 (Mt)	T	L14	4 hours	LA	532	Nd9-D
37	90 (Mt)	S	L14	1 hour	DA	532	Nd9-S
38	91	I	L11	1 hour	DA	532	Nd9-S
	92 (LM)	I	L11	1 hour	DA	532	Nd9-S
	93	I	L11	1 hour	DA	532	Nd9-S
39	94-96	I	L11	1 hour	DA	532	Nd9-S

Table 2 ... continued

RHESUS

Plate Number	Figure Number	Retinal Position	Lesion Number	Lesion Age	DA/LA/CL	Wavelength λ (nm)	Animal
40	97 (LM)	I	L8	1 day	LA	1064	Nd10-D
	98 (LM)	I	L8	1 day	DA	1064	Nd10-S
	99	I	L8	1 day	LA	1064	Nd10-D
	100	I	L8	1 day	DA	1064	Nd10-S
41	101	S	(L6)	-	LA	control	Nd10-D
	102 (LM)	S	L6	1 day	LA	1064	Nd10-D
	103-104	S	L6	1 day	LA	1064	Nd10-D
42	105-108	I	(L8)	-	DA	control	Nd10-S
43	109-112	T	L5	1 day	LA	1064	Nd10-D
44	113-116	T	(L5)	-	LA	control	Nd10-D
45	117-120	N	L7	1 day	LA	1064	Nd10-D
	121-122	T	L7	1 day	DA	1064	Nd10-S
46	123 (Mt)	S	L6	1 day	LA	1064	Nd10-D
	124 (Mt)	Mac/S	L9	1 day	LA	532	Nd10-D
46 A	I (LM)	Mac/S	L9	1 day	LA	532	Nd10-D
	II	Mac/S	(L9)	-	LA	control	Nd10-D
	III	Mac/S	L9	1 day	LA	532	Nd10-D
	IV	Mac/S	(L9)	-	LA	control	Nd10-D
47	125 (Mt)	F	L10	1 day	LA	532	Nd10-D
	126	F	L10	1 day	LA	532	Nd10-D
48	127 (LM)	F	L10	1 day	LA	532	Nd10-D
	128-129	F	L10	1 day	LA	532	Nd10-D
49	130 (LM)	Mac/T	L13	1 day	LA	532	Nd10-D
	131-132	Mac/T	(L13)	1 day	LA	control	Nd10-D
50	133-136	Mac/T	L13	1 day	LA	532	Nd10-D
51	137 (LM)	Mac/T	L12	1 day	LA	532	Nd10-D
	138-140	Mac/N	L12	1 day	LA	532	Nd10-D
52	141-143 (LM)	Mac/I	L11	1 day	LA	532	Nd10-D
53	144 (LM)	Mac/I	L11	1 day	DA	532	Nd10-S
	145 (Mt)	Mac/I	L11	1 day	DA	532	Nd10-S
54	146-147	Mac/I	L11	1 day	DA	532	Nd10-S
	148-149	Mac/I	L11	1 day	LA	532	ND10-S

Table 2 ... continued

CYNOMOLGUS

Plate Number	Figure Number	Retinal Position	Lesion Number	Lesion Age	DA/LA/CL	Wavelength λ (nm)	Animal
55	150 (Mt)	Mac/T	L4	1 day	CL	1064	Nd11-S
56	151 (Mt)	Mac/T	L4	1 day	-	1064	Nd11-S
56 A	(Mt)	T	(L4)	1 day	CL	control 55-56	Nd11-S
57	152-155	N	L5	1 day	CL	1064	Nd11-S
58	156-159	N	L6	1 day	CL	1064	Nd11-S
59	160-163	T	L12	1 day	CL	532	Nd11-S
60	164 (Mt)	T	L12	1 day	CL	532	Nd11-S
61	165	far N	(L51)	-	CL	control	Nd11-S
	166-168	far N	L51	1 day	CL	532	Nd11-S
62	169-171	Mac/T	L5	1 day	Dose-F CF	1064	Nd11-D
	172	Mac/T	(L5)	-	CL	control	Nd11-D
63	173-176	F	L2	1 day	Dose-F CL	1064	Nd11-D
64	177-180	Mac/N	L4	1 day	Dose-F CL	1064	Nd11-D
65	181	I	L11	1 day	DA	1064	Nd12-S
	182	N	L8	1 day	DA	1064	Nd12-S
	183	N	L8	1 day	DA	1064	Nd12-S
	184	F	L2	1 day	DA	1064	Nd12-S
	185	F	L2	1 day	Dose-F DA	1064	Nd12-D

FIGURE LEGENDS

Figures 1 - 17, Rabbit

Figures 21 - 40; 150 - 185, cynomolgus

Figures 41 - 149, Rhesus monkey

Except where specified as light micrographs (LM) the illustrations are transmission electron micrographs. The lesions have clearly demarcated borders in the RPE, and the cells in the lesion centre are more severely affected than those in the periphery.

Several transmission electron micrographs of a single lesion are presented, as well as montages, to emphasize the variations exhibited within one lesion, depending on whether the section is from the lesion far periphery, mid-area, or lesion centre, and to reduce the tendency to generalize from information garnered from one section only.

RABBIT RETINA

Plates 1 - 5

Lesions and controls are all in the retinal area inferior to the visual streak.

Plate 1 Rabbit Lesions, one day old (damage limited to outer retina)

Figure 1 (LM x 1,500)
Figure 2 (x 3,400), at edge of lesion.
Figures 3 and 4 (x 6,250)

The changes as a result of laser irradiation are limited mainly to the retinal pigment epithelium (RPE). In the lesion centre, the RPE is saucer-shaped (Figures 1, 3, 4). Elsewhere in the lesion the RPE cells bulge out at their apical borders (Figure 1). Some RPE cells detach from Bruch's membrane (BM) and lie freely in the subretinal space as macrophage-like cells (Figure 1). The photoreceptors (PR) are disorganized. Large lipid globules are normally seen in rabbit RPE (Figures 2, 3). The RPE nucleus is shrunken and deformed (Figure 2).

Basal infolds (BI) are not seen in the RPE cells in the lesion centre (Figures 2, 3, 4). In Figure 2, one cell contains BI only in that part of the cell more distant from the lesion. Tongue-like extensions of RPE cells slide over to line the denuded BM in the lesion centre (Figures 2, 3, 4) and they form junctional complexes (Figures 3, 4).

Overlying the RPE "tongues" are layers of membranes, probably from the retracted apical microvilli (Figures 2 and 3), and necrotic coagulated RPE cytoplasm (Figures 2, 3, 4).

Some outer segments contain disordered discs and convoluted outer segments (Figure 2).

The endothelium of the choriocapillaries (CC) is thickened, with electron-dense cytoplasm and reduced or absent fenestrations (Figures 2, 3, 4). In the lumen of the CC are small electron-dense "globules" (Figures 2, 3, 4) and erythrocyte (RBC) "ghosts" (Figure 4).

Bruch's membrane contains cell processes and is not disrupted (Figures 3, 4).

Plate 2 Rabbit, one day old lesion (damage limited to the outer retina)

Figure 5 (x 6,250) - lesion centre.
Figure 6 (x 5,000) a few cells distant from the very centre of the lesion.
Figure 7 (x 10,000) lesion centre.

Some outer segments (OS) in the lesion centre appear normal, or nearly normal, while their neighbouring OS are disorganized (Figure 5). Lying among these OS are two membrane-limited bodies each enclosing a number of OS in various stages of disintegration, as well as mitochondria (Figure 5). Figure 6 displays such a structure which also contains melanin granules (MG).

Many phagosomes of differing sizes line the apical border of the RPE (Figure 6). RPE microvilli are absent, rudimentary or disorganized (Figure 6). Some basal infolds (BI) are present in RPE cells away from the lesion centre (Figure 6) but are absent from the lesion centre itself (Figure 7). A whorl of membranes in RPE, apical to the RPE tongue, is probably derived from the RPE apical microvilli (Figure 7). There are junctional complexes between two tongue-like extensions of the RPE cells and between endothelial cells of the choriocapillaris (Figure 7).

The basement membranes of Bruch's membrane (BM) appear to be intact (Figure 7). A cell lies within BM. The endothelial cells show thickening and densification, and contain vacuoles (Figure 7).

Plate 3 Rabbit, one day old lesions (extending through the entire retina)

Figure 8 (x 3,400)
Figure 9 (x 2,500)
Figure 10 (x 5,000)

The outer nuclear layer (ONL) shows extensive pyknosis, necrosis, disorganization and vacuolization **(Figure 8)**. Amidst all the organelle destruction and damage, mitochondria appear to be relatively resistant to laser induced damage **(Figures 8, 9)**, as do the striated rootlets and centrioles of the inner segments **(Figure 9)**.

In the inner and outer segment areas, there is vacuolization, disorganization in varying degrees, of the outer segments. The parts of the inner segments closer to the outer-limiting membrane are less damaged than the proximal areas closer to the outer segments **(Figure 9)**.

Choroidal cells show vacuolization, degenerative changes and areas of bleeding **(Figure 10)**.

Plate 4 Rabbit.

Figure 11 (x 3,400) one week old.
Figure 12 (x 3,400) 2 weeks old.
Figure 13 (x 3,400) control area (10 cells distant from edge of lesion in **Figure 11**).

The normal rabbit RPE has clearly demarcated zones of basal infolds (BI), mitochondria, and dense apical cytoplasm; and the RPE apical border is convexly rounded. Apical microvilli (AMV) contain melanin granules (MG). A large lipid droplet is present, and nearby it, a phagosome. Small black round spots can be seen in the basal RPE, in Bruch's membrane (BM) and in the choroid (**Figures 11, 13**).

Laser-damaged RPE cells hump up into the subretinal space (**Figure 11**), and between these humps the RPE is reduced in height. One RPE cell has a club-shaped extension, lined at its periphery by MG, and contains a large lipid droplet, a phagosome, a nucleus, and mitochondria and it has very reduced AMV. The basal plinth-like portions of this cell consists mainly of basal infolds (**Figure 11**).

At 2 weeks post-laser-irradiation, the RPE cells display electron-dense apical cytoplasm (**Figure 12**). One RPE cell (left-hand) has only a very narrow neck-like connection to the basal RPE (**Figure 12**).

Plate 5 Rabbit

Figures 14 and 15 (x 3,400) one week old lesions.
Figure 16 (LM x 1,000)
Figure 17 (x 3,400) Controls.

Figure 14 displays the humping of the laser-affected RPE cells and the array of the melanin granules (MG) at their apical borders. Note the small electron-dense small globules in the basal RPE, Bruch's Membrane and the choroid. There are 3 cells in the subretinal space which have irregular margins and appear to be free cells (Figure 15). One of these cells contains large phagosomes; another contains many MG; and the third (with an abnormal nucleus) lies over a thinned portion of the RPE. The outer segments are distant from the RPE but are only slightly disarrayed. The MG in the RPE lie in the apical RPE cytoplasm and not in the apical microvilli as they normally do (Figure 15).

Figures 16 and 17 show the slightly undulating apical surface of the normal RPE. Figure 17 displays the prominent basal infolds and the apical dense cytoplasm of the RPE, and the very close association of the outer segments and RPE.

Cynomolgus Retina, male

Plates 7 - 12 one day old lesions, 1064 , different lesions all from same eye.

Plate 7 Cynomolgus retina

Figure 21 (x 2,500) montage of a lesion, temporal region, close to macula.

The outer segments (OS) show the range of changes that occur after laser irradiation: irregular staining and distances between disks, convoluted OS, finger-print whorls of disks, OS empty of disks, misaligned OS.

The RPE cells at the edge of the lesion have apical microvilli. In the lesion centre melanin granules are in the necrotic, apical, separated parts of the RPE cells, the RPE cells appear vacuolated and hypopigmented. Bruch's membrane is intact. Endothelial cells are electron-dense. The lumen of the choriocapillaris contains erythrocytes, a platelet and a number of small black globule-bodies.

Plate 8 Cynomolgus retina (details of lesion displayed in **Plate 7**, temporal to macula)

Figure 22 (LM x 2,000)

The lesion at its largest diameter affects about 10 RPE cells which are hypopigmented and multilayered. Cells with dark inclusions lie in the subretinal space. Outer segments (OS) are misaligned, and some inner segments are affected.

Figure 23 (x 3,800)

The RPE is 3-layered and all layers show disruption and necrotic changes, in a gradient from base to apex. Basal infolds are absent. Mitochondria and lipofusin granules are present in the basal regions and melanin granules in the most apical regions, alongside phagosomes. The OS show mild to severe damage. Vacuolar spaces are seen throughout the RPE. Microvilli are absent.

Figure 24 (x 19,600)

The basal part of a RPE cell and Bruch's Membrane (BM). BM is not disrupted and contains small electron-dense globules (EDG) in addition to the usual collagen fibres. In the RPE, the endoplasmic reticulum (ER) is fragmented, mitochondria (dark-staining) are present as well as a lipid-like body with elements of ER closely applied to its margin (as seen also in **Figure 23**).

Figure 25 (x 19,600)

Apical part of RPE cell in lesion contains a large phagosome with OS disks, 2 lipofuscin granules, mitochondria, disrupted ER and one EDG resembling those seen in BM in **Figure 24**.

Plate 9 Cynomolgus retina (details of lesion, nasal to the macula)

Figure 26 (x 2,800)

The cone nuclei and most of the cone inner segments (CIS) appear normal, but one CIS is necrotic. Debris-type material is in the Müller cell, immediately vitreal to the outer limiting membrane.

Figure 27 (x 2,800)

Basal part of RPE showing two cells, the right-hand one more damaged that the left-hand one, which has melanin granules in its apical microvilli, and a closely associated outer segment. The choroid and choriocapillaris (CC) show degenerative changes. The lumen of the CC contains erythrocytes, platelets, debris, and many small electron-dense droplets (EDG). The endothelium is fragmented.

Figure 28 (x 14,000)

Basal part of a disrupted RPE cell, showing mitochondria, junctional complex, a lipoidal body (LB) with "spots" on its margin, spaces and vacuoles, swollen and fragmented endoplasmic reticulum. Normal basal infolds are absent. Note 3 EDG: one in the RPE (between the LB and left-hand edge of photomicrograph) and one in the lumen of the CC, and both have fuzzy halos. Another EDG is in the endothelium. Bruch's membrane is intact.

Plate 10 Cynomolgus retina (lesion in temporal area of macula)

Figure 29 (LM x 2,000)

The lesion spans six RPE cells in the maximum diameter of the lesion, and the RPE cells show hypopigmentation and layering. The margins of the lesion are clear. The unaffected RPE cells have apical microvilli with melanin granules. A large "bubble-space" is seen scleral to the RPE. The choriocapillaris is congested.

Figure 30 (x 3,400)

In the lesion area there are two pyknotic rod photoreceptor nuclei.

Figure 31 (x 3,600)

Basal part of disrupted RPE cell and intact Bruch's membrane (BM). The RPE cell has many cystic and vacuolar spaces and lipoidal bodies (LB) with a rim of small electron-dense bodies on their margins. Basal infolds (BI) are absent. The coagulated apical parts of the RPE contain phagosomes, lipofuscin granules, melanin granules and other small electron-dense circular bodies.

Figure 32 (x 10,600)

Disrupted basal RPE cell and intact BM. The choriocapillaris contains electron-dense globules (EDG). The endothelium is thickened and contains small vacuoles; fenestrations are reduced. Note one EDG in the basal RPE, and two LB each with a marginal rim of apposed electron-dense bodies.

Plate 11 **Cynomolgus retina** (lesion in the fovea)

Figure 34 (x 2,700)

A large "bubble" (more than twice the height of the RPE cells) lies immediately vitreal to the lesion, and it appears to be membrane-limited. The lesion is one of the smallest seen. Note the pale RPE cell with very reduced cytoplasm containing lipofuscin, and prominent microvilli (MV). Basal infolds are absent. The cell to the left is hypopigmented, and its microvilli are not apical.

Figure 35 (x 36,000)

The RPE cell in the lesion shows details of the smooth and rough endoplasmic reticulum (ER) in the left-hand cell and the junctional complex between the two cells of the RPE. The right-hand cell has dispersed, swollen and fragmented ER.

Figure 36 (x 36,000)

A portion of the RPE, showing part of a nucleus at the left-hand edge of the photomicrograph. Three mitochondria contain electron-dense inclusions; one is very elongated. A body of concentric membrane layers may be of mitochondrial origin.

Plate 12 **Cynomolgus retina** (Controls)

Figure 37 (x 2,800)

Control area for foveal lesion **(see Plate 11).** RPE, Bruch's membrane (BM) and choroid. Some outer segments do not have typically well-arrayed disks.

Figure 38 (x 2,800)

Control area for nasal lesions near macula **(see Plate 9).** The basal infolds are better developed than in **Figure 37.**

Figure 39 (x 2,800)

Control area for temporal lesion close to the macula **(see plates 7 and 8).**

In **Figures 37-39,** there are small electron-dense globules in choriocapillaris and BM and similar sized bodies in the RPE.

Figure 40 (x 2,800)

Control area for temporal lesion close to the macula **(see plates 7 and 8; and Figure 39).** The outer segments (OS) show separation of disks (D), irregular staining of D within one OS, whorled OS D, swollen OS and misaligned OS **[extension of Figure 39].**

RHESUS RETINA

Plates 13 - 22

One animal, age estimated to be 20 years, female. Right eye, lesions one hour old; left eye, lesions one day old.

Plate 13 Rhesus retina Controls for one day old lesions in the left eye in the macula close to the fovea

Figure 41 (x 3,400)

Outer limiting membrane, inner segments, and Muller cells. Note electron-dense material (debris?) in some of the Müller cells.

Figure 42 (x 3,400)

RPE is crowded with lipofuscin granules of varied sizes. Melanin granules (MG) are present in the apical microvilli and in the RPE cell body. Basal infolds (BI) are present. Bruch's membrane (BM) contains electron-dense bodies. The endothelium of the choriocapillaris (CC) is thickened and layered and the CC contains RBC "ghosts".

Figure 43 (x 3,400)

RPE as in **Figure 42**, but it also contains a large number of lipid bodies and some mitochondria are elongated. The B1 are reduced. BM is electron-dense and has an unusual undulating border with the basal RPE where there are accumulations of debris-material.

Figure 44 (x 3,400)

RPE as in **Figures 42 and 43**, but note the number of platelets in the CC.

Figure 45 (x 10,000)

Basal RPE and BM. Note the densification areas in BM and 4 electron-dense globules (EDG); the BI in the basal RPE, a few bodies in the RPE visually resembling the EDG of BM, smooth and rough endoplasmic reticulum and mitochondria.

Plate 14 Rhesus retina Controls for one hour old lesions in the fovea in the right eye

Figure 46 (x 3,000)

Elongated cones displaying inner segments (IS) and outer segments (OS). The disks of the OS are irregularly aligned in the proximal OS and there are many whorls of disks close to the cone IS-OS junction.

Figure 47 (x 15,300)

RPE and Bruch's membrane (BM). BM has vacuoles and electron-dense inclusions. Six elongated mitochondria in the RPE are approximately parallel to each other and contain elongated parallel longitudinal cristae. Hemidesmosomes can be seen at RPE-BM interface.

Figure 48 (x 6,000)

RPE, BM and choriocapillaris (CC). In the RPE, there are abundant lipofuscin and melano-lipofuscin granules. BM contains a cluster of small electron-dense globules (EDG). Many EDG, of varied sizes, are in the CC. Two small EDG can be seen in the basal RPE near the left-hand margin of the photograph, between a large lipofuscin granule and BM.

Figure 49 (x 30,500)

Detail of BM and RPE border. Basement membrane can be seen between or within basal infolds. The part of the BM that contains a clump of debris-material (including membrane-bounded bodies) creates an invagination into the basal RPE. BM contains collagen fibrils and many vesicles.

Plate 15 Rhesus retina One hour old lesion in fovea (right eye)

Figure 50 (x 5,000)

Montage of lesion. The outer segments (OS) look normal. Condensations of interphotoreceptor matrix lie between RPE and the OS, on the left of the photograph, alongside a group of "bubbles" in the subretinal space. Below the large "bubbles" are smaller vacuolar spaces. The apical microvilli (AMV) are reduced. Many of the melanin granules (MG) are in the apical RPE but not in the AMV. The RPE nuclei are shrunken and misshapen. Mitochondria are basal, and the abundant lipofuscin granules occupy a mid-region of the RPE cells. The choriocapillis (CC) contains red blood cells (RBC), RBC ghosts and many electron-dense globules (EDG). Bruch's membrane also contains small electron-dense globules.

Figure 51 (LM x 2,400)

There are many "bubbles" in the subretinal space. The RPE contains many lipofuscin granules. The OS are displaced. The CC is congested.

Plate 16 **Rhesus retina** one hour old lesion, peripheral and superior to macula in the fundus. (right eye)

Figure 52 (LM x 1,500)

"Bubbles" of space in subretinal space vitreal to RPE. The lesion area forms a hillock protruding towards the vitreous. A "bubble" can be seen in the RPE at Bruch's membrane (BM).

Figure 53 (x 3,800)

Montage. The "bubbles" between the RPE (only moderately disorganized and not necrotic) and the outer segments (OS) appear membrane-bounded and contain sparse flocculent material. The OS appear normal. Areas of the interphotoreceptor matrix show electron-density (left hand side of photomicrograph). Apical microvilli are absent. The RPE contains many small vacuoles apically and fewer large vacuoles basically. Some mitochondria are swollen. BM contains electron-dense bodies. The choriocapillaris is congested and contains electron-dense globules and some of these are also seen in the choroidal tissue. Note the choroidal melanocyte in the right-hand lower corner of the photograph.

Plate 17 Rhesus retina one hour lesion, temporal to the macula (right eye) in the fundus **(see Plate 19,** temporal closer to fovea)

Figure 54 (x 3,000)

About 6-8 RPE cells are affected in the largest diameter of the lesion. The RPE cells beyond the lesion but bordering it contain many lipofuscin granules, apical microvilli (AMV) with melanin granules (MG). The RPE cells in the lesion appear less dense (lighter), their nuclei are shrunken and misshapen, the AMV are present but tend to be swollen. Vacuolar spaces among the basal infolds in the basal RPE beyond the lesion are larger within the lesion, and are also seen in the mid-zone of the RPE cell beyond the lesion. Bruch's membrane (BM) has electron-dense inclusions. The choriocapillaris is congested and contains red blood cells (RBC) and RBC ghosts and many electron-dense globules (EDG). Similar, but sparser, EDG are seen in the choroid and a few in BM. Spaces between the apical RPE and the outer segments contain flocculent and amorphous material and are not membrane-bounded.

Plate 18 Rhesus retina one hour old lesions, nasal and close to the macula (right eye)

Figure 55 (LM x 1,500)

The rod nuclei are dark-staining. Some OS are contorted. There are "bubble" spaces between the RPE and the outer segments (OS). The RPE in the lesion is hypopigmented, with pale nuclei. Melanin granules can be seen apically in the RPE beneath (scleral) to the "bubbles".

Figure 56 (x 9,300)

Basal portion of RPE and Bruch's membrane (BM). RPE contains electron-dense lipofuscin, mitochondria with unusual cristae, a shrunken nucleus, a large vacuolar space and smaller vacuolar spaces. Basal infolds (BI) are absent. BM contains electron-dense areas and electron-dense globules (EDG) and the basement membrane at the choriocapillaris (CC) is not continuous at the left-hand side of the photograph. Fenestrations in the endothelium are absent.

Figure 57 (x 15,600)

Basal region of RPE, BM and CC. The RPE contains swollen mitochondria, many vacuoles, lipofuscin granules, and only a very few BI. The endothelium is disrupted and fenestrations are absent. The lumen of the CC contains erythrocytes, a platelet and leukocyte, and many EDG of various sizes.

Figure 58 (x 19,600)

Detail of basal RPE and BM.

In the RPE, there are three groups of whorled membranes and membrane-bounded vacuoles. The endothelium lacks fenestrations.

Plate 19 Rhesus retina one hour old lesion, temporal, close to fovea (right eye)
(see Plate 17, temporal, outside of macula)

Figure 59 (LM x 1,500)

Small lesion affecting only a few RPE cells with displacement of photoreceptor outer and inner segments, vitreally. Apical melanin granules are present in the microvilli of the RPE. The laser-affected RPE cells contain vacuolar spaces. Two large "bubbles" of space and a few smaller ones lie between the RPE and outer segments.

Figure 60 (x 10,400)

Base of RPE cell and Bruch's membrane (BM). In the RPE the smooth endoplasmic reticulum (SER) is disrupted. The nucleus is misshapen and shrunken and shows signs of disintegration. Basal infolds are very altered. BM contains patches of densification. The endothelium lacks fenestrations and displays open pores.

Figure 61 (x 26,000)

Portion of two RPE cells showing a junctional complex, disrupted SER, cystic spaces and complex lipofuscin granules.

Plate 20 Rhesus retina one hour lesion, temporal to the macula in the fundus (right eye) **(see Plate 17,** montage, same lesion)

Figure 62 (LM x 1,500)

Very few RPE cells are involved but the lesion nevertheless creates a hillock in the retina towards the vitreous. Apical melanin in microvilli are present below the "bubbles" in the subretinal space. Two RPE cells are hypopigmented with pale nuclei. The choriocapillaris is congested.

Figure 63 (x 3,400)

Basal RPE, Bruch's membrane (BM) and choriocapillaris (CC). There are large cystic spaces in the basal RPE, and basal infolds are absent. Nuclei are necrotic. BM contains electron-dense patches. The CC contains many electron-dense globules (EDG) and "ghosts".

Figure 64 (x 8,400)

Basal RPE and BM. The RPE contains lipofuscin granules, cystic spaces, lipoidal globules and a whorled membrane structure. The mitochondria are abnormal. Basal infolds are swollen or absent. BM contains electron-dense patches and EDG.

Figure 65 (x 6,000)

Detail of CC. Fenestrations are absent and there is layering in the endothelium (left-hand side of photograph) and the cells contains vacuoles. In the lumen are EDG.

Plate 21 **Rhesus retina** one hour lesions (right eye)

Figure 66, lesion superior to and near fovea. **Figure 67-69,** lesion inferior to and close to macula.

Figure 66 (LM x 1,500)

A large area of bubble-like spaces between the RPE and outer segments (OS).

Figure 67 (LM x 1,500)

An area of bubble-like spaces between the RPE and OS which show disorganization.

Figure 68 (x 3,800)

OS region, showing contorted OS and swollen OS with disks confined to the margins.

Figure 69 (x 11,000)

OS and apical RPE. RPE has melanin granules in structures that may be re-arranged retracted microvilli. Note the condensations of interphotoreceptor matrix around the OS.

Plate 22 Rhesus retina (x 2,000) one day-old lesion in the macula, nasal and inferior to the fovea, right eye.

Two montages of same lesion.

Figure 70 (less central part of lesion)

Some outer segments (OS) appear normal, while others show disarrayed disks (D). In the subretinal space are two irregularly shaped macrophage-like bodies containing melanin granules (MG) and lipofuscin (LF), coagulated cytoplasm and a few vacuoles. The RPE cell (on the right-hand margin of the photograph) contains three phagosomes, LF and pale cytoplasm. Bruch's membrane (BM) contains electron-dense material.

Figure 71 (x 2,000) (more central part of lesion)

"Bubble"-like spaces, larger and smaller, in the subretinal space appear to be spaces in the interphotoreceptor matrix (IPRM) surrounding the OS. The IPRM appears as a fine and lightly stippled background. RPE cells to the left of the photomicrograph have apical microvilli (AMV) which contain MG. Vitreal to these cells are "bubbles". The RPE cells on the right-hand side of the photomicrograph lack the usual array of AMV and the OS are more distant from the RPE apical border. The basal part of the RPE has small vacuolar spaces. BM contains electron-dense material. Electron-dense globules (EDG) (appearing here as pinhead points) can be seen in the most basal RPE and in BM.

EDG are seen in the choriocapillaris of this retina but much less frequently than in the left eye.

Plates 23 - 30 Rhesus retina one day-old lesions, same animal, right eye dark-adapted (overnight-morning); left eye light-adapted (4 1/2 hours, afternoon)

Plate 23 Light-adapted Rhesus retina, control, in the macula, nasal to the fovea.

Figure 72 (x 3,400) Montage

There are only 3 phagosomes, near or at the apical RPE. Melanin granules are mainly in the apical microvilli. There are many lipofuscin granules and mitochondria occupy mainly a basal position in the RPE. The basal infolds are present as a continuous border, but are not prominent, and hemidesmosomes are abundant. The cytoplasmic matrix of the RPE cell is dense and darkly-staining. Bruch's membrane contains electron-dense material. The endothelium of the choriocapillaris (CC) is fenestrated and there are electron-dense globules in the lumen of the CC.

Plate 24 Rhesus retina dark-adapted, control, in the fovea (but not in the central fovea)

Figure 73 (x 4,000)

There are four phagosomes and condensations of interphotoreceptor matrix at the apical RPE border. The apical microvilli are retracted and devoid of melanin granules which are seen more sclerally along a region of cystic spaces in the RPE. Lipofuscin granules of varied sizes and shapes are abundant. The cytoplasmic matrix of the RPE contains cystic spaces, as do two nuclei and the central nucleus is shrunken. The basal infolds are irregular. Electron-dense globules (EDG) are present in the lumen of the choriocapillaris and EDG of similar size and staining can be seen in Bruch's membrane (left of centre) and several between the RPE nucleus and Bruch's membrane at the right-hand margin of the photograph. The endothelium appears not to be continuous.

Plate 25 Rhesus retina controls, extra-foveal

Figure 74 (x 3,400)

Dark-adapted retina, temporal to the fovea in the macula (see Figure 76)

Apical microvilli (AMV) contain melanin granules. Electron-dense globules (EDG) are present in the lumen of the choriocapillaris.

Figure 75 (x 3,400)

Dark-adapted retina, in the superior retina, beyond the macula.

The AMV are retracted. There are cystic spaces in the RPE cytoplasmic matrix, some of which may be the result of loss of lipofuscin granules during tissue preparation. The basal infolds are not distinct. EDG are seen in the lumen of the choriocapillaris.

Figure 76 (x 3,400)

Dark-adapted retina temporal to the fovea in the macula (see Figure 74).

Some outer segments (OS) show swelling and convolutions. One large swollen organelle contains remains of OS disks and swollen mitochondria.

Figure 77 (x 3,400)

Light-adapted retina in the nasal macula. Some of the OS are convoluted, others are swollen with disks in disarray.

Plate 26 Rhesus retina one day-old lesion, light-adapted. Macular, nasal to the fovea

Figure 78 (x 2,500) Montage

The lesion spans about 7 cells in its largest diameter in the RPE.

Most outer segments (OS) are distant from the RPE apical surface. "Bubbles" vitreal to the apical RPE appear as spaces in the interphotoreceptor matrix. Portions of the RPE cells form separated units, containing many lipofuscin granules (LF), melanin granules (MG), OS disks packets and coagulated electron-dense cytoplasm. Apical microvilli (AMV), swollen fragmented, retracted, can be seen between the free RPE units and the remaining RPE cells abutting Bruch's membrane (BM). At one place BM is denuded and tongues of RPE cells extend towards this small denuded zone. On the left-hand edge of the micrograph is a RPE cell with AMV containing MG. Basal infolds are absent except in this RPE cell. The lumen of the choriocapillaris contains many electron-dense globules (EDG) resembling pinhead points. A few very similar-looking EDG can be seen in BM and in the basal RPE.

Plate 27 Rhesus retina one day-old lesion, **light-adapted.** Macular, superior to fovea

Figure 79 (x 3,400) Montage

The lesion spans about six cells in its longest diameter in the RPE. The RPE is two-tiered. Apically coagulated dense cytoplasm, vacuoles, cystic spaces, melanin granules (MG) and lipofuscin granules (LF), and some apical microvilli (AMV). AMV are more prominent on the RPE cells at both margins of the lesion, at the edges of the photograph. Basally the RPE attached to Bruch's membrane (BM) is saucer-shaped. Basal infolds are absent in this saucer-shaped area. A terminal bar can be seen above the nucleus (on the left). Bruch's membrane is intact and contains many clear vesicles and fewer electron-dense vesicles. The endothelium is fenestrated. The lumen of the choriocapillaris contains electron-dense globules (EDG) and is not congested. Similar EDG can be seen in the basal RPE and in BM.

The three clumps of apical RPE, containing necrotic and vacuolated cytoplasmic matrix, melanolysosomes and melanin granules, resemble detached macrophage-like bodies seen in Figure 70.

Plate 28 Rhesus retina one day-old lesion, **dark-adapted** for 16 hours, Macular, temporal to fovea

Figure 80 (x 4,000) Montage

Some outer segments (OS) are convoluted, and several distinct packets of OS disks (D) can be seen within one OS plasma membrane. A membrane-bounded unit of stippled cytoplasm lies among the OS. "Bubbles", large and small, can be seen at the apical RPE, in the interphotoreceptor matrix. The RPE is much disrupted and the apical parts especially contain electron-dense flocculent cytoplasm, melanin granules, cystic spaces, vacuoles, lipofuscin granules, autophagic vacuoles, and some OS D packets. One such portion of apical RPE forms a pillar, devoid of apical microvilli, extending into the subretinal space. The basal RPE lacks basal infolds but has many hemidesmosomes. Bruch's membrane contains many vesicles, luscent and electron-dense.

Plate 29 Rhesus retina one day-old lesion, dark-adapted for 16 hours.
Superior fundus, outside the macula

Figure 81 (x 4,000) Montage

Large lesion spanning many RPE cells. The outer segments (OS) are convoluted and swollen, and the OS and their disks are in disarray. Large OS packets lie on the border of the RPE or within the RPE. "Bubble" spaces occur in among the disturbed OS.

The RPE is severely affected: flattened; there is no semblance of the normal polarity of the RPE except that some melanin granules are in the apical RPE. There are large and small cystic spaces at Bruch's membrane (BM); vacuolar spaces can be seen throughout the RPE. The nuclei are necrotic. Basal infolds are absent.

The intact Bruch's membrane contains many vesicles. The endothelium is discontinuous and fenestrations are absent. The choriocapillaris contains many electron-dense globules (EDG) of varied size.

Plate 30 **Rhesus retina** one day-old lesion, **dark-adapted.** Temporal fundus, outside the macula

Figure 82 (x 3,000) Montage

The centre of this lesion shows large "bubble" spaces in the region between the outer segments (OS) and the apical RPE. These contain some flocculent material. The OS are in disarray.

The RPE below the large "bubbles" is reduced to only a few strands of material along Bruch's membrane (BM). There are cystic spaces in the RPE on the BM border. There are no apical microvilli, basal infolds, or hemidesmosomes. The cytoplasm of the RPE cells that contain nuclei and lipofuscin granules has cystic spaces and swollen endoplasmic reticulum.

The endothelium is discontinuous and lacks fenestrations. The lumen of the choriocapillaris contains electron-dense globules.

Plates 31 - 33 Rhesus retina Retinas were **light-adapted,** exposed to 1064 λ laser light in the morning.

Plate 31 Rhesus retina four hour old lesion, **light-adapted.** Fovea, near the centre

Figure 83 (x 3,000) Montage

Six RPE cells, from the lesion edge to the lesion centre.

The tall RPE cells of the fovea are pale in the lesion and palest in the lesion centre. Melanin granules tend to be in an apical position in the RPE and on the remaining microvilli (AMV) but the AMV are scleral to apical borders of the RPE cells which extend vitreally. The RPE cells contain cystoid and vacuolar spaces, dispersed and fragmented endoplasmic reticulum, phagosomes (vitreally); lipofuscin granules, spherical, ovoid and elongated mitochondria, and swollen basal infolds (BI) (sclerally). Bruch's membrane is intact and contains luscent and electron-dense vesicles. Electron-dense 'pinhead' particles can be seen in the BI. The endothelium is fenestrated.

Some outer segments (OS) are swollen, and a few are convoluted. There are many ovoid vacuolar spaces in the subretina, some of which may be swollen OS, but others are more likely to be spaces in the interphotoreceptor matrix. Two of the three RPE nuclei present are necrotic.

Plate 32 **Rhesus retina** four hour-old lesion, **light-adapted,** at the edge of the macula, temporal to the fovea

Figure 84 (x 3,000) Montage

The lesion affects only four cells at its and another few cells at its margins (in this micrograph). Some outer segments (OS) are swollen and disorganized and spaces can be seen in the interphotoreceptor matrix but other OS appear normal. Melanin granules (MG) can be seen between the OS.

The RPE cells in the lesion centre appear pale and swollen, or contain pale cytoplasm. The apical border of two cells in the lesion centre bear some microvilli (AMV), and have an irregular margin extended into broad finger-like projections containing the same pale-staining 'stippled' cytoplasm as is seen in the rest of these central cells. Phagosomes can be seen in the apical RPE (see especially the left-hand side of the micrograph). Some mitochondria are elongated in the long axis of the cell.

The basal infolds are swollen and contain electron-dense particulate matter, as do the lumen of the choirocapillaris and Bruch's membrane.

Plate 33 Rhesus retina four hour-old lesion, **light-adapted**, at the edge of the macula,inferior to the fovea

Figure 85 (x 3,000) Montage

The centre of the lesion contains four pale-staining RPE cells and is bordered in its periphery by two darker-staining cells. Some outer segments (OS) are swollen, show convolutions, and disorganization; others appear to be normal. Melanin granules can be seen, among the OS, free in cystic spaces, in swollen apical microvilli (AMV), and at the apical RPE border. The central pale RPE cells are swollen and show extensions into the subretinal space, terminal bars (near the apical border), some cystic spaces, and swollen basal infolds containing particulate matter. The elongated mitochondria tend to align close to and parallel to the lateral plasma membrane cell borders.

Plates 34 - 35 Rhesus retina one hour-old lesions, **dark adapted** for 1 1/2 hours at mid-day and then exposed to 1064λ laser light

Plate 34 Rhesus retina, dark-adapted. Macula, inferior to the fovea

Figure 86 (x 3,400) Montage

Many large phagosomes are present at the apical RPE border. In the centre of the micrograph is a very large outer segment portion surrounded by layers of membranes. There are swirls of membranes in the lesion centre. The most damaged RPE is thinned and is in a saucer-shape. Basal infolds are absent. An electron-dense globule (EDG) can be seen in Bruch's membrane (BM) near the endothelium and near cell processes within BM. The choriocapillaris is congested with erythrocytes, and some EDG are present. There are 1-5 layers of cells and cell processes at the choriocapillaris endothelium on the choroidal side.

Plate 35 Rhesus retina dark-adapted for 1 1/2 hours, mid-day.
One hour lesion, in the macula, temporal to the fovea

Figures 87 and 88 (x 2,500) Montages, same lesion

Figure 87 The more peripheral part of the lesion.

Figure 88 The central part of the same lesion.

The damage is more severe and extensive in the lesion centre **(Figure 88)** than in its peripheral area **(Figure 87)**. This can be seen in the:

(1) outer segments, and the greater number of OS disks packets within the RPE **(Figure 88)**. Note swollen, enlarged, vesiculated and necrotic OS in Figure 88;

(2) RPE necrosis;

(3) the extent of the vacuolization in the RPE;

(4) large lipofuscin granules and melanolysomal bodies;

(5) greater vacuolization at the RPE-Bruch's membrane (BM) border;

(6) mitochondria which can be distinguished in **Figure 87** but not in Figure 88;

(7) BM, in which there is greater focal densification in **Figure 88.**

Note: RPE cell with a 'tongue' extending in towards the lesion centre (left-hand margin, **Figure 88**); the cell process in BM vitreal to the endothelium; in the choriocapillaris leukocytes and sparse electron-dense globules.

Plate 36 **Rhesus retina light-adapted,** for 3 3/4 hours in the morning. Four hour-old lesion **λ** 532 nm. Temporal, in the peripheral fundus

Figure 89 (x 3,000) Montage

Normal outer segment (OS) are seen abutting on the RPE apical surface, which has extrusions into the subretinal space. Apical microvilli are present in places. Terminal bars can be seen at the apical RPE border. Two RPE nuclei are necrotic. Swollen, reduced and distorted basal infolds are present. Mitochondria are elongated especially alongside and parallel to the lateral cell membranes. Lipofuscin granules are abundant. Bruch's membrane contains electron-dense material.

Plates 37 - 39 Dark-adapted for 1 1/2 hours, at mid-day. 1 hour lesion.
λ 532 nm.

Plate 37 Rhesus retina dark-adapted for 1 1/2 hours at mid-day. One hour-old lesion in the periphery, superior to the macula. λ 532 nm.

Figure 90 (x 2,000) Montage

Photoreceptor inner segments (IS) and outer segments (OS), RPE and choroid.

Most of the IS are swollen and contain swollen mitochondria. The cone OS are less damaged than are the rod OS; and the cone IS mitochondria also appear to be more resistant than the rod IS mitochondria. OS are in disarray. Packets of OS disks can be seen at the RPE apical border. Apical microvilli are sparse. The RPE is reduced in height, parts are hypopigmented and other parts have denser cytoplasm and many lipofuscin granules are present, some of which appear fragmented. One nucleus (near right-hand margin of the micrograph) is necrotic. The mitochondria are swollen, and basal infolds are absent.

Plate 38 Rhesus retina dark-adapted for one and half hours, mid-day. One hour lesion, λ 532 nm, inferior in the peripheral fundus (see Plate 39, same lesion).

Figure 91 (x 8,400) Basal RPE, Bruch's membrane (BM) and choroid

The basal RPE is necrotic. The basal lamina of BM at the choroidal surface is indistinct. One cell in the choroid shows necrotic changes in the nucleus and cytoplasm; another shows necrotic pyknotic cytoplasm and many vacuoles.

Figure 92 (LM x 1,500)

There is bleeding within the retina (outer plexiform and inner nuclear layers). Photoreceptors including their nuclei are pyknotic.

Figure 93 (x 3,400) Montage from the edge of the lesion towards its centre

The right-hand margin of the micrograph shows a normal RPE cell with a tongue extending along Bruch's membrane (BM). The cell next to it has vesiculated cytoplasm. The other RPE cells are more severely necrotic, with vacuoles along the BM-RPE border, cytoplasm fragmented with many cystic spaces and many melano-lipofuscin bodies, lysosomes and melanolysosomes. Only a few microvilli (AMV) are present, but there are whorls of membrane at the apical RPE surface, probably derived from the AMV. The choroid is cystic.

Plate 39 Rhesus retina dark-adapted for 1 1/2 hours, mid-day. One hour lesion, inferior in the peripheral fundus. λ 532 nm
[see Plate 38 - same lesion]

The series illustrates the different appearances of parts of the same lesion.

Figure 94 (x 2,500)

Outer segments (OS) are in disarray, convoluted, and show disorganization and pyknotic staining of disks, creating in some OS an irregular banded appearance. Phagosomes are present in the apical cytoplasm of the RPE. Only a few microvilli and basal infolds (BI) remain; some mitochondria are very elongated. Melanin granules are in the RPE. The lumen of the choriocapillaris (CC) is congested and contains many platelets. The choroid contains cystic spaces.

Figure 95 (x 6,300)

Enlargement of part of **Figure 94.**

The BI are sparse and there are electron-dense inclusions in Bruch's membrane (BM) and the apparent absence of the BM basal lamina, on its inner margin at the CC. The endothelium is fenestrated.

Figure 96 (x 2,500)

Part of the lesion shows damaged RPE with apical phagosomes, no microvilli and no basal infolds, and many vacuolar spaces. The CC contains leukocytes. The choroidal melanocytes contain cystic spaces, clumped melanin granules (MG) as well as loss of MG.

Plates 40 - 53 Rhesus retina one day-old lesions, 532 λ in the macula, 1064 λ in the periphery of the fundus, around the macula.

One eye was **light-adapted** and exposed to light in the morning after 3 1/2 hours in the light; the other eye was **dark-adapted** and exposed to laser light in the early afternoon, after 3 1/2 hours in the dark.

Plate 40 Rhesus retina light-adapted, all figures from are from a single, one day-old lesion (1064 λ).

Figure 97 (LM x 1,900)

Lesion in the inferior peripheral retina, on the macular border.

The lesion creates a hump in the retina towards the vitreous. The cone nuclei stain lightly, the rod nuclei stain deeply. Some rod inner segments (RIS) are pyknotic. Outer segments (OS) are disarrayed and contorted and there is a space between the RPE and the OS.

Figure 98 (LM x 1,200)

The inner nuclear layer is intact, but some of the synaptic spherules are pyknotic. The RPE is hypopigmented (as in Figure 97).

Figure 99 (x 2,900)

The RPE displays swollen apical microvilli with melanin granules (MG) and condensations of interphotoreceptor matrix at the apical border of the RPE. The RPE contains a large phagosome; the nucleus is shrunken; the basal RPE contains a row of cystic spaces. Bruch's membrane contains electron-dense material.

Figure 100 (x 2,900)

RPE. The microvilli are retracted and MG are seen inside the cell. There is a prominent terminal bar, and cystic spaces among the lipofuscin granules. Basal infolds are swollen or absent. Elongated mitochondria in parallel array are present.

Plate 41 Rhesus retina, light-adapted one day-old lesion in the superior periphery (λ1064)

Figure 101 (x 1,300)

Control for lesion illustrated in **Figures 102, 103 and 104.**

Many inner segments and outer segments (OS) are swollen. In many of the OS, the disks are in disarray, pyknotic and some disks form whorled figures. Condensations of interphotoreceptor matrix can be seen as structureless grey material around some OS.

Figures 102 (x 1,300)

The basal lamina in the lesion centre is denuded and large cystic spaces extend from Bruch's membrane (BM) into the subretinal space to the outer segments. Some RPE cells abut on the large cystic spaces and not on BM. There are also small cystic spaces within the basal RPE. The choroidal capillaries are congested.

Figure 103 (LM x 3,000)

The outer segments show many of the features displayed in the control tissue **(Figure 101)**, but the extent of the changes is greater and many cystic spaces are present.

Figure 104 (x 4,000)

Detail of cystic spaces, in the subretina, between the outer segments and the remains of the apical RPE, devoid of microvilli. One cystic space is empty; the other contains pale flocculent material.

Plate 42 Rhesus retina, light-adapted Controls for the lesion (inferior, peripheral) illustrated on **Plate 40.**

Figure 105 (x 2,700)

Figure 108 (x 2,800)

Note the congested choriocapillaris. In the RPE there are apical microvilli, phagosomes, prominent terminal bars, abundant lipofuscin granules, dense endoplasmic reticulum and mitochondria (mainly basal). Outer segments are closely associated with the apical border of the RPE.

Figure 106 (x 3,500)

Inner segments, outer limiting membrane, and cone and rod nuclei. Cystic spaces are present. Two cone nuclei are necrotic.

Figure 107 (x 2,500)

Some outer segments are swollen and/or convoluted and contain disks that are in disarray.

Plate 43 Rhesus retina, light-adapted one day-old lesion (1064λ) in the temporal periphery.

Figures 109 and 110 (x 2,000)

There are cystic spaces between RPE and outer segments (OS), and small cystic spaces can be seen in the RPE at Bruch's membrane. The melanin granules are apical in retracted microvilli. OS are swollen with disarrayed and necrotic disks. Lipoidal globules are present, and surround the nucleus. Bruch's membrane has pyknotic inclusions.

Figure 111 (x 2,700)

Swollen outer segments (OS) show disks in disarray, pyknotic, with whorls of disks, and empty OS portions.

Figure 112 (x 2,000)

The RPE cell shows melanin granules apically (in disarrayed apical microvilli). Terminal bars are present. The lipofuscin granules occupy a central position. Basal infolds are absent in the basal RPE. There are small cystic spaces in the RPE.

Plate 44 Rhesus retina, light-adapted controls for one day-old lesion (1064λ) in the temporal periphery **(Plate 43)**

Figures 113, 114 and 115 (x 2,700)

Figure 116 (x 2,000)

Note the close association of the outer segments (OS) and RPE, and large phagosomes in the apical RPE. Hemidesmosomes are abundant **(Figure 113).** Some outer segments are swollen and disks are absent, or disarrayed, or whorled **(Figures 114, 115).** Some inner segments have swollen mitochondria **(Figure 115).** The choriocapillaris is congested **(Figures 113 and 116).** Lipofuscin granules occupy all but the basal region of the RPE and the apical microvilli.

Plate 45 Rhesus retina, light-adapted one day-old lesion (λ1064) in the nasal periphery

Figures 117 - 120 - light adapted

Figures 121 and 122 - dark-adapted

Figure 117 (x 2,000)

A portion of the RPE cell is separated off in the subretinal space. It contains melanin granules, lipofuscin granules and coagulated cytoplasm, and between this structure and the basal RPE a terminal bar can be seen. Bruch's membrane has electron-dense contents. Disarrayed outer segments (OS) are present.

Figure 118 (x 14,000) and Figure 119 (x 6,700)

The RPE. Note: the terminal bar, the retracted apical microvilli without melanin granules, a large phagosome (Figure 118) and a portion of extruded necrotic RPE seen on the left-hand side of photograph in Figure 118) and bottom right hand corner in Figure 119.

Figure 120 (x 4,000)

Details of the RPE - OS zone. Note: swollen empty OS and pyknotic disks, alongside normal OS abutting on the RPE and the extruded melanin granules and areas of condensed interphotoreceptor matrix.

Figure 121 (x 2,000)

There are large cystic spaces between the RPE and the OS, at the basal RPE and within the RPE cell. Note the large phagosome.

Figure 122 (x 4,000)

Detail of Figure 121, showing the basal cystic spaces, some necrotic mitochondria, the congested choriocapillaris and swollen endothelium.

Plate 46 Rhesus retina, light-adapted one day-old lesions (λ 1064 nm).

Figure 123 (x 3,000) λ 1064 nm, in the superior fundus.

The lesion has torn the RPE and Bruch's membrane is denuded in places. Large vacuolar spaces are seen in both the basal and apical RPE in the lesion centre. Smaller vacuoles, basal in the RPE, are seen at both sides of the lesion centre. The outer segments are more severely disarranged proximally than distally. This lesion measured 185 μ in the RPE.

Figure 124 (x 3,000) λ 532 nm, in the superior border of the macula.

This lesion measured 360 μ in the RPE. Both proximal and distal parts of the outer segments are in disarray. Large 'bubble-spaces' are seen between the necrotic apical RPE and the outer segments. Vacuolar spaces are present in the basal RPE where parts of Bruch's membrane are denuded. The choriocapillaris is abnormal.

Plate 46 A Rhesus retina, light-adapted one day-old lesion (λ 532) in the superior macula; and control.

Figures I and III one day-old lesion

Figures II and IV control area

Figure I (x 1,320)

Most of the RPE is separated from Bruch's membrane (BM) and in the centre the RPE is discontinuous. Large cystic spaces can be seen at Bruch's membrane and between the separated RPE and the outer segments (OS). The OS are considerably disrupted. One pyknotic inner segment can be seen in the right-hand lower part of the photograph.

Figure III (x 3,400)

Detail of choriocapillaris (CC), Bruch's membrane (BM) and RPE. The CC contains erythrocytes and a leukocyte. The endothelium is present only as a thin line, and the basal lamina of the inner side of BM is not apparent. A thin irregular strip of RPE cell extends between BM and the large cystic space, but is absent at the base of the photomicrograph.

Figure II (x 3,000) and **Figure IV** (x 5,600)

Controls. Many newly-shed OS disk packets (phagosomes) are present in the RPE or at the RPE surface (**Figure II**). Small cystic spaces are present especially in the basal RPE (**Figures II and IV**). BM has electron-dense material (**Figure II and IV**) and is similar to the BM seen in **Figure III**. The CC is congested, and necrotic (**Figure IV**). Cystic spaces can be seen in the choroid (**Figure II**).

Plate 47 Rhesus retina, light-adapted for 3 1/2 hours in the morning. One day-old lesion, λ 532 nm, in the foveal centre

Figure 125 (x 2,200) Montage

The damaged area in the RPE and outer segments (OS) is extensive. The RPE is disorganized and necrotic and small cystic, vacuolar spaces are present within the RPE.

Packets of OS disks are present in the RPE. Large cystic spaces line Bruch's membrane (BM), vitreally, and are present also in the RPE and among the OS. OS are in considerable disarray and many are swollen.

The choriocapillaris is very congested and the choroid itself shows necrotic changes.

Figure 126 (x 2,200)

The OS show a range of degenerative changes, as do the inner segments (IS), including swollen mitochondria, pyknotic mitochondria and pyknotic, coagulated cytoplasm.

Plate 48 Rhesus retina, light-adapted for 3 3/4 hours in the morning. One day-old lesion, λ 532 nm, in the fovea (as in Plate 47)

Figure 127 (LM x 1,300)

There is a humping of the outer retinal layers and large cystic spaces occupy a space between Bruch's membrane (BM) and the RPE, which is largely detached from BM. There are also cystic spaces between the RPE and the outer segments (OS). Note the pyknotic photoreceptor nuclei and inner segments, as well as OS in disarray.

Figure 128 (x 3,600)

The outer nuclear layer displays several necrotic, pyknotic nuclei and general necrosis and disorganization.

Figure 129 (x 6,700)

A magnified portion of the right-hand side of micrograph **Plate 47, Figure 125,** showing the large cystic spaces, with flocculent contents, in the basal RPE, resting either on a thin layer of RPE or directly on BM. The choriocapillaris shows portions of fragmented swollen and discontinuous endothelium, and necrotic changes.

Plate 49 Rhesus retina, light-adapted for 3 3/4 hours in the morning. One day-old lesion, λ 532 nm, on the temporal margin of the macula

Figure 130 (LM x 1,300)

Instead of the usual humping of the lesion resulting in a convexity of the outer limiting membrane, this lesion displays a concavity. The margin of the lesion in the RPE can be seen clearly to the right of centre of the photograph yet further to the right there is pyknosis of inner segments, rod nuclei and Henle fibres as can also be seen in the centre and at the far left of the photograph. There are cystic spaces between the RPE and outer segments (OS) and between RPE and Bruch's membrane.

Figures 131 and 132 Controls for lesion shown in **Figure 130.**

Figure 131 (x 3,800)

Swollen OS contain disorganized disks (D), spaces devoid of D, and pyknotic D. Some OS are not swollen, one OS is convoluted. The inner segment apex (at the upper right-hand side of photograph) is devoid of mitochondria, and its OS contains a whorl of OS D.

Figure 132 (x 3,400)

A continuation of **Figure 131,** showing a few OS closely abutting on the RPE apical surface. Melanin granules and a phagosome are in the apical microvilli. The RPE shows normal polarity. Bruch's membrane is electron-dense, and there are cell processes in BM.

Plate 50 Rhesus retina, light-adapted for 3 3/4 hours in the morning. One day-old lesion, λ 532 nm, on the temporal margin of the macula (same lesion as Plate 49)

Figure 133 (x 9,400)

Details of four photoreceptors. The inner segments (IS) contain swollen pale mitochondria, empty; or with remains of cristae; or small rounded dark-staining mitochondria, with cristae, and electron-dense spots. The cytoplasm of the IS is cystic, swollen, dark-staining. Remains of a striated rootlet are present in the middle IS.

The outer segment (OS) disks (D) are in disarray and the middle OS has vesiculated D. The interphotoreceptor matrix is condensed around some parts of the photoreceptors.

Figure 134 (x 3,800)

Detail of the RPE and Bruch's membrane (BM). The RPE is torn cystic and necrotic. Apical microvilli and basal infolds are absent. The normal polarity of the RPE is disturbed. Large lipofuscin granules (LG) and small electron-dense globules (EDG) can be seen in the basal RPE.

Figure 135 (x 7,000)

Basal RPE, Bruch's membrane and choroid. The RPE contains many electron-dense bodies (lipofuscin); mitochondria; cystic spaces; 2 nuclei; a junctional complex; and near Bruch's membrane (BM) a membranous body which resembles an outer segment phagosome. Basal infolds are absent. BM contains vesicles and electron-dense material. The choriocapillaris is lined by discontinuous and fragmented endothelium and the lumen is occluded

Figure 136

The basal RPE is cystic, lacks basal infolds, and small electron-dense globules (EDG) are present, in addition to lipofuscin.

The choriocapillaris is lined by thickened endothelium, and contains cell processes and one large necrotic body.

Plate 51 Rhesus retina, light-adapted for 3 3/4 hours in the morning. One day-old lesion, λ 532 nm, on the nasal margin of the macula.

Figure 137 (LM x 1,500)

The lesion produces a hillock-hump in the retina towards the vitreous. The outer segments (OS) are disorganized. Cystic spaces can be seen between the RPE and OS. There are apical microvilli (AMV) with melanin granules (MG). Some RPE nuclei are pyknotic.

Figure 138 (x 3,400)

The apical RPE has retracted apical microvilli (AMV) containing melanin granules. A prominent terminal bar is present. One outer segment is inserted into the apical RPE, and another in the subretinal space is swollen and disorganized.

Figure 139 (x 5,000)

Apical RPE, with outer segment packets (one of them disorganized), fragmented AMV and condensations of interphotoreceptor matrix.

Figure 140 (x 3,800)

Inner segments with swollen mitochondria and apical centrioles. Outer segments are disorganized.

Plate 52 **Rhesus retina, light-adapted** for 3 3/4 hours in the morning. One day-old lesion, λ 532 nm, on the inferior margin of the macula

Figures 141, 142 and 143 are three views of the same lesion.

Figures 141 and 142 (LM x 1,500)

Figures 141 and 142 show inner segment pyknosis.

Figure 143 (LM x 2,000) (same as **Figure 142**).

Note that the lesion appears concave in **Figure 141** and convex in **Figures 142 and 143.** In **Figure 141,** there are a few pyknotic cone nuclei. In **Figures 141 and 142,** there are many pyknotic rod nuclei. There is disorganization of the outer segments (OS) and cystic spaces in subretina and between the RPE and Bruch's membrane (BM) **(Figures 141 - 143).**

In **Figure 143,** there are small cystic spaces in the basal RPE at Bruch's membrane. A few RPE nuclei are pyknotic. The melanin granules, while apical in position in the RPE, are more vitreal than is usual.

Plate 53 Rhesus retina one day-old lesions λ 532 nm, on the *inferior margin* of the macula

Figure 144 (LM x 1,500)

Dark-adapted for 3 3/4 hours at mid-day.

The basal RPE has cystic spaces at the border with Bruch's membrane (BM). Despite the changes, the melanin granules (MG) are positioned apically. Large cystic spaces are seen between the RPE and the outer segments (OS). OS are somewhat disarrayed. Some rod nuclei are pyknotic.

Figure 145 (x 2,200) Montage

Light-adapted, 3 3/4 hours in the morning.

Note the similarities with **Figure 144**; basal RPE with small cystic spaces at the BM border, and MG are present in the apical RPE. Large spaces are seen between the RPE and the OS.

Plate 54 Rhesus retina one day-old lesions, λ 532 nm, on the inferior margin of the macula

Figures 146 and 147 dark-adapted for 3 3/4 hours mid-day.

Figures 148 and 149 light-adapted for 3 3/4 hours in the morning.

Figure 146 (x 3,400)

In the RPE, there is a large cystic space containing structures that resemble the apical microvilli (AMV). There are no basal infolds. Terminal bars are present. The apical RPE in particular is necrotic. The outer segments are in disarray and disorganized, and some are swollen.

Figure 147 (x 5,000)

Apical RPE displays some AMV. An extruded portion of RPE, contains necrotic, coagulated cytoplasm, melanin granules, and lipofuscin granules.

Figure 148 (x 12,500)

Basal RPE, Bruch's membrane (BM) and choroid.

The sparse basal infolds are swollen. BM contains electron-dense material. There is no choriocapillaris abutting on BM. Basement membrane material surrounds a large structure in the choroid containing parts of cells, and debris.

Figure 149 (x 6,300)

Basal RPE and necrotic choroid with no choriocapillaris present. Necrotic materials and debris and fragments of choroidal melanin granules are present.

Plate 55 **Cynomolgus retina** **constant light for 26 hours** before first exposure to laser, one day-old lesion, λ 1064 nm, on the temporal border of the macula

Figure 150 (x 2,500) Montage

The outer segments (OS), RPE, Bruch's membrane, and choroid. Some of the OS are disorganized. The RPE is disorganized, necrotic, cystic, and layered.

The choriocapillaris (CC) is not patent and the choroid, near the RPE, shows disorganization and necrotic changes. Towards the bottom of the micrograph the choroid appears more normal.

Plate 56 Cynomolgus retina constant light for 26 hours before first exposure to laser, one day-old lesion, λ 1064 nm, on the temporal border of the macula

Figure 151 (x 2,500) Montage

This is a continuation of the lesion shown in **Figure 150.**

The choroid immediately below Bruch's membrane shows the same degenerative changes across the entire extent of the lesion, as seen in **Figure 150.**

Bruch's membrane (BM) has a regular border with the RPE and the basal lamina can be seen. On the choroidal surface of BM, the basal lamina is not apparent throughout. BM contains electron-dense material, and looks "moth-eaten" in places.

The RPE is necrotic, pyknotic in its apical parts. Portions of RPE, apically, have separated from basal RPE. These separated portions contain coagulated cytoplasmic matrix, melanin granules, lipofuscin granules, packets of outer segment (OS) disks, cystic spaces. There is also a large space which appears as a tear in the interphotoreceptor matrix (IPRM). Condensations of IPRM can be seen below this clear space between two clumps of separated apical RPE portions. Apical microvilli are absent except at the edge of the lesion on the right-hand edge of the photograph.

Cynomolgus retina, one day constant light for 26 hours. Temporal border of the macula

Plate 56 A (x 2,500) Montage

Control for lesion displayed in **Plates 55 and 56.**

The basal RPE, in the upper left-hand corner, is normal, as in Bruch's membrane. Note that the basal lamina on the RPE side is far wider and clearer than is the basal lamina on the choroidal side. The choriocapillaris is clearly displayed. In the choroid, some melanocytes are deeply staining and one contains lipoidal bodies.

Plates 57 and 58 Cynomolgus retina, constant light for 26 hours before exposure to λ 1064 nm laser. The same one day-old lesion in the nasal periphery of the fundus.

Plate 57

Figure 152 (x 3,700)

In the lesion, 6-8 cells away from the lesion centre. The RPE, Bruch's membrane (BM) and the choriocapillaris (CC). Apical microvilli (AMV) contains melanin granules (MG). MG are also present in the apical RPE. The basal infolds (BI) are swollen or absent. Terminal bars, mitochondria, lipoidal globules and lipofuscin granules (LFG) can be seen in the RPE. One very large electron-dense inclusion in the RPE contains membranes similar to those of outer segment (OS) disks (D). In the RPE, on the right-hand side of the photograph, are two smaller electron-dense bodies which include membrane-like whorls. There are parts of the endoplasmic reticulum (ER) which show electron-dense "pinched" profiles.

The endothelium on the retinal side of the CC is thin and fenestrated. The endothelium on the choroidal side appears multi-layered.

Figure 153 (x 6,800)

In the lesion 3-4 cells away from the lesion centre. There are only a few small AMV. The RPE cytoplasm appears darker and denser, and the ER shows more "pinched" profiles than are seen in Figure 152. Very few BI are present.

Three large electron-dense inclusions can be seen towards the basal RPE. Each contains a very dense core and rim, between which are membrane-like whorls of membranes.

Figure 154 (x 6,800) The lesion centre

Very large structures (at the top of the micrograph) are swollen, disorganized OS and their D. The RPE appears to be three-layered: (a) basally there is a saucer-shaped cell, with ER, devoid of BI and separated by membrane material from (b) a portion of the RPE cytoplasm coagulated and containing LFG, a few mitochondria (with electron-dense inclusions) and many melano-lipofuscin granules. The disordered OS abut on (b), and (c) a membrane-bounded portion of the RPE (on the left-hand side of the photograph) which appears devoid of cell organelles.

BM is intact and both its basal laminae are well-developed (as in Figure 153).

Figure 155 (x 19,000)

In the outer segment area, a large collection of debris, membranous material, flocculent cytoplasm and lipofuscin granules.

Plate 58 Cynomolgus retina (same lesion as shown in **Plate 57**)

In the nasal periphery of the fundus (λ 1064 nm)

Figure 156 (x 5,400)

Four of the five inner segments (IS) contain elongated mitochondria. The IS on the extreme left of the photograph contains striated rootlets. The central IS, devoid of mitochondria, contains some electron-dense membranous material. Its outer segment has no typical disks (D) and has two electron-dense globules. One outer segment (OS) contains a large whorled arrangement of D.

Figure 157 (x 3,400)

IS from the outer limiting membrane (OLM) to OS. Two of the IS are necrotic. One of these is disintegrating (on the right-hand side), and the other contains D-like membranes at its apex. Its OS contains 3 electron-dense globules similar to two in **Figure 156.** Vitreal to the OLM, the Muller cells contain electron-dense material.

Figure 158 (x 5,400) RPE and choroid in the lesion

The RPE is two-layered. Its apical part consists of extruded coagulated cytoplasmic matrix, melanin granules and lipofuscin granules. The basal part is less disorganized, bears remnants of apical microvilli, contains "pinched" endoplasmic reticulum profiles, some mitochondria and lipoidal globules, but lacks basal infolds.

Bruch's membrane has a "moth-eaten" appearance. The choriocapillaris is very disorganized; the endothelium is not apparent; the lumen is occluded but not with blood cells.

Figure 159 (x 2,700)

The choroid displays degenerative changes with densifications, pyknosis and vacuolisations.

Plates 59 and 60 Cynomolgus retina, constant light for 26 hours before exposure to λ 532 nm laser. One day-old lesion in the temporal periphery of the fundus

Plate 59

Figure 160 (x 5,400)

Most of the inner segments and outer segments (OS) show degrees of disorganization and necrotic changes.

Figure 161 (x 10,000)

The inner segment (IS) is disorganized. It contains dark staining mitochondria with prominent electron-dense inclusions. There are 14 structures with electron-dense rims which contain whorls of membranes. The neighbouring IS is not severely affected.

Figure 162

The RPE in the lesion periphery contains two large packets of OS disks. RPE basal infolds are much reduced, and the apical microvilli are either reduced or disorganized. "Pinched" profiles of endoplasmic reticulum are present. OS abut on the apical surface of the RPE. The RPE cell on the upper left-hand margin of the photograph is reduced in height.

Figure 163 (x 18,000)

Coagulated cytoplasm of RPE overlies Bruch's membrane which appears both dense and "moth-eaten". Below Bruch's membrane lies a large clot of blood in the choroid.

Plate 60 Cynomolgus retina, constant light for 26 hours before exposure to λ532 nm laser light. One day-old lesion in the temporal periphery of the fundus. Same lesion as in **Plate 59.**

Figure 164 (x 3,000) Montage. Choroid and RPE

There are at least 10 large packets (of irregular shapes) of outer segment disks at or in the RPE, at its apical border. The RPE cell is coagulated and cystic. Lipofuscin granules, melanin granules and a very few mitochondria remain. There are no apical microvilli and no basal infolds. In places the RPE has lifted away from Bruch's membrane. The normal structure of the choriocapillaris has been destroyed, and its lumen is full of electron-dense debris. The choroid shows some damaged choroidal melanocytes, and cystic spaces.

Plate 61 Cynomolgus retina, continuous light for 26 hours prior to exposure to laser (λ 532 nm), one day-old lesion in periphery, nasal to the optic disc

Figure 165 (x 2,500) control

There are large packets of outer segments (OS) disks (D) in the RPE itself and one large and one small lipid globule is present. A whorl of pale D can be seen at the distal end of one OS.

Figure 166 (LM x 1,200)

The lesion creates an irregular apical RPE border. Cystic spaces can be seen in the hypopigmented RPE. OS are in disarray and some are pyknotic, as are also some cone inner segments and rod nuclei.

Figure 167 (x 5,000)

The RPE in the lesion centre is severely disorganized and layered. A basal portion of the RPE contains cystic spaces, lipoidal globules, and some mitochondria. Basal infolds (BI) and apical microvilli are absent. The more apical part of the RPE appears to be separated from the basal part. Its cytoplasmic matrix is coagulated and cystic. Some lipofuscin granules appear to be fragmented. Portions of RPE cells can be seen in membrane-bounded bodies in the subretina among swollen and disrupted OS which line the apical RPE.

Figure 168 (x 10,000)

In the basal RPE in the lesion there are many lipoidal bodies, a few mitochondria, and cystic spaces. Prominent in this photograph are units of whorls of membranous material with electron-dense cores and rims.

Plate 62 Cynomolgus retina, continuous light for 26 hours prior to exposure to λ1064 nm dose-fractionated, in the temporal macula. One day-old lesion.

Figure 169 (x 2,000) and

Figure 170 (x 2,000)

Bruch's membrane (BM) has "moth eaten" appearance. The RPE is so disrupted that much of BM is denuded. Portions of RPE cell material (with necrotic cytoplasmic matrix) lie free in the subretina, between BM and the outer segments (OS). These RPE cell portions contain melanin granules (MB), lipofuscin granules and mitochondria. Debris lies on BM on the RPE side. The OS are in disarray, and show pyknosis, swelling, vesiculation and disruption. The endothelium of the choriocapillaris appears to be intact, and the lumen is patent.

Figure 171 (x 4,000)

The inner segments (IS) are shown extending from their nuclei, and the outer limiting membrane (OLM). They contain the usual organelles, including many mitochondria. One IS contains a large unit of OS disks (D) in its proximal (vitreal) end, and a small whorl of OS D at its distal (scleral) end. IS (on the left) is necrotic.

Figure 172 (x 5,000)

Control for the above lesion. The proximal (vitreal) ends of the OS contain misaligned and whorled D.

Plate 63 **Cynomolgus retina** prior exposed to 26 hours of **continuous light** before delivery of λ 1064 nm, dose fractionated, in the fovea. One day-old lesion.

Figure 173 (x 2,800)

At the periphery of the lesion in the RPE, the boundary line of the lesion is in the centre of the photograph, with the lesion to the right. The lesion contains lipoidal bodies and very large cystic spaces and small cystic spaces, both within the RPE and on its apical border. Apical microvilli (AMV) and basal infolds (BI) are absent. To the left, the RPE bordering on the lesion bears AMV with melanin granules (MG), and BI are present. The endothelium of the choriocapillaris is thickened.

Figure 174 (x 4,000)

The inner segments (IS) are swollen and their mitochondria, instead of being mainly elongated, are mainly circular and dark-staining or swollen. There are many cystic spaces in the IS.

Figure 175 (x 4,00)

The apical RPE is wholly disrupted, its MG and lipofuscin granules, as well as some outer segments, are "exploded". Bruch's membrane (BM) is denuded and is lined, discontinuously, by electron-dense material.

Figure 176 (x 9,000)

The endothelium of the choriocapillaris shows many fenestrations and it has a thickened cell with a process projecting into BM, which has a "moth-eaten" appearance. The basal RPE is disrupted and contains a large cystic space, bounded by what appears a membrane.

Plate 64 Cynomolgus retina, continuous light for 26 hours prior to exposure to λ1064 nm. One day-old dose fractionated lesion in the nasal part of the macula.

Figure 177 (x 5,000)

Figure 178 (x 5,000)

The RPE is humped up apically in one part and thinned in another. The RPE is layered. The apical RPE is necrotic and contains melanin granules (MG), lipofuscin granules, and autophagic vacuoles. There are very few apical microvilli (AMV) and no basal infolds. The RPE contains empty cystic spaces. The basal RPE contains mitochondria. The outer segments and their disks are in disarray. Two tongues of RPE along Bruch's membrane (BM) almost meet in the centre of the photographs.

Figure 179 (x 24,000)

Details of the fenestrated endothelial cells, BM and basal RPE. The endoplasmic reticulum (ER) of the RPE is swollen and disrupted. Some ribosomes are present. Some of the mitochondria are elongated. Basal infolds are very sparse.

Figure 180 (x 24,000)

BM, basal RPE with a few basal infolds, one mitochondria, dispersed SER, and some ribosomes. There are two large empty cystic spaces. Electron-dense bodies near the cystic spaces are probably residual bodies.

Plate 65 Cynomolgus retina, dark-adapted, one day-old lesions from single exposures to λ1064 nm (except Figure 185, dose fractionated).

Figure 181 (LM x 1,200)

In the inferior periphery. The lesion appears hyperpigmented in the RPE. Inner segments and photoreceptor nuclei are pyknotic.

Figure 182 (x 2,000)

In the nasal periphery. Bruch's membrane (BM) is pyknotic. The RPE is layered; bordering BM there is a small pale basal region devoid of organelles and basal infolds (BI) and also a larger layer of slightly denser cytoplasm containing two phagosomes. Between this region and the apical necrotic RPE is a region of microvilli and a cystic space. The apical necrotic cytoplasm contains phagosomes and some melanin granules, but no apical microvilli (AMV).

Figure 183 (x 3,400) In the nasal periphery.

Some of the outer segments (OS) are convoluted and some are disrupted. The RPE is essentially similar to that shown in Figure 182, except that remains of AMV are present.

Figure 184 (x 15,000) In the nasal periphery.

There are large phagosomes with OS disks in this portion of separated RPE material, which also contains residual bodies, necrotic endoplasmic reticulum, and autophagic vacuoles.

Figure 185 (x 5,000) Dose fractionated. In the fovea.

Necrotic apical RPE, with apical microvilli scleral to it.

ADDENDA

ABSTRACT

ARVO Suppl. to Invest. Ophthalmol. Vis. Sci. 27(3) 1986, p 202, #74.

NEODYMIUM-YAG THRESHOLD AND SUBTHRESHOLD RETINAL LASER LESIONS

Bessie Borwein, Dept. of Anatomy, The University of Western Ontario, London, Ontario.

A pulsed Nd-YAG laser (wavelength 1.06 μ; output energy ≥ 100J/pulse; max. pulse rate frequency 20 pulses/sec.) was used on pigmented rabbits and cynomolgus monkeys. An ophthalmologist prior-examined all eyes. Animals were sedated and anaesthetized. Rabbits were killed 1 hour, 1 day, 4 days, 1 week and 25 days after exposure; monkeys 1 hour, 1 day. Experimental lesions (L) ranged from 0.15-0.4 x 10^{-5} J. Fundus photography revealed a few lesions at 1 hr and a few more at 1 day. Retinas were examined by light and transmission electron microscopy. L areas were compared to control areas nearby. One rabbit was prior dark adapted (DA) for 18 hours. The pigment epithelium (PE) and photoreceptors showed no differences compared to light-adapted retinas. For the same energy and spot sizes, no two lesions are identical. L shows graded damage from centre to periphery. Each L affects only a few pigment cells and related outer segments (OS); inner segments are less affected. In L basal infolds of the PE are much reduced in height, or absent, in L centres (C) but not peripherally; in rabbit the apical part of the PE cells humps up dramatically, in monkey "humping" is less pronounced; PE cells in LC are reduced in height or absent; within an affected PE cell three distinct strata develop, and the cells themselves may become multi-layered; PE cells shed into the subretinal space act as free macrophage and contain large phagosomes with OS discs (D), as do also PE cell in situ; shed packets of OS D often line the apical PE as a continuous border; junctional complexes of PE cells, mono- or multi-layered, are morphologically intact if the cell itself is not disrupted. In monkey retinas clear "bubbles" of space appear at the apical PR. PE microvilli disappear or seem inverted into the cell. Debris is sequestered at the basal PE and dense small particles are seen in the lumens of the choriocapillaries. In a monkey that had 29 L in the macula the entire area is rippled and all PE cells contain myriad small vacuoles. The experiment is being repeated to see if the number and proximity of the lesions create this condition. (Supported by USAMRD)

Abstract 2.

Proc. Canadian Federated Biological Societies Annual Meeting (CFBS) (Guelph) 29: p.213, June 1986.

B. BORWEIN. Department of Anatomy, University of Western Ontario, London, Canada. Subthreshold Nd-YAG laser lesions in mammalian retinas.

Small lesions were created in the maculae of anaesthetised cymologous monkeys and rabbit retinae by a pulsed Nd-YAG laser (λ 1064 nm). An ophthalmologist prior-examined all eyes. Animals were killed by injection 1 hr. and 1 day post-exposure. Retinae were examined by light and transmission electron microscopy. For same energy and spot sizes no two lesions (L) are identical. Each L affects only a small group of pigment epithelium cells (PE) and related outer segments (OS) of the photoreceptors; inner segments are less affected. If PE cells are not disrupted in the L, the PE junctional complexes are morphologically intact. The PE basal infolds are reduced or absent in the L centres (C) but not in the L periphery (P). L show graded damage from LC to LP. Debris is sequestered at the basal PE and dense small particles are seen in the choriocapillaries. Affected PE cells develop three distinct internal strata and the PE itself may become multilayered. In rabbit, in the LP PE cells hump up markedly into the subretinal space (SRS); in monkey, less so. In the LC PE cells are reduced in height or absent. In monkey clear bubbles appear in the SRS at the apical PE. PE cells are shed into the SRS and there act as scavengers. Shed OS discs often line the apical PE as a continuous border. PE microvilli are absent, reduced or appear to be inverted into the cell. (Supported by USAMRDC)

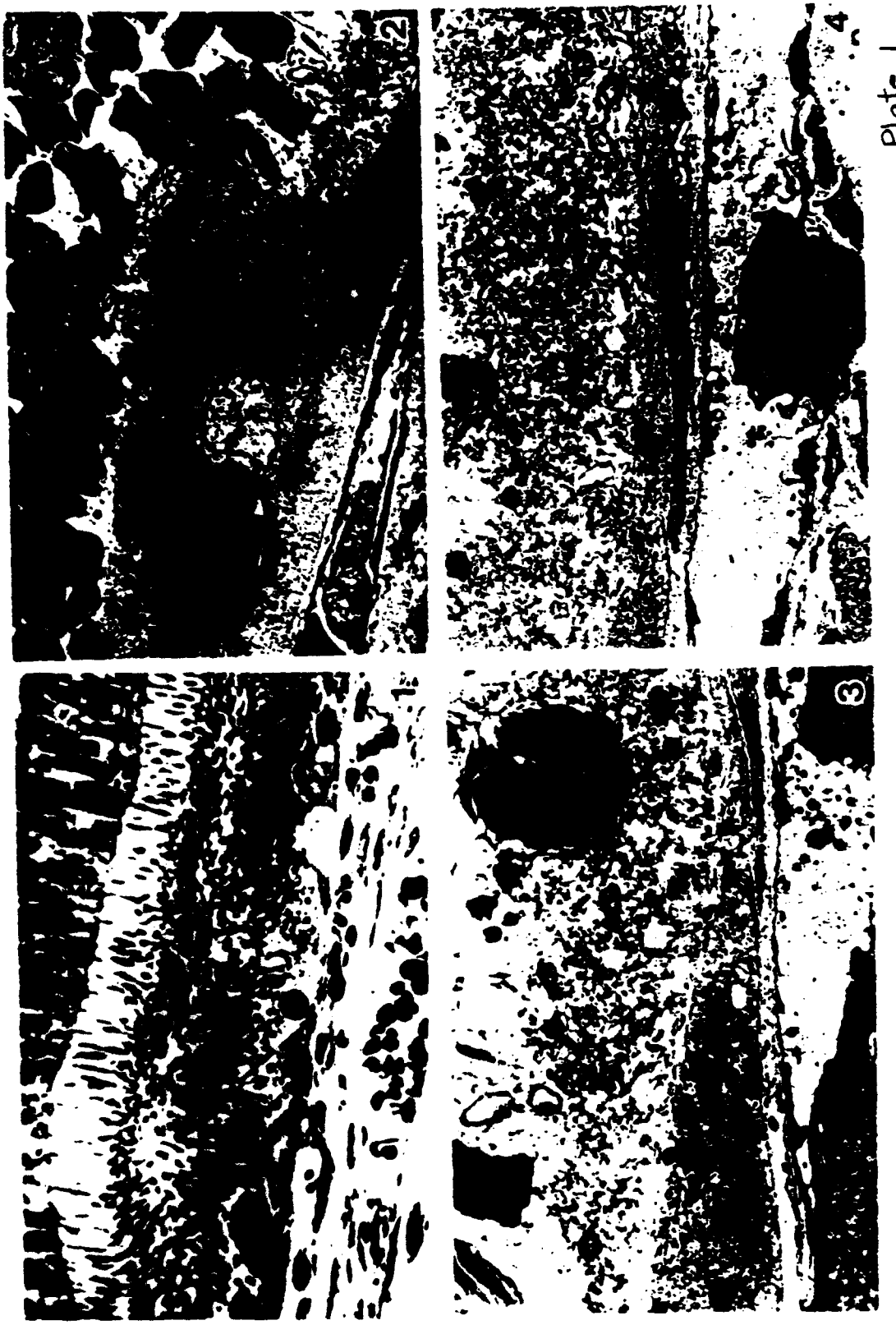

Plate I

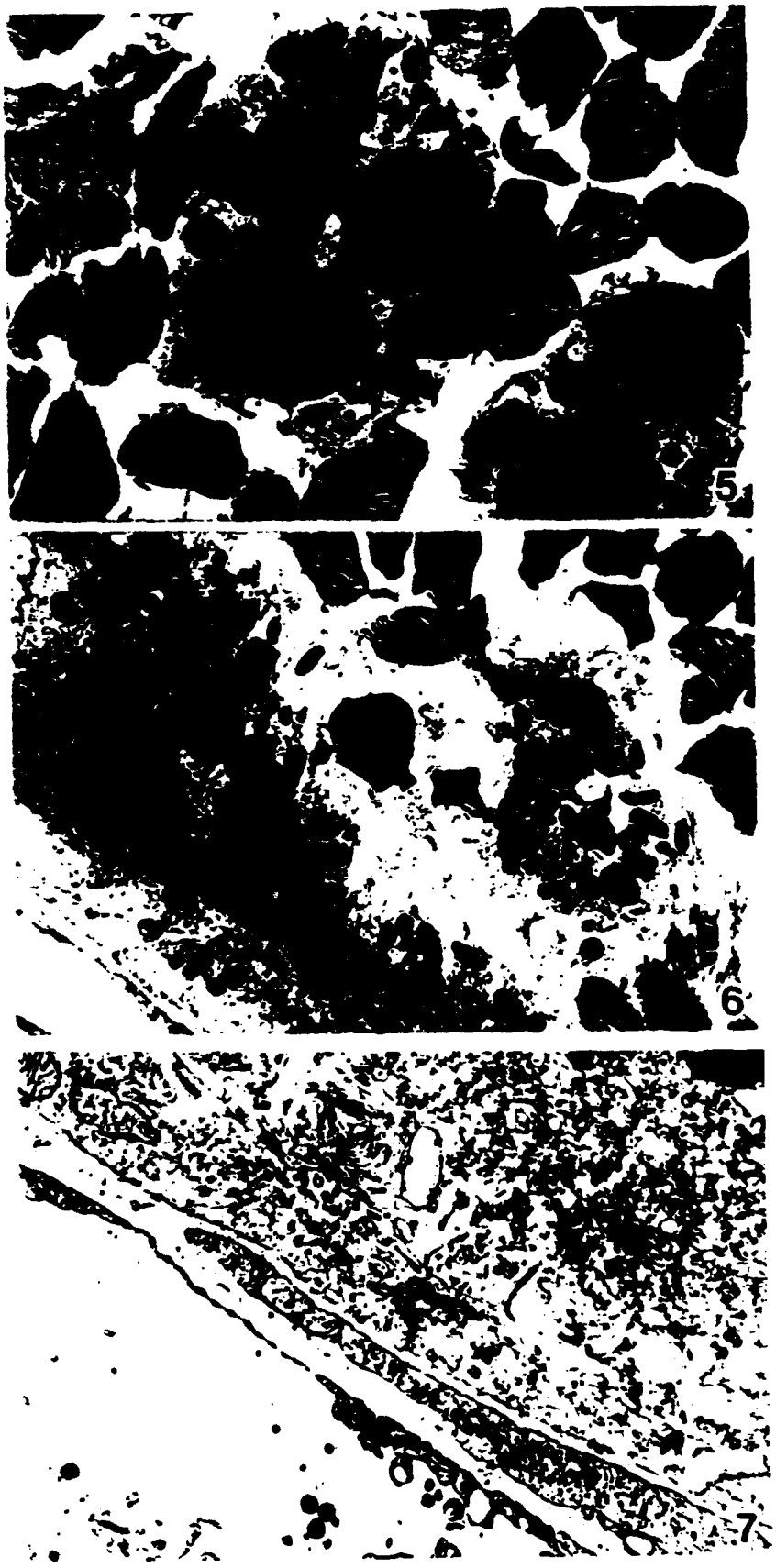

Plate 2

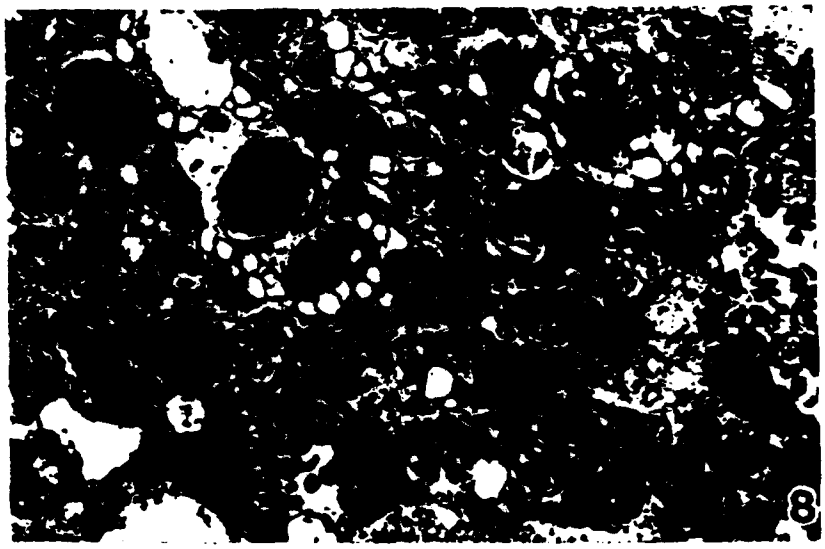

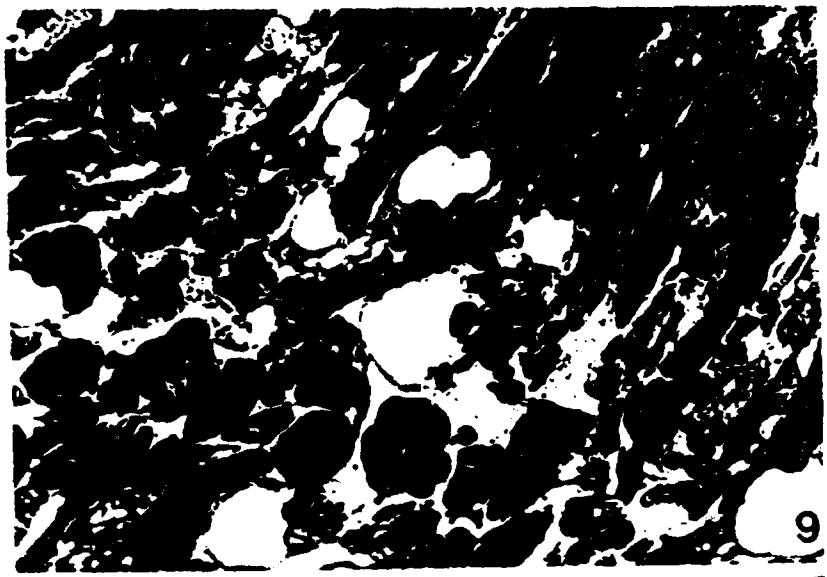

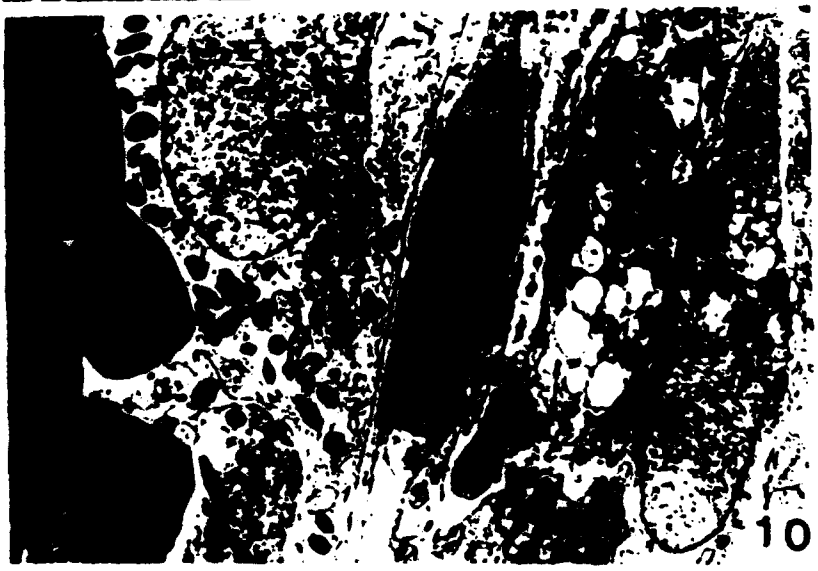

Plate 3

Plate 4

Plate 5

PLATE 6 INTENTIONALLY OMITTED


Plate 7

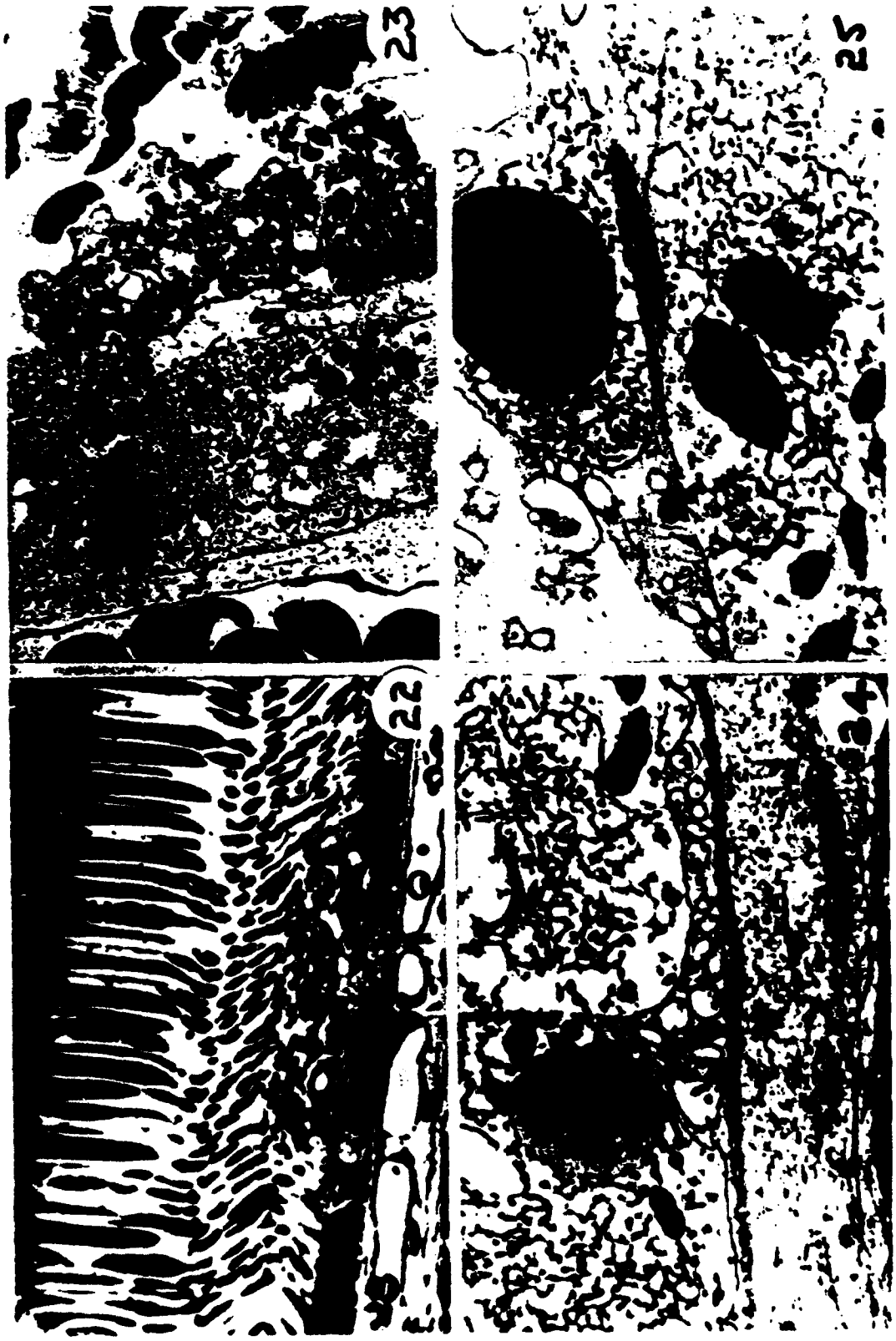

Plate 8

Plate 9

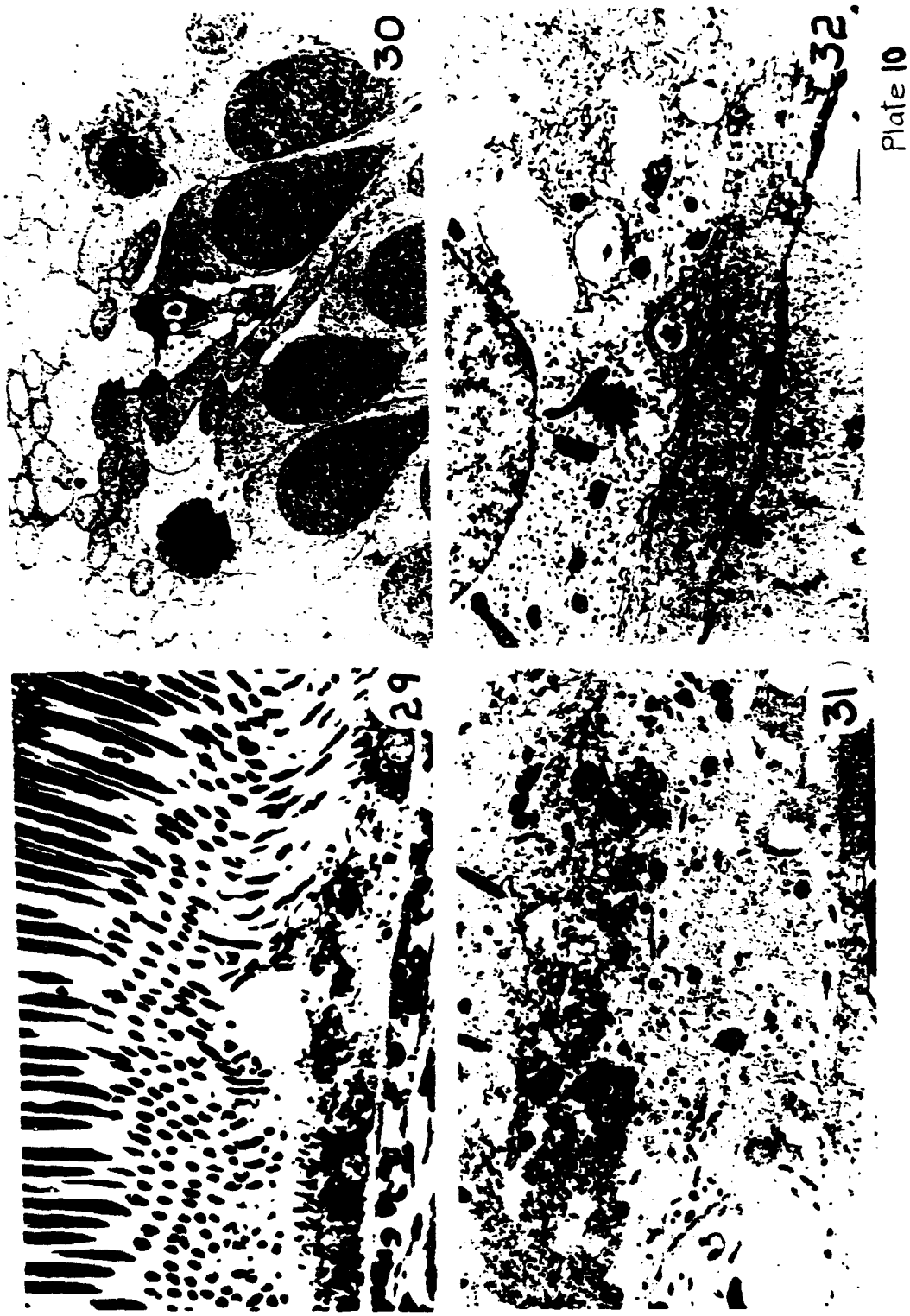

Plate 10

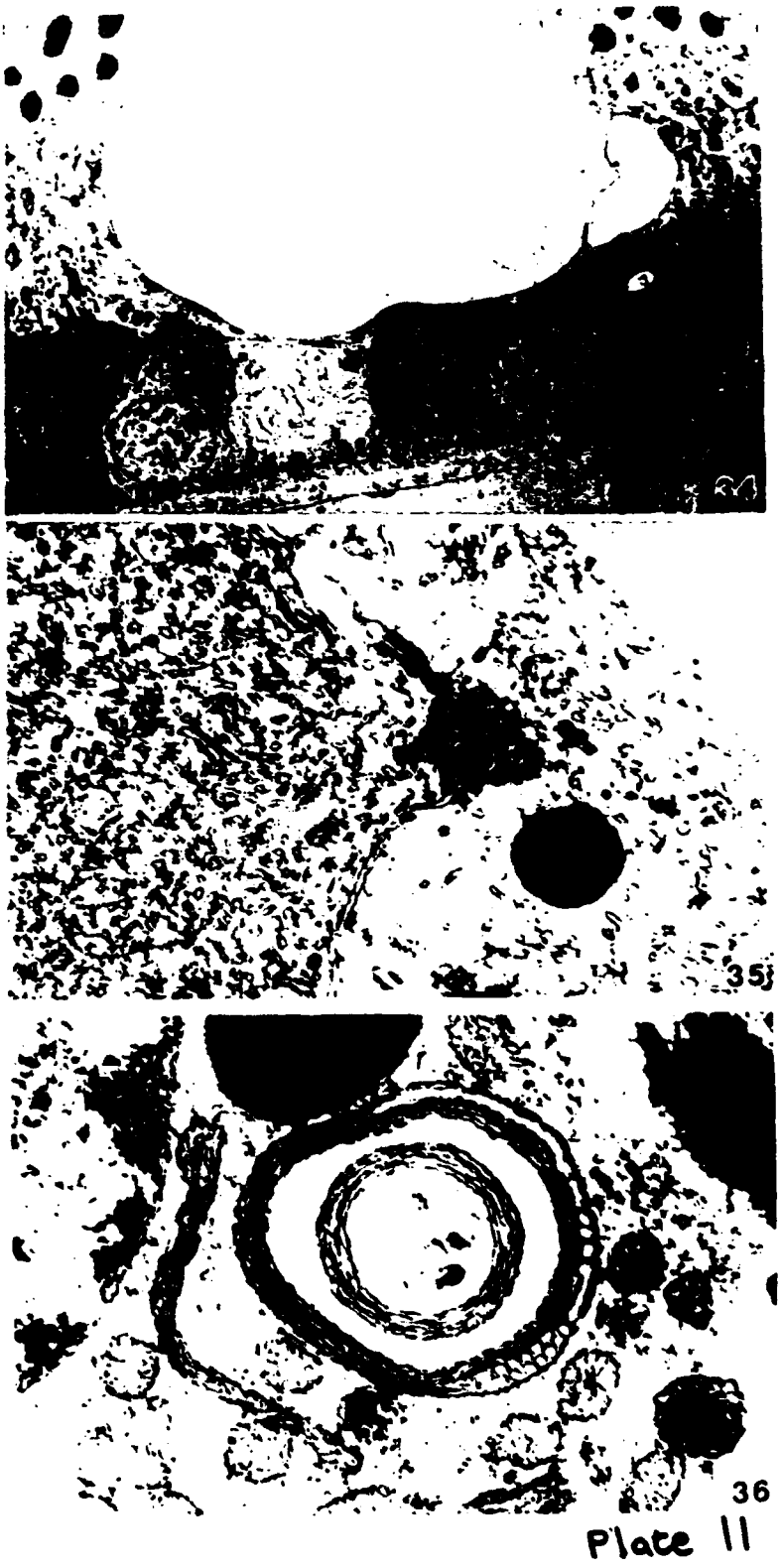

Plate II

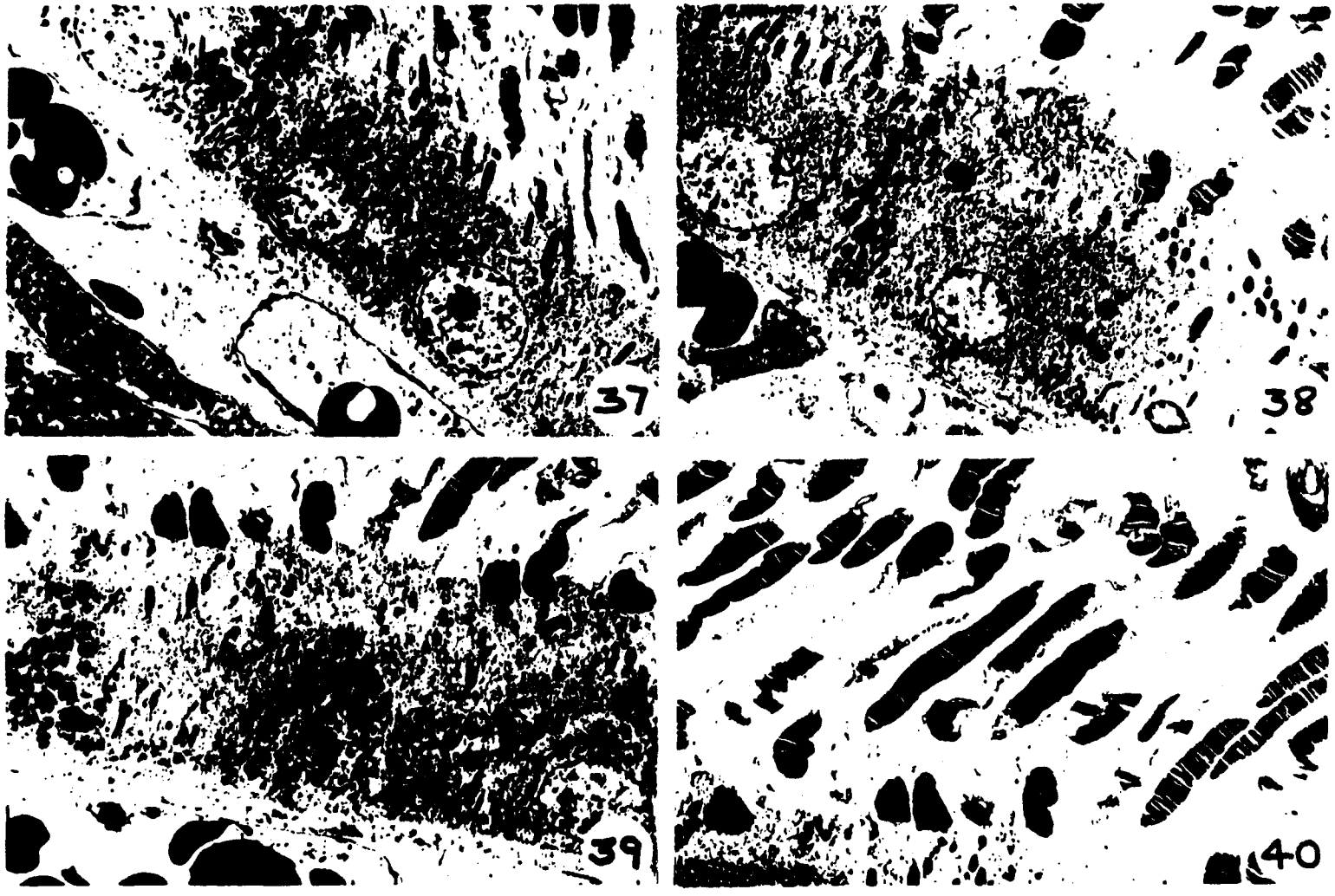

Plate 12

Plate 13

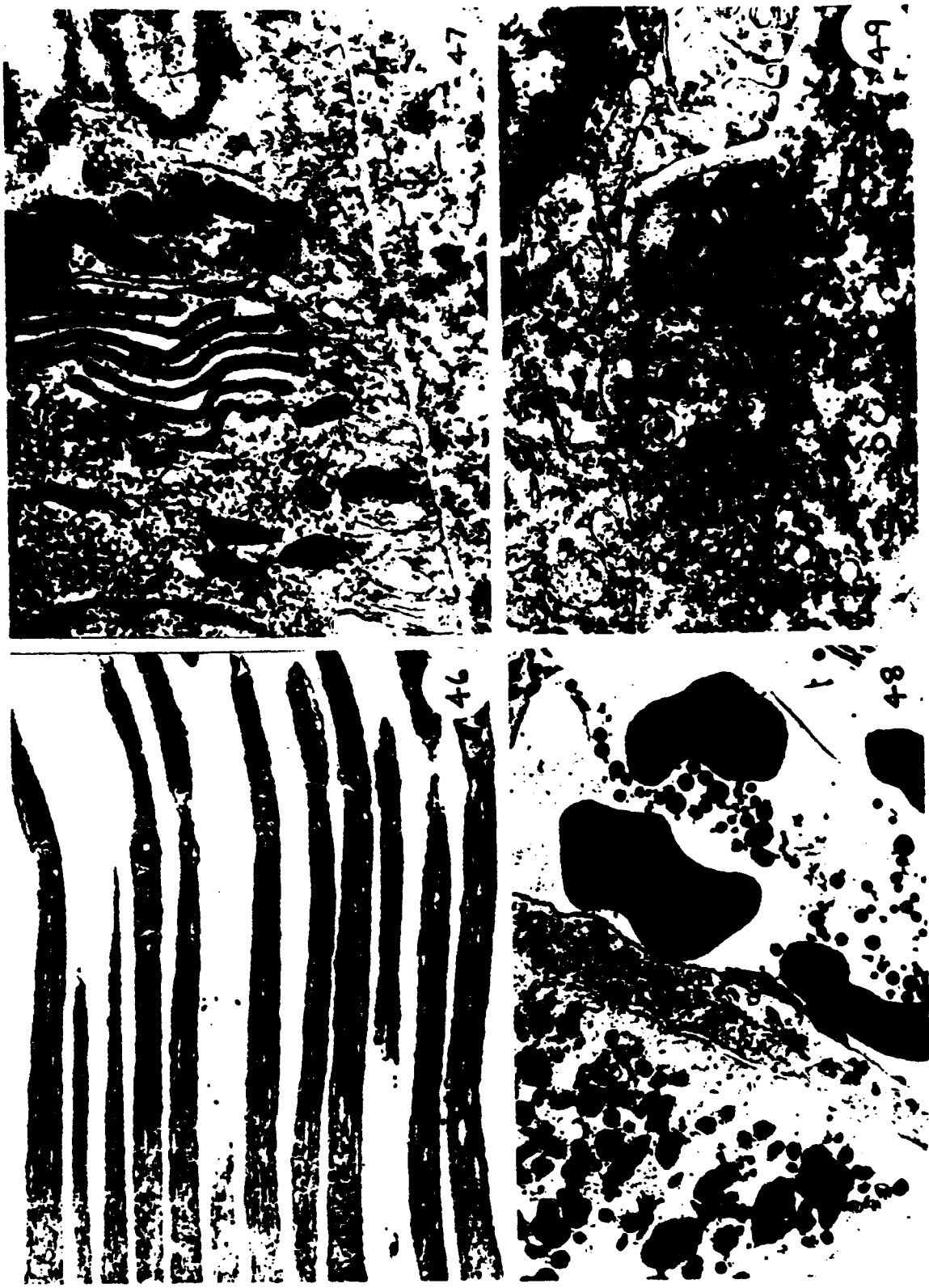

Plate 14

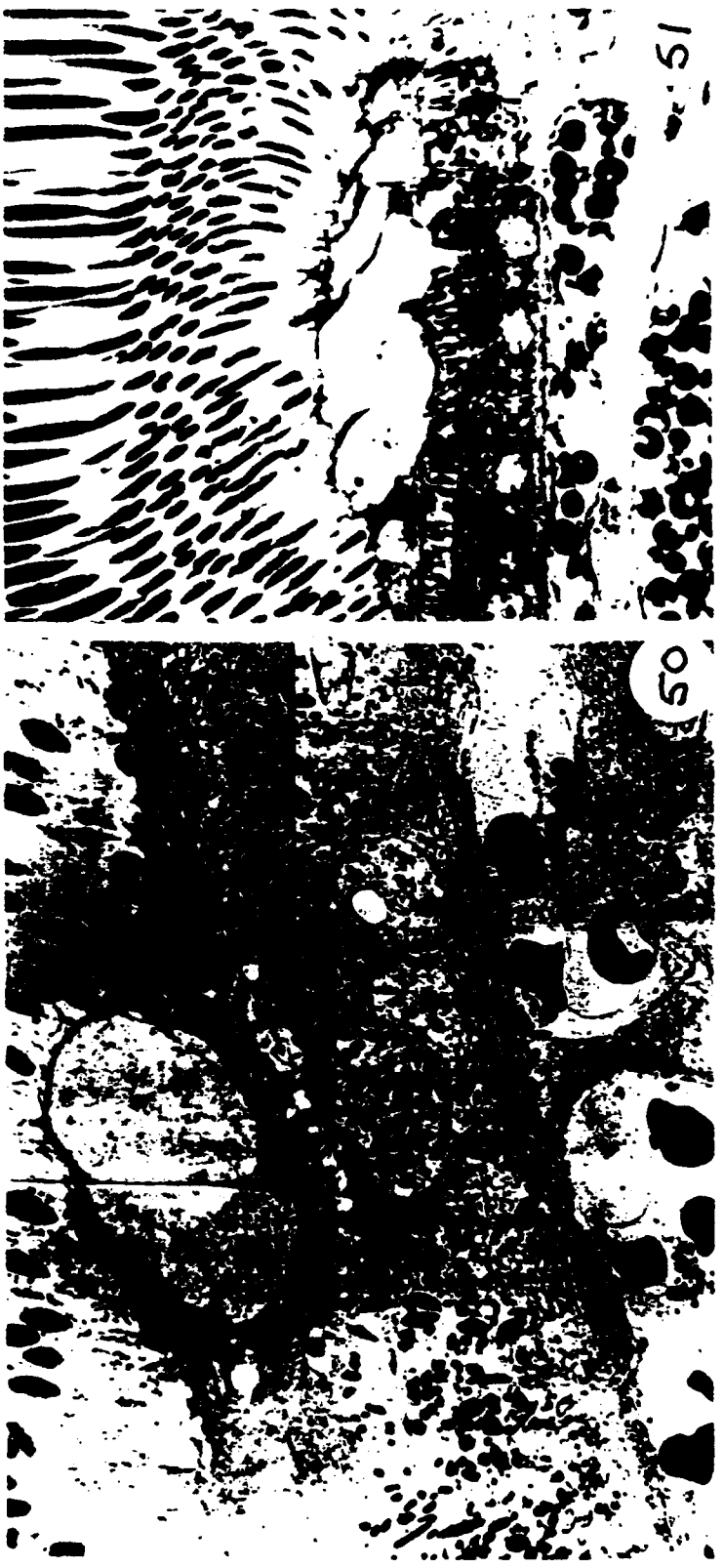

Plate 15

Plate 16

Plate 17

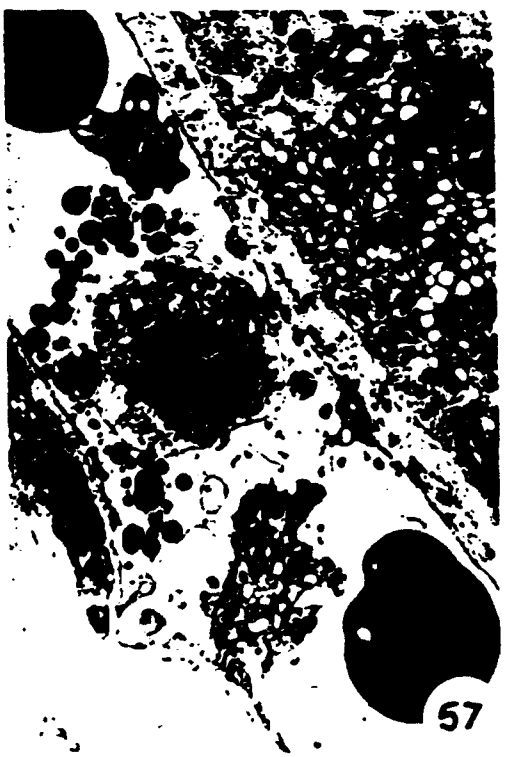

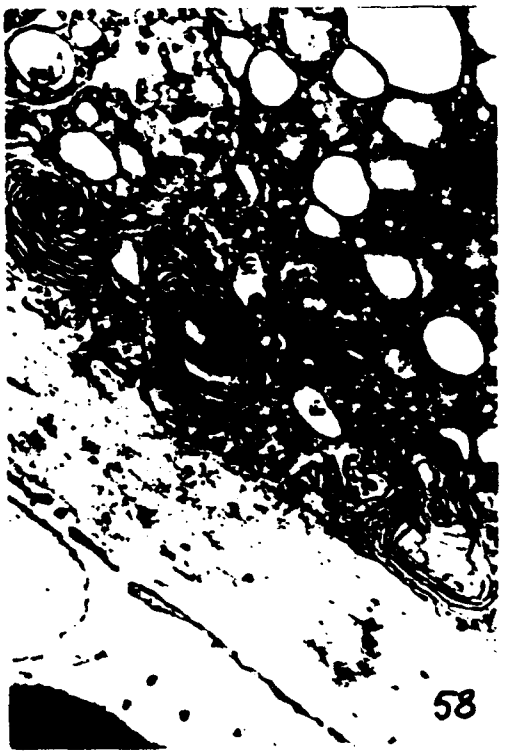

Plate 18

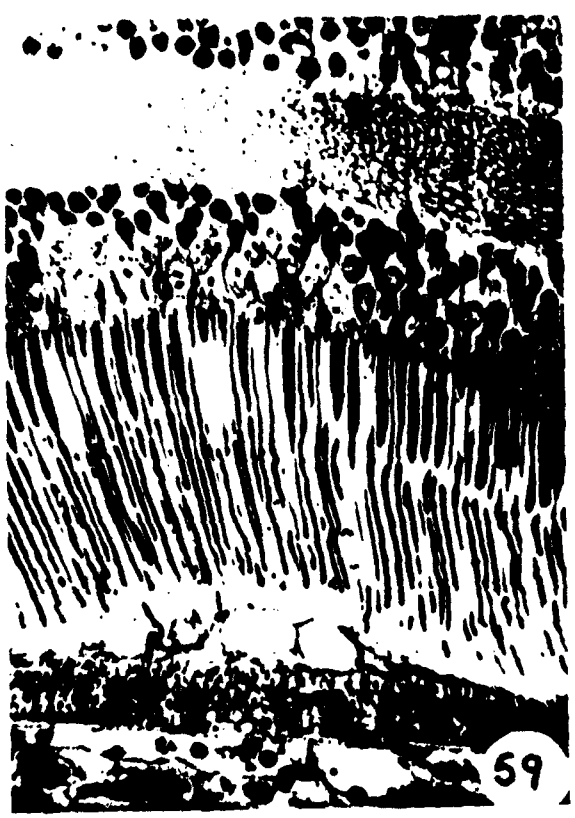

Plate 19

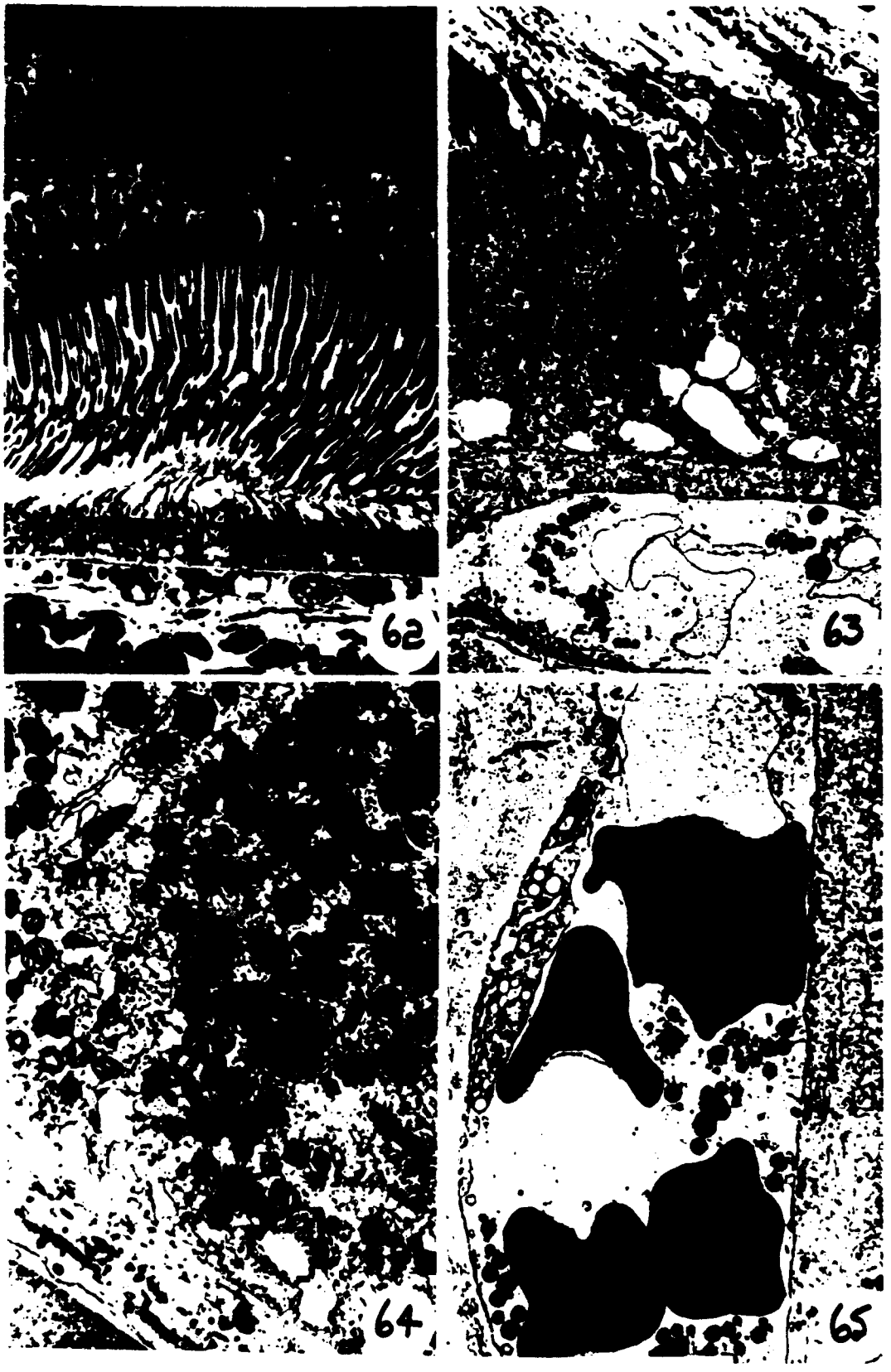

Plate 20

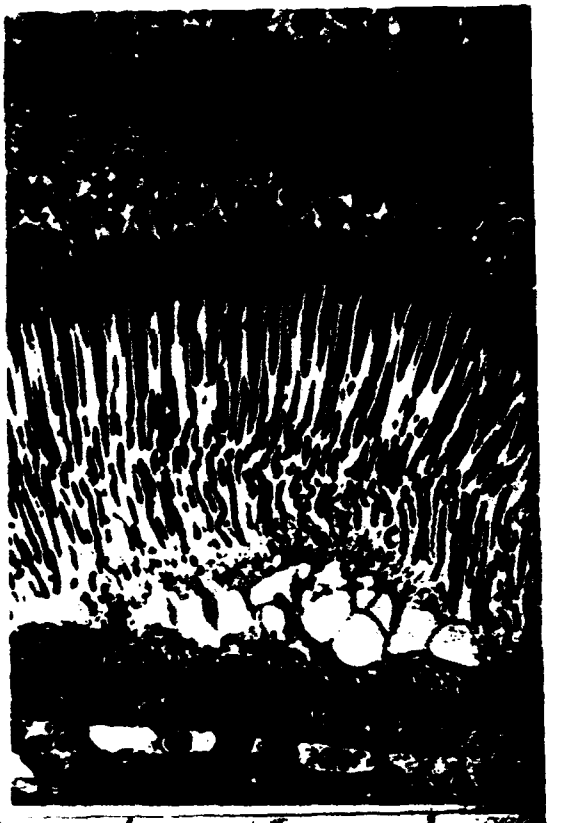

Plate 21

Plate 22

Plate 23

Plate 24

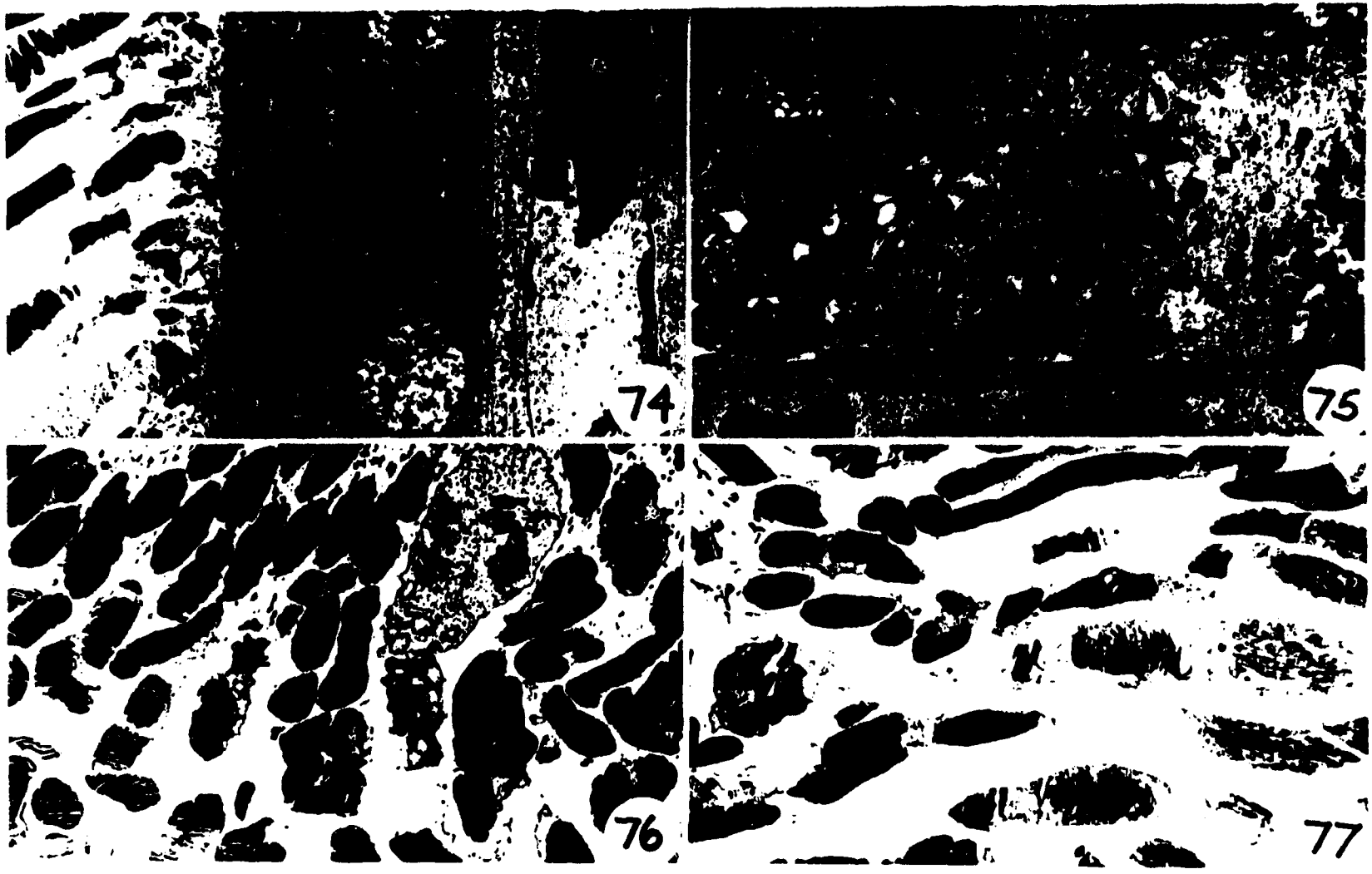

Plate 25

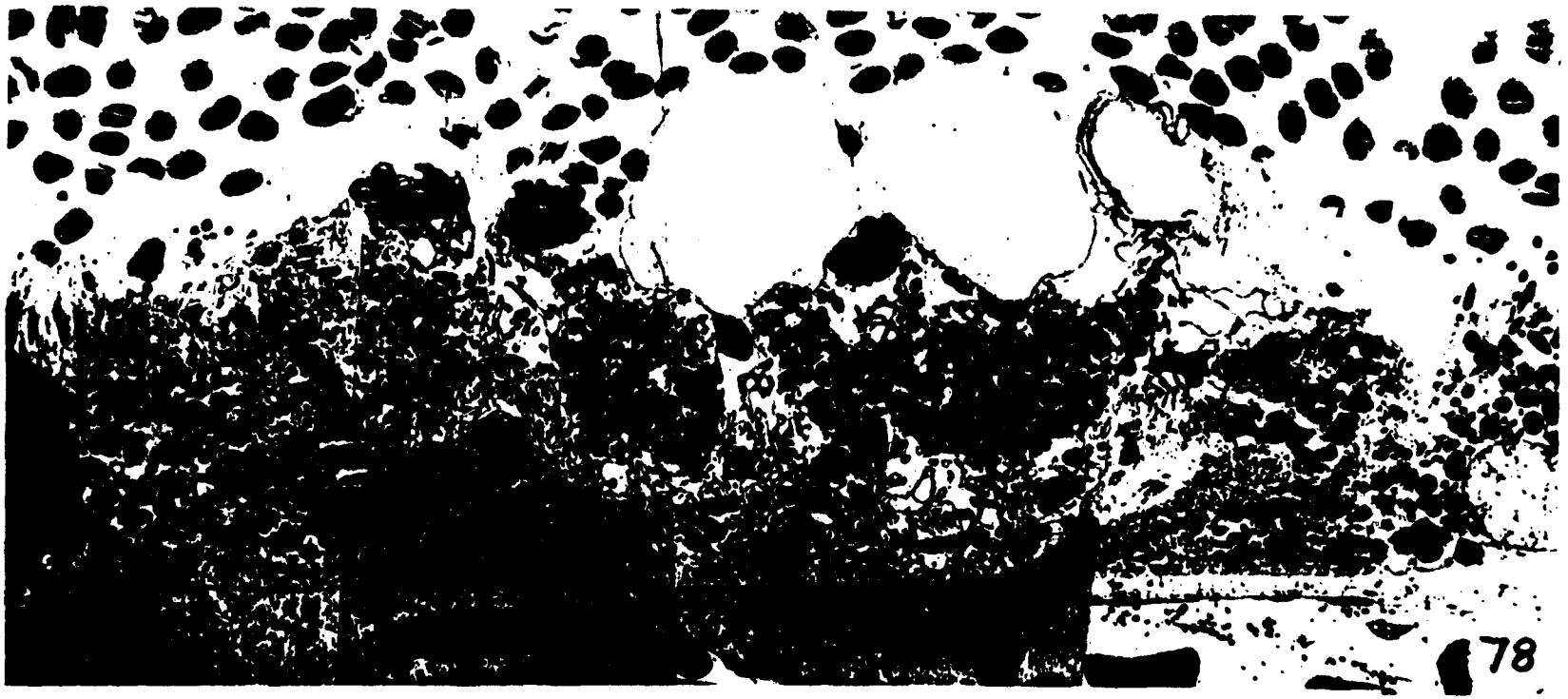

Plate 26

Plate 27

Plate 28

Plate 29

Plate 3D

Plate 31

84

Plate 3

Plate 33

86

Plate 34

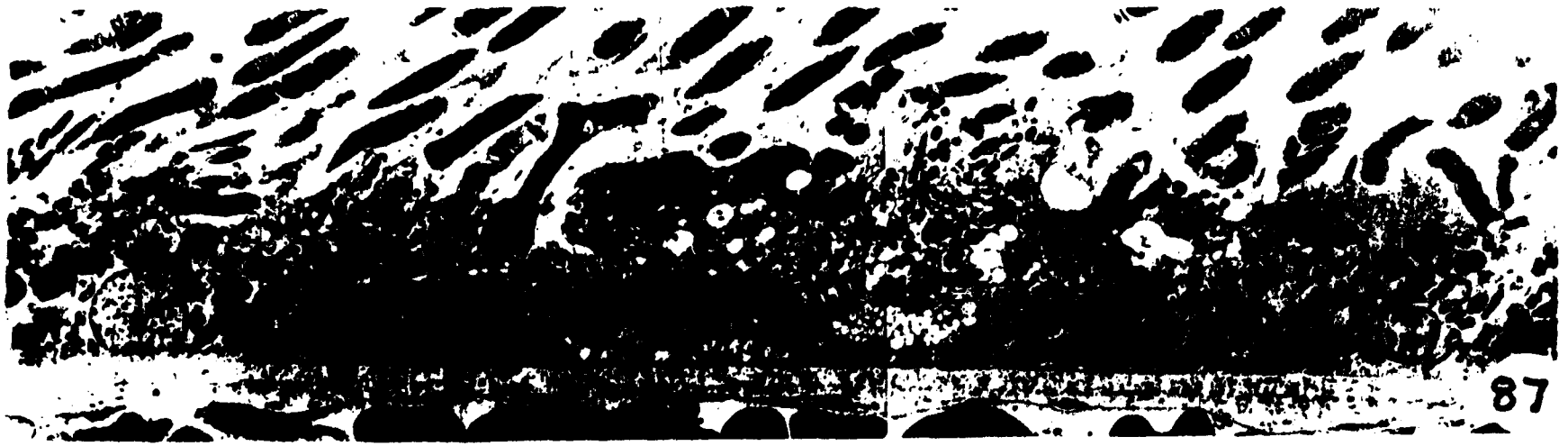

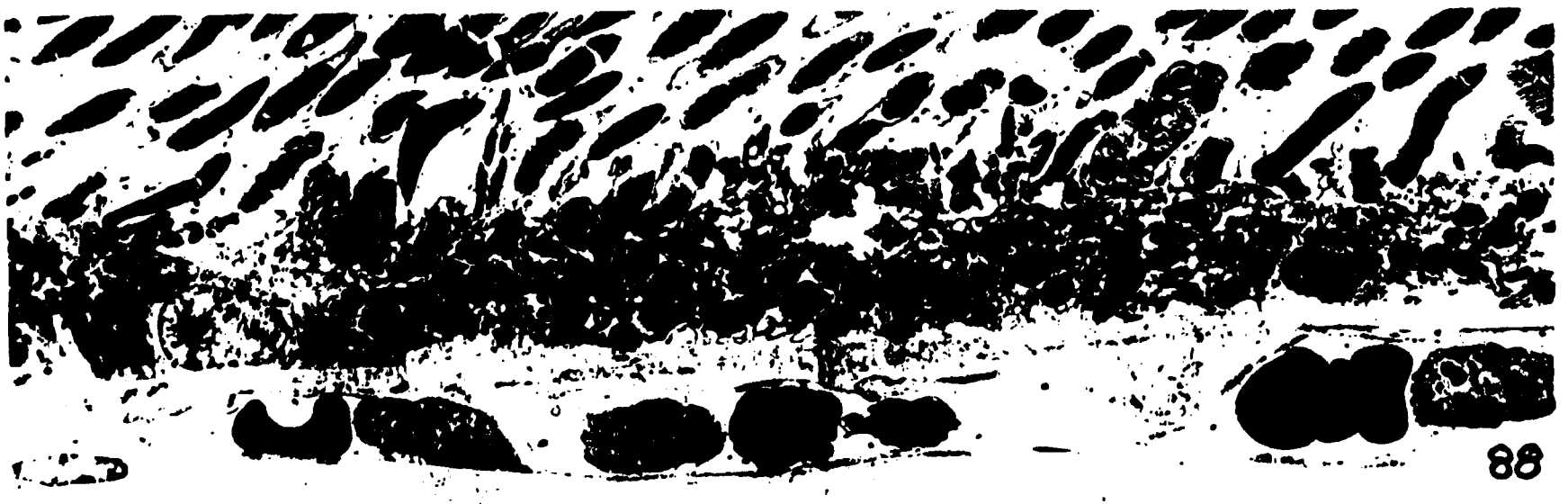

Plate 35

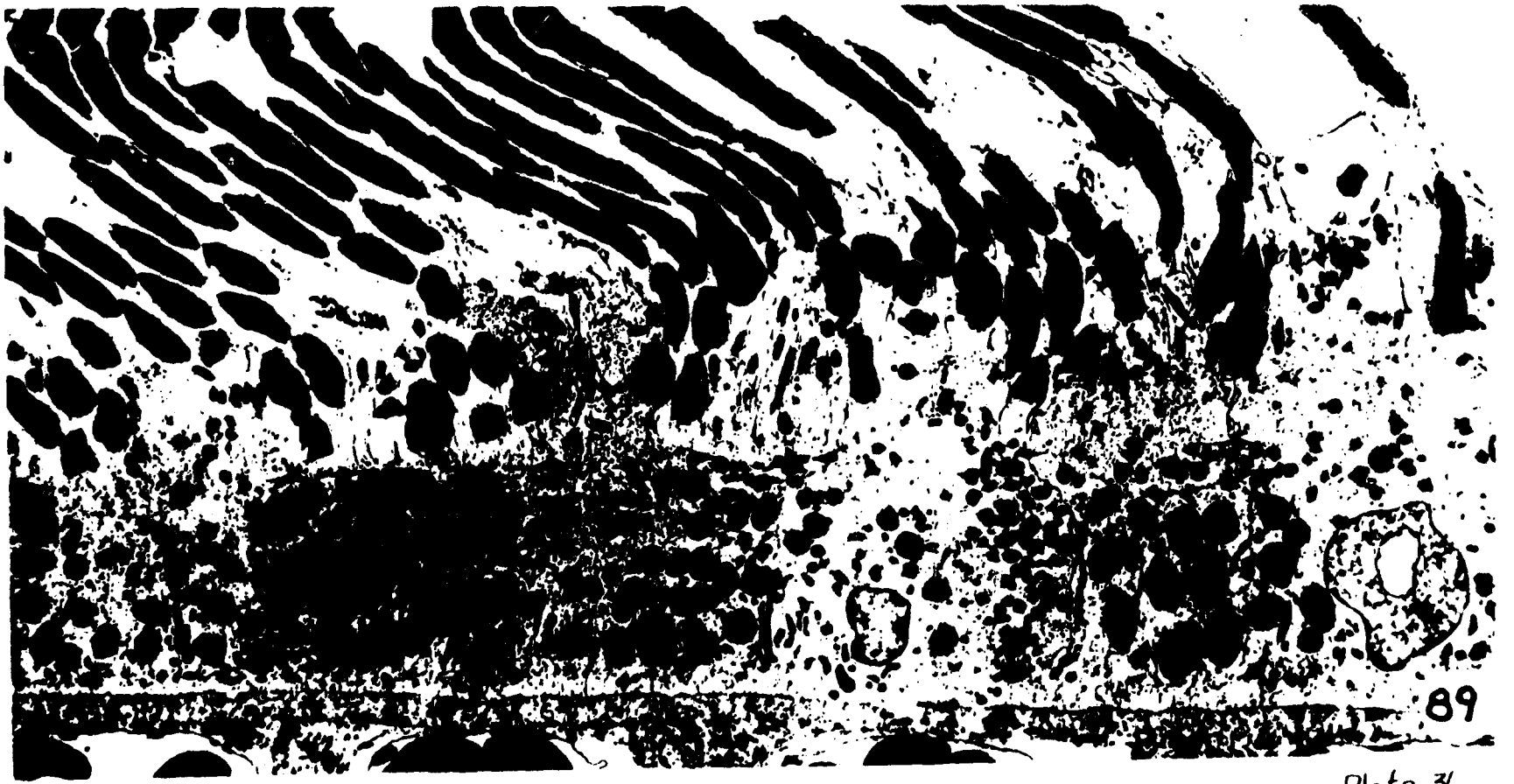

Plate 36

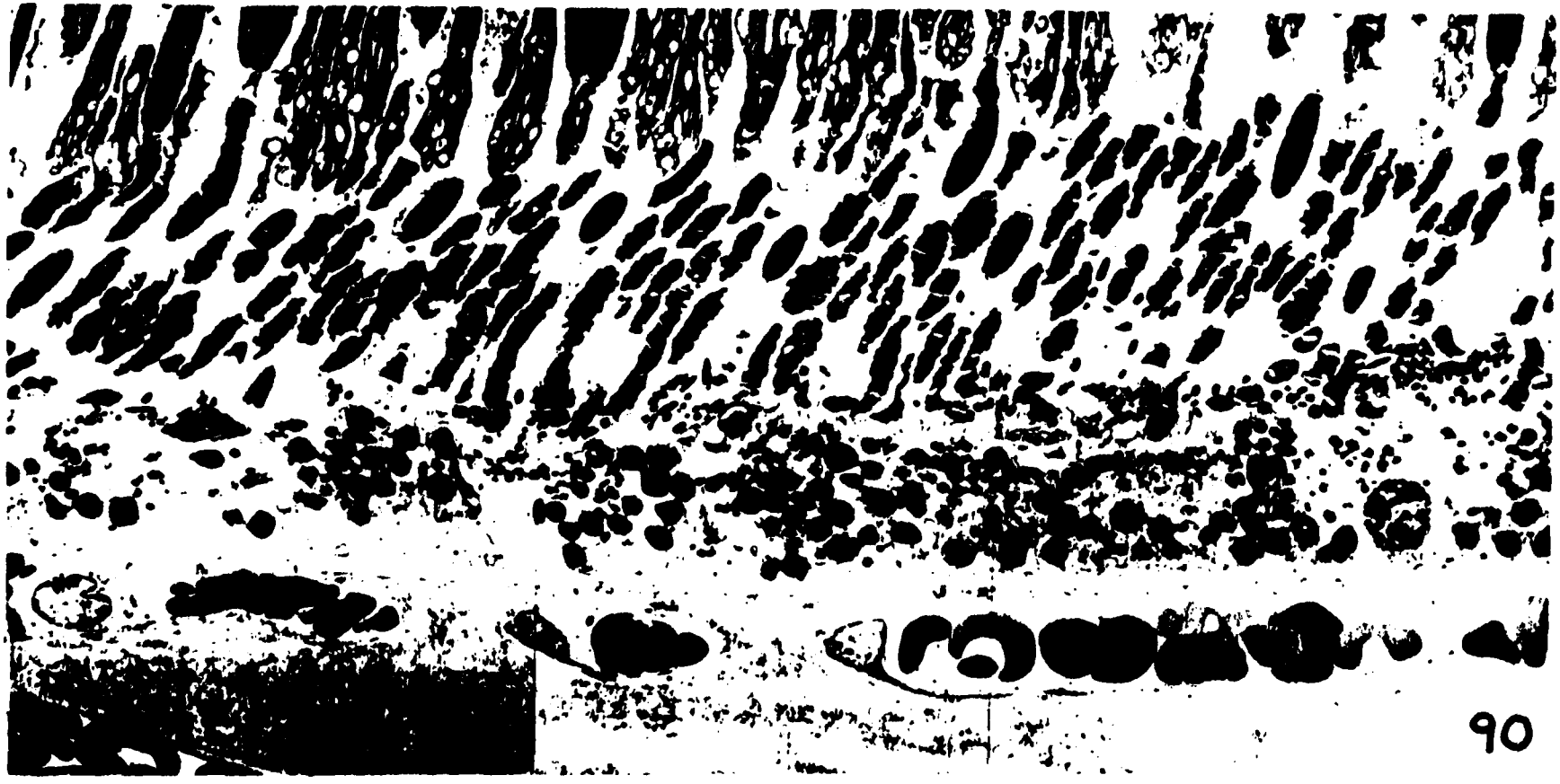

90

Plate 37

Plate 38

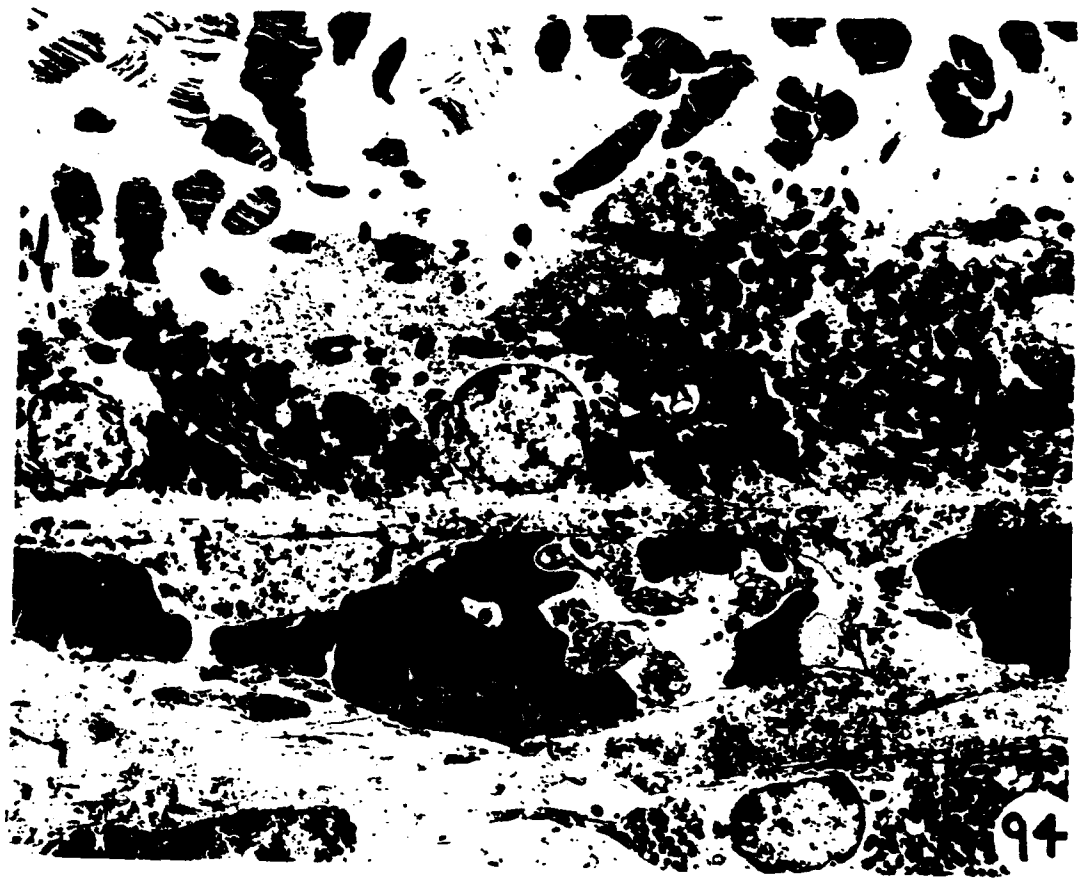

Plate 39

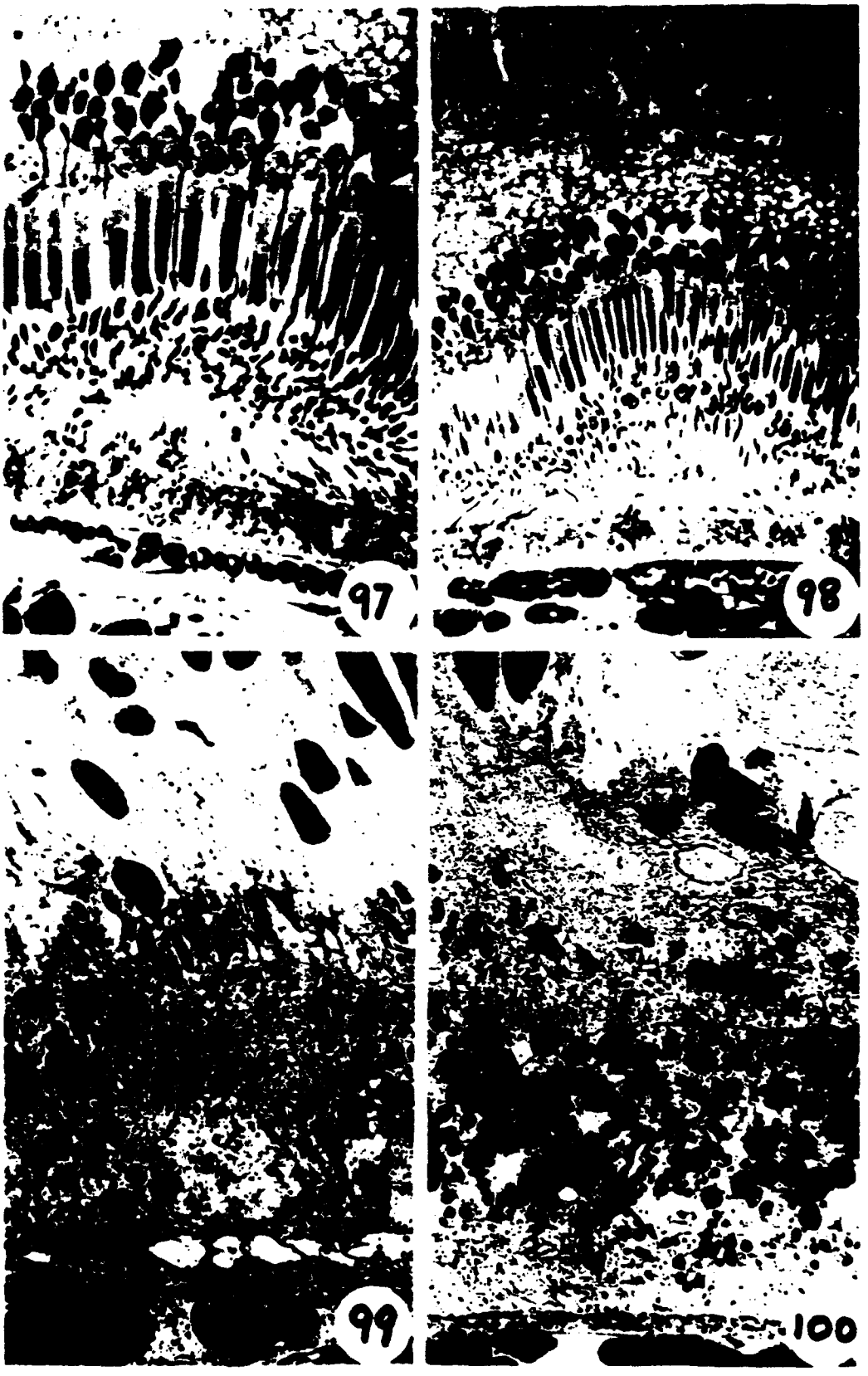

Plate 40

Plate 41

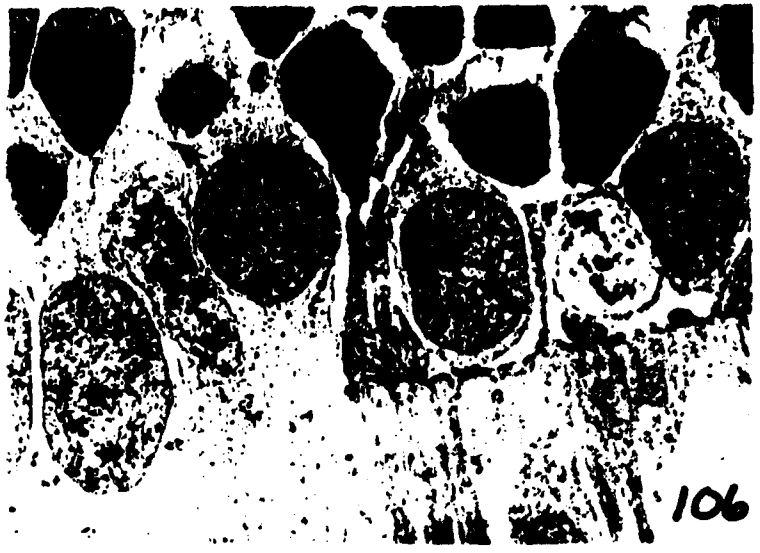

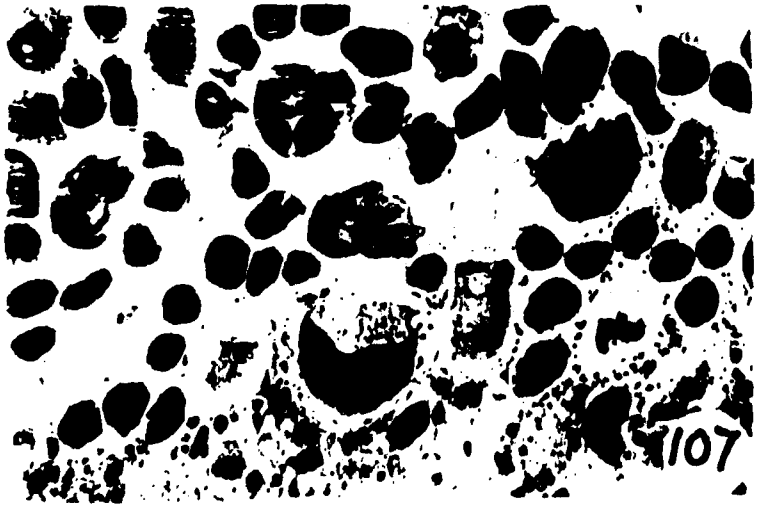

Plate 42

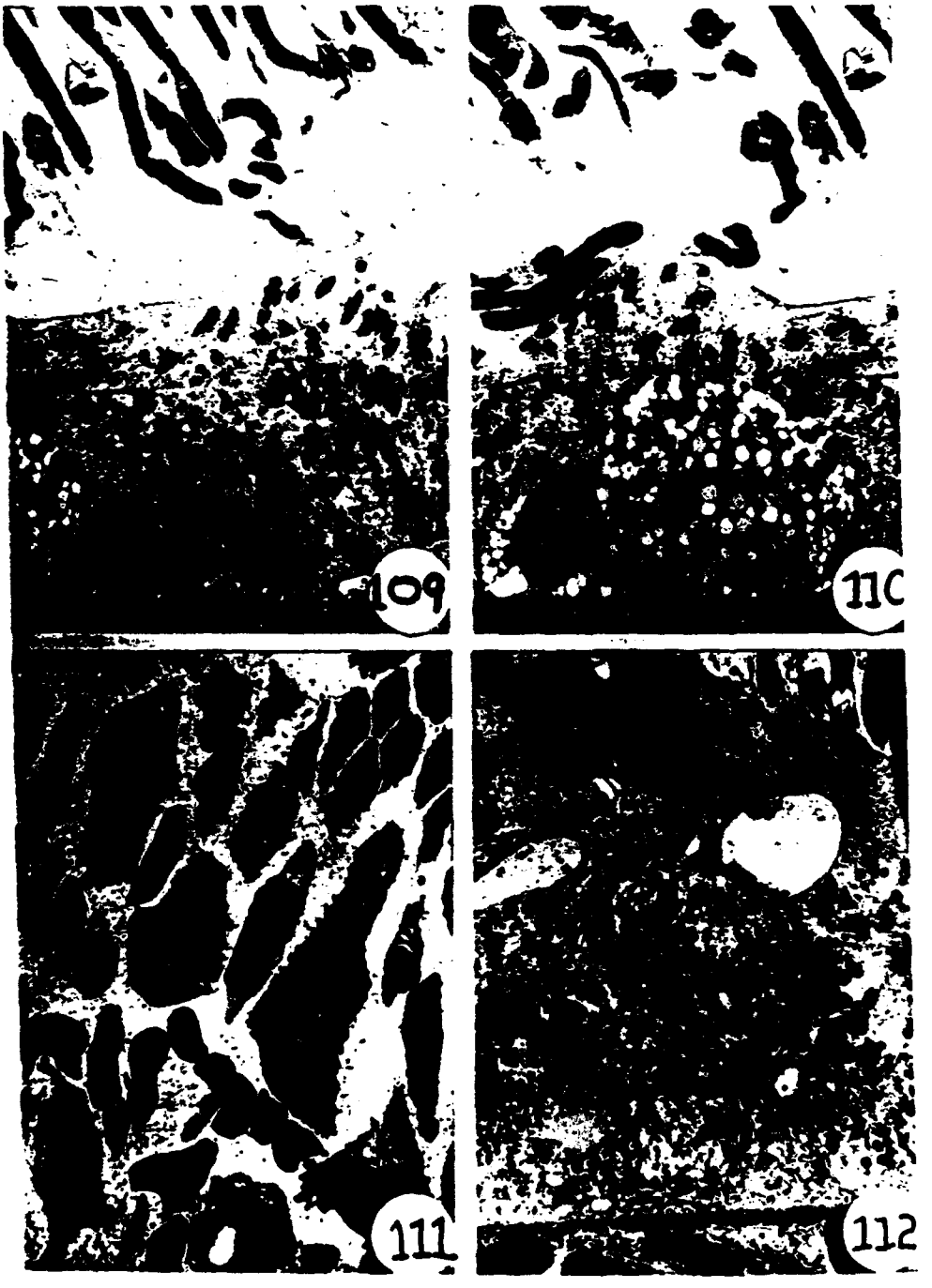

Plate 43

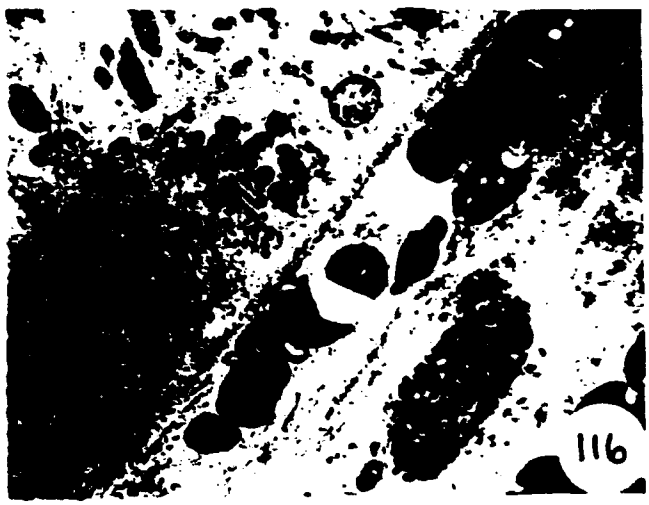

Plate 44

120

117

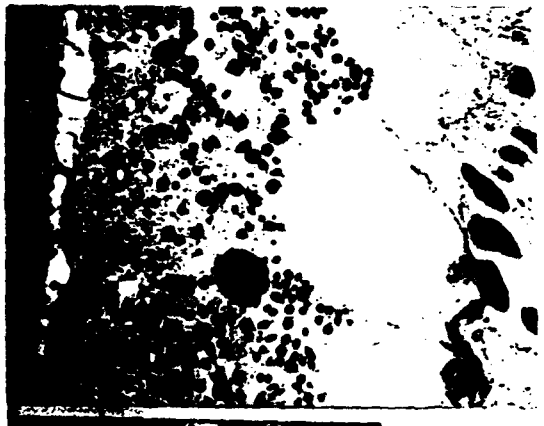

121

118

122

119

Plate 45

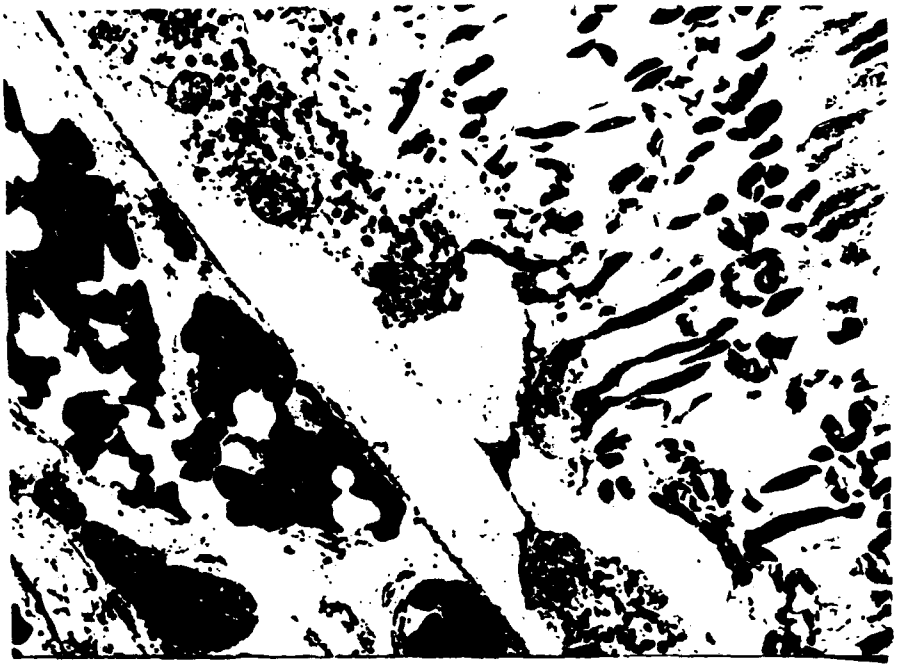

123

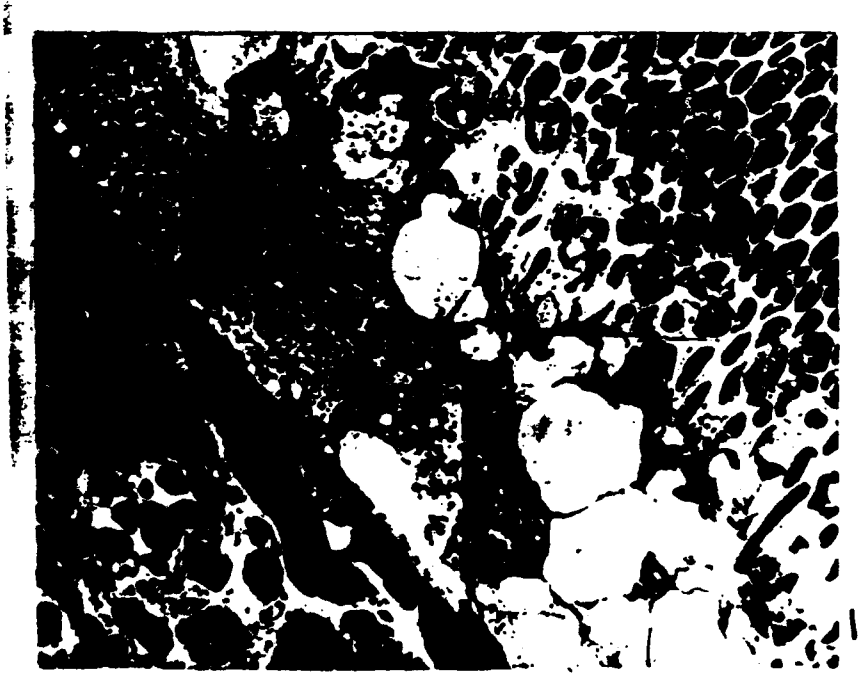

124

Plate 46

I

II

III

IV

Plate 46A

158

125

Plate 47

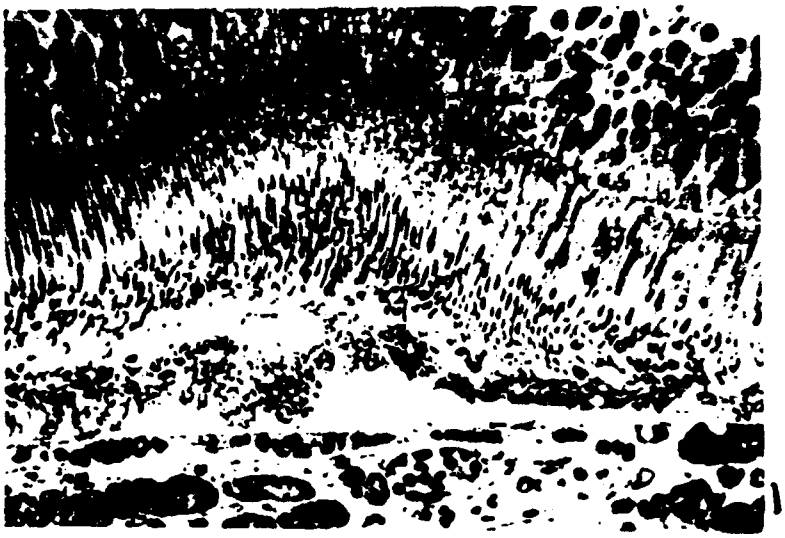

127

128

129

Plate 48

Plate 49

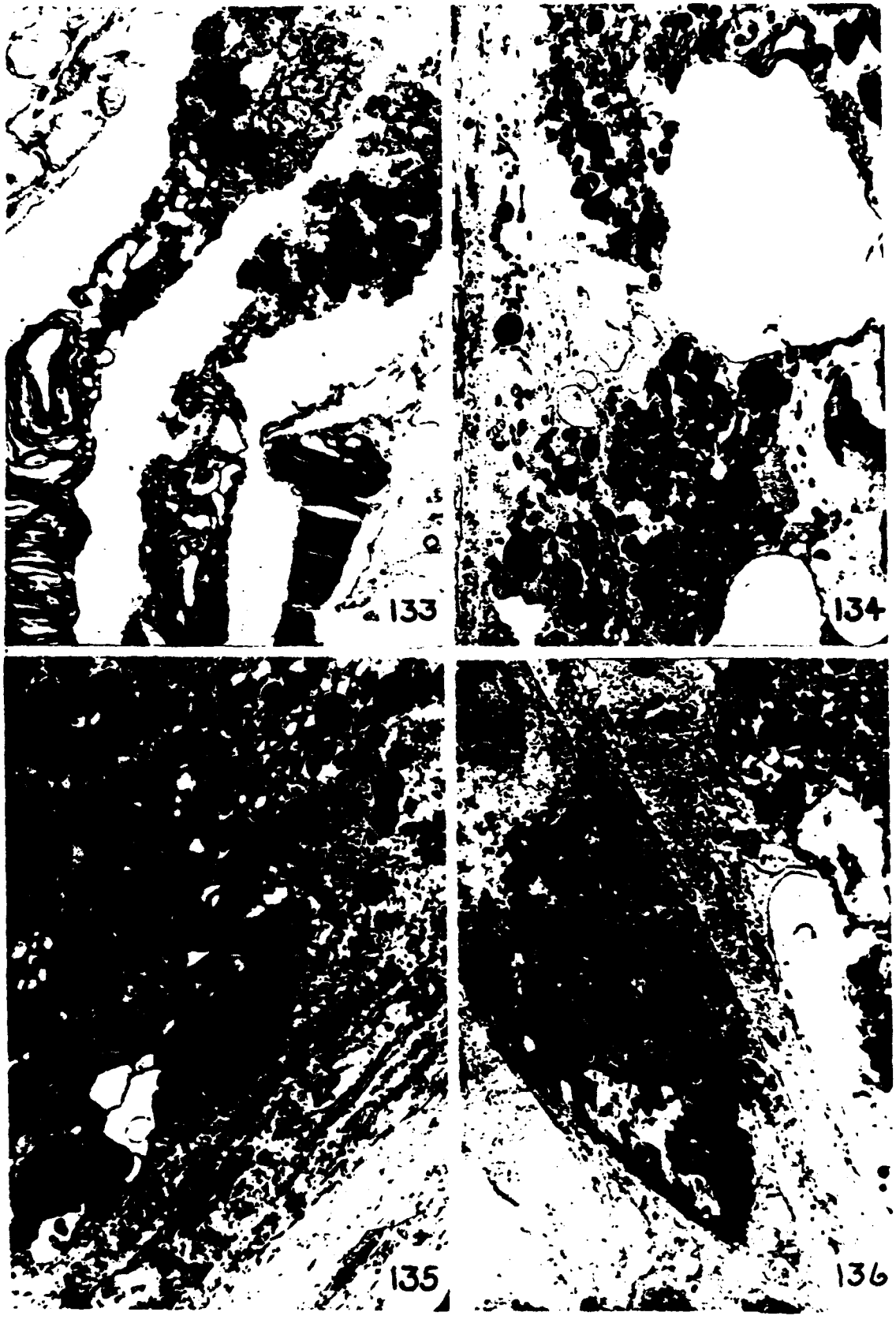

Plate 50

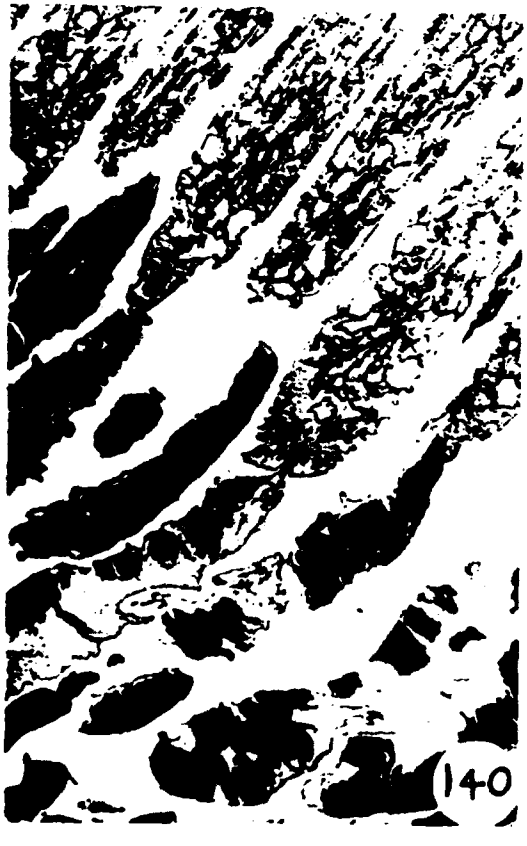

Plate 51

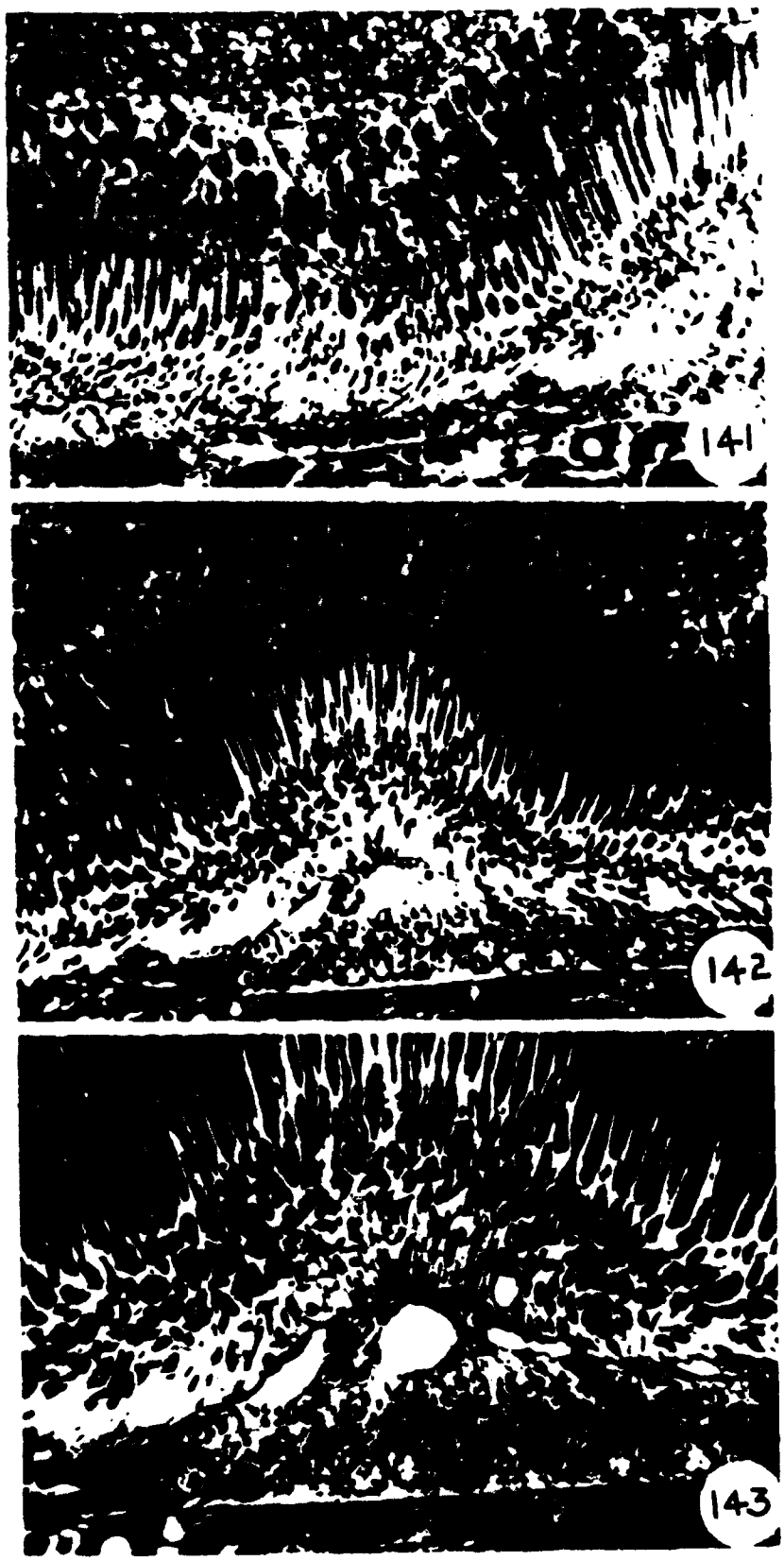

Plate 52

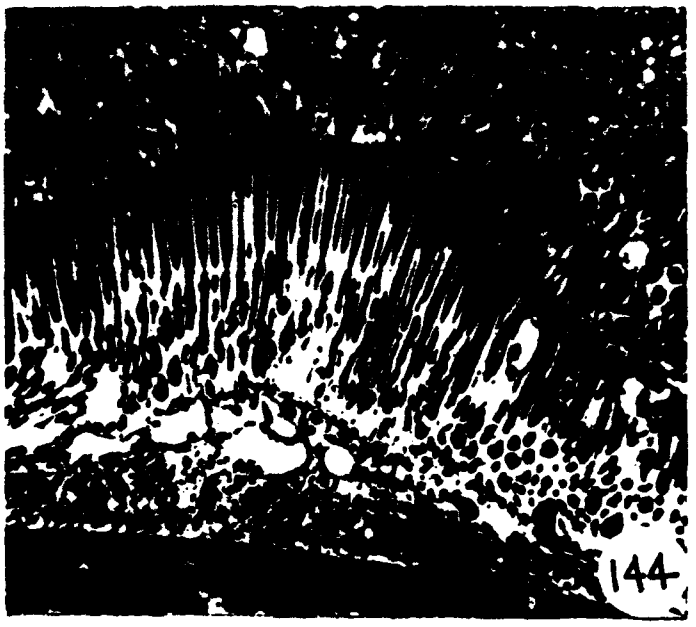

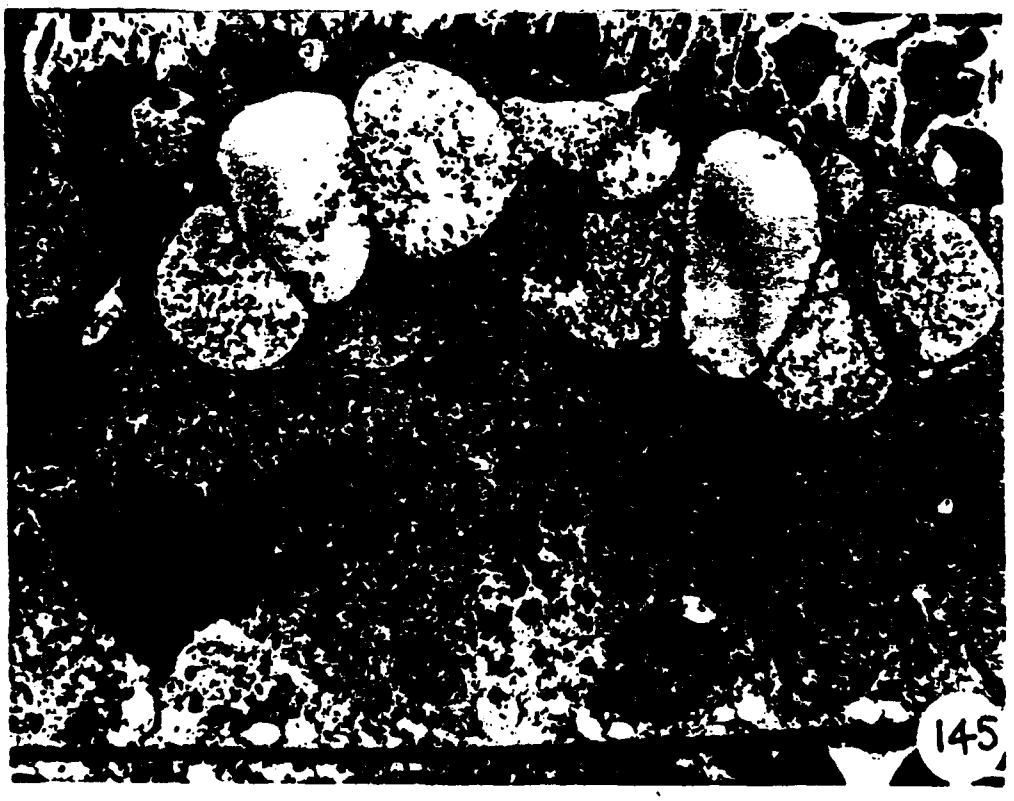

Plate 53

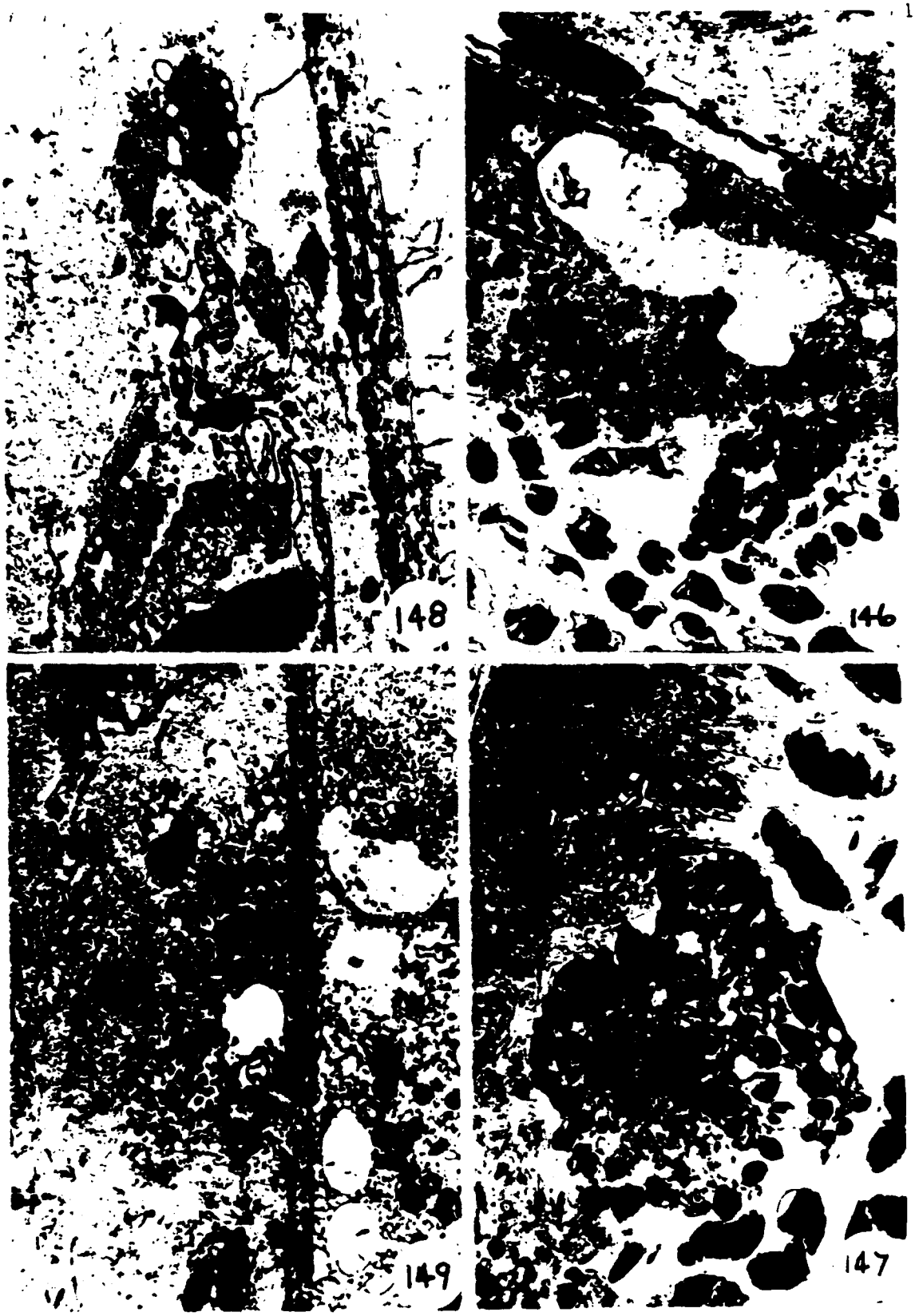

Plate 54

150

Plate 55

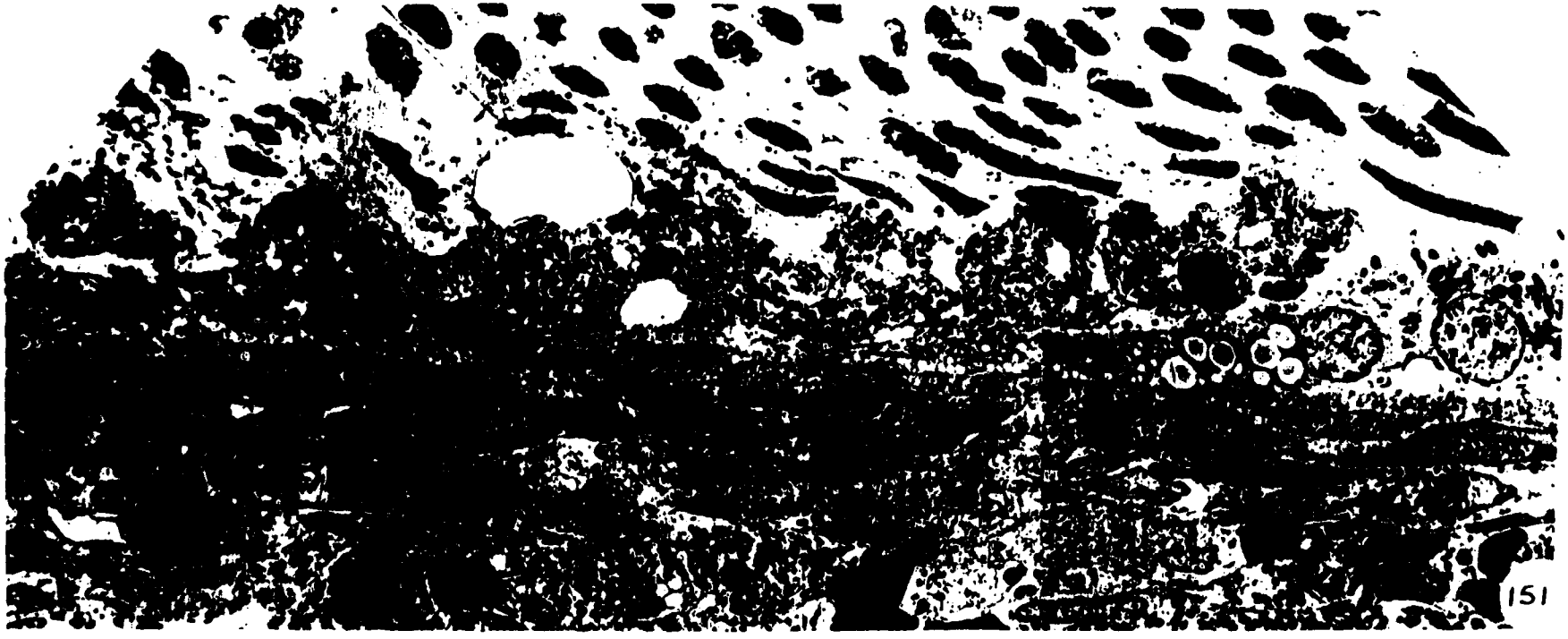

Plate 56

Plate 56A

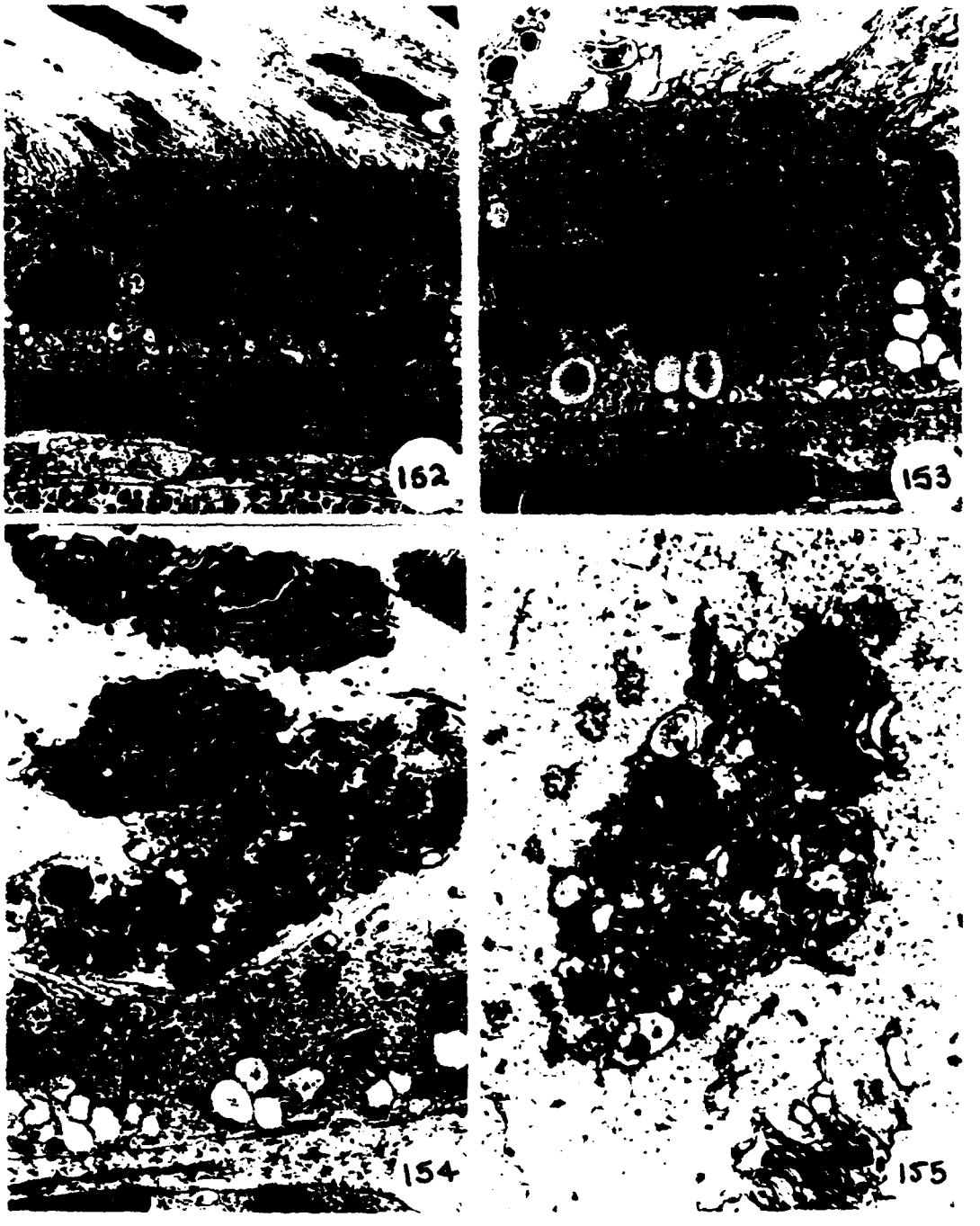

Plate 57

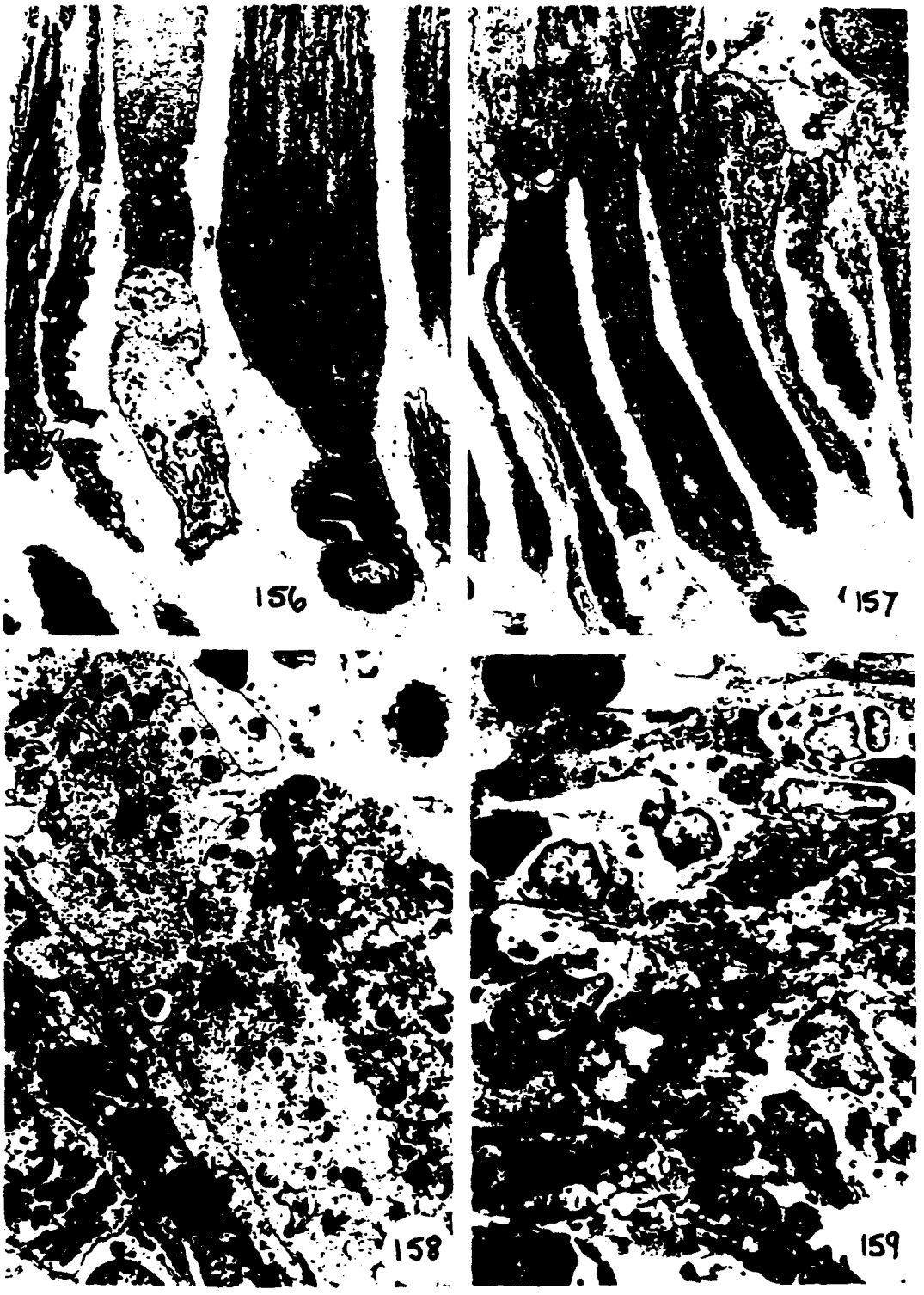

Plate 58

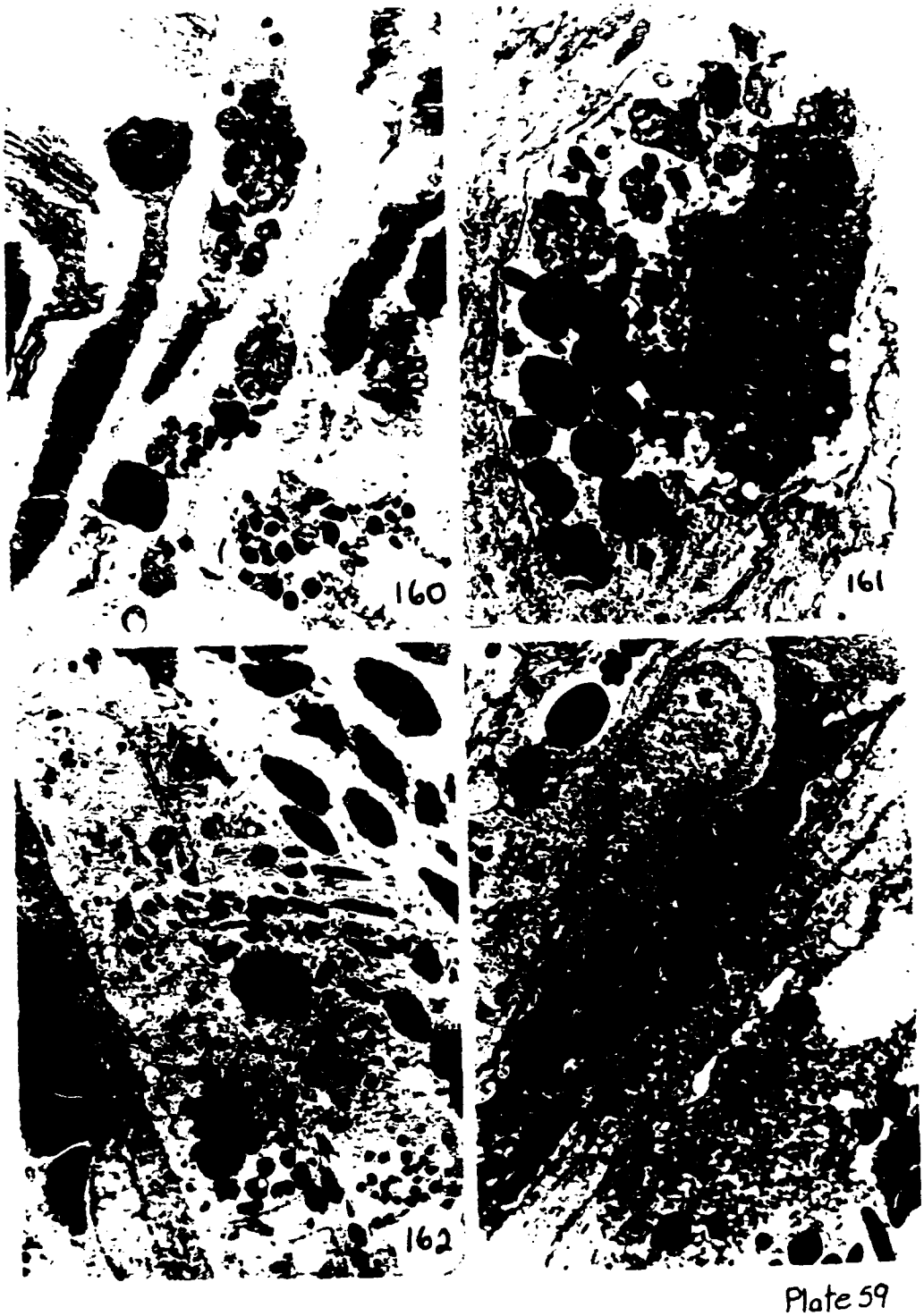

Plate 59

Plate 60

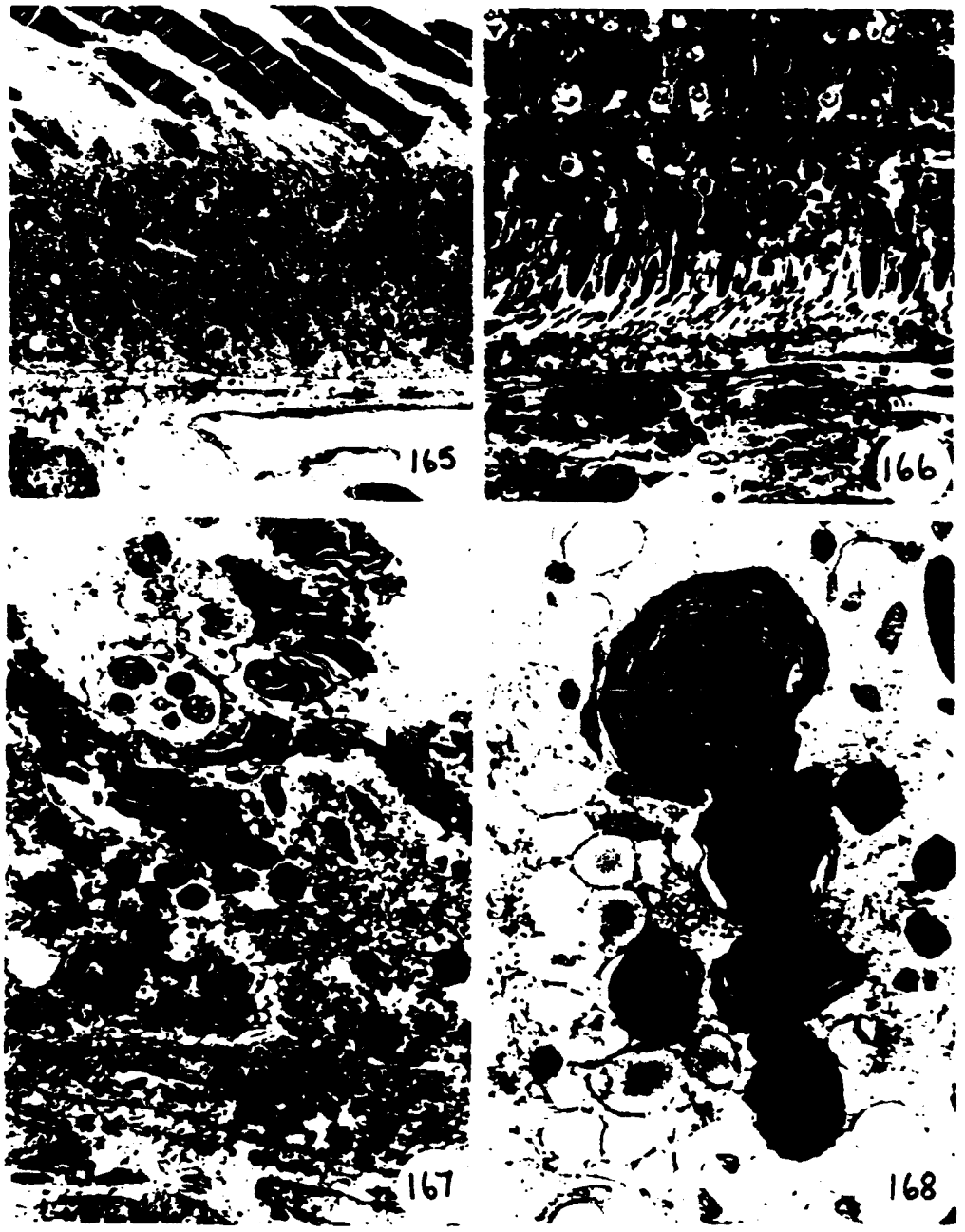

Plate 61

169

170

171

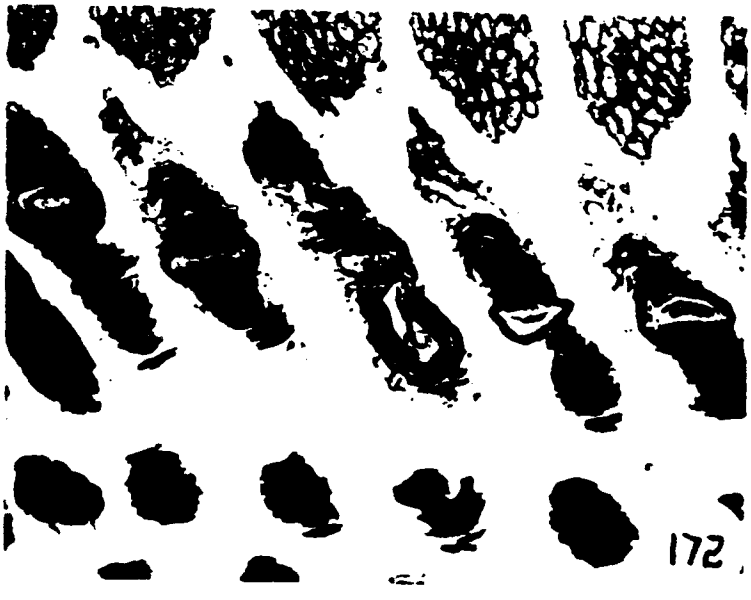

172

Plate 62

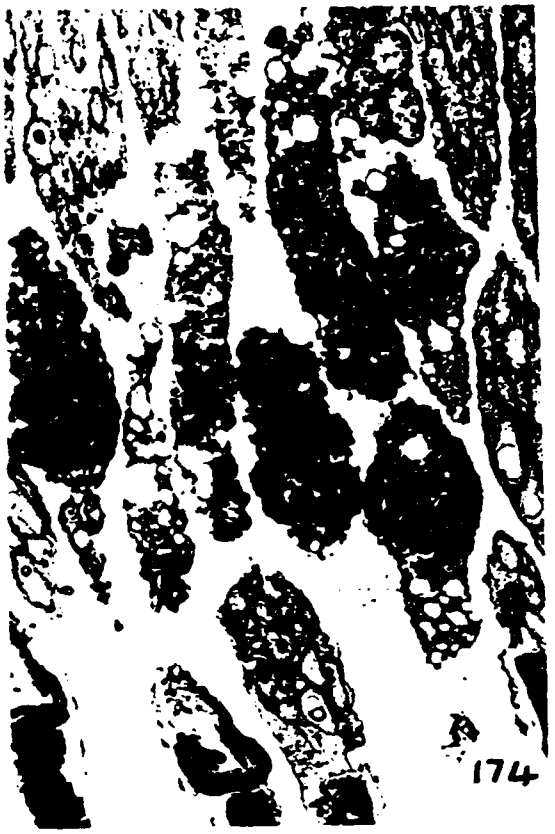

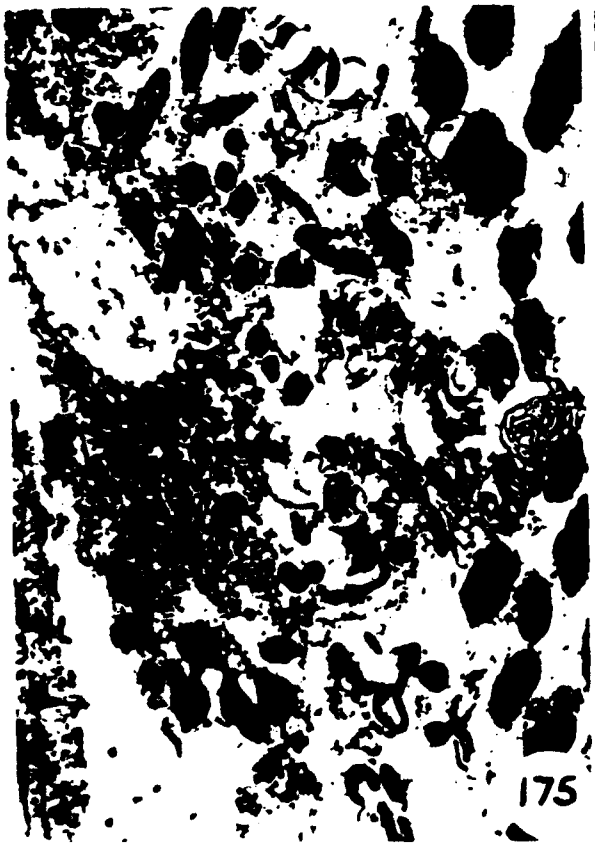

Plate 3

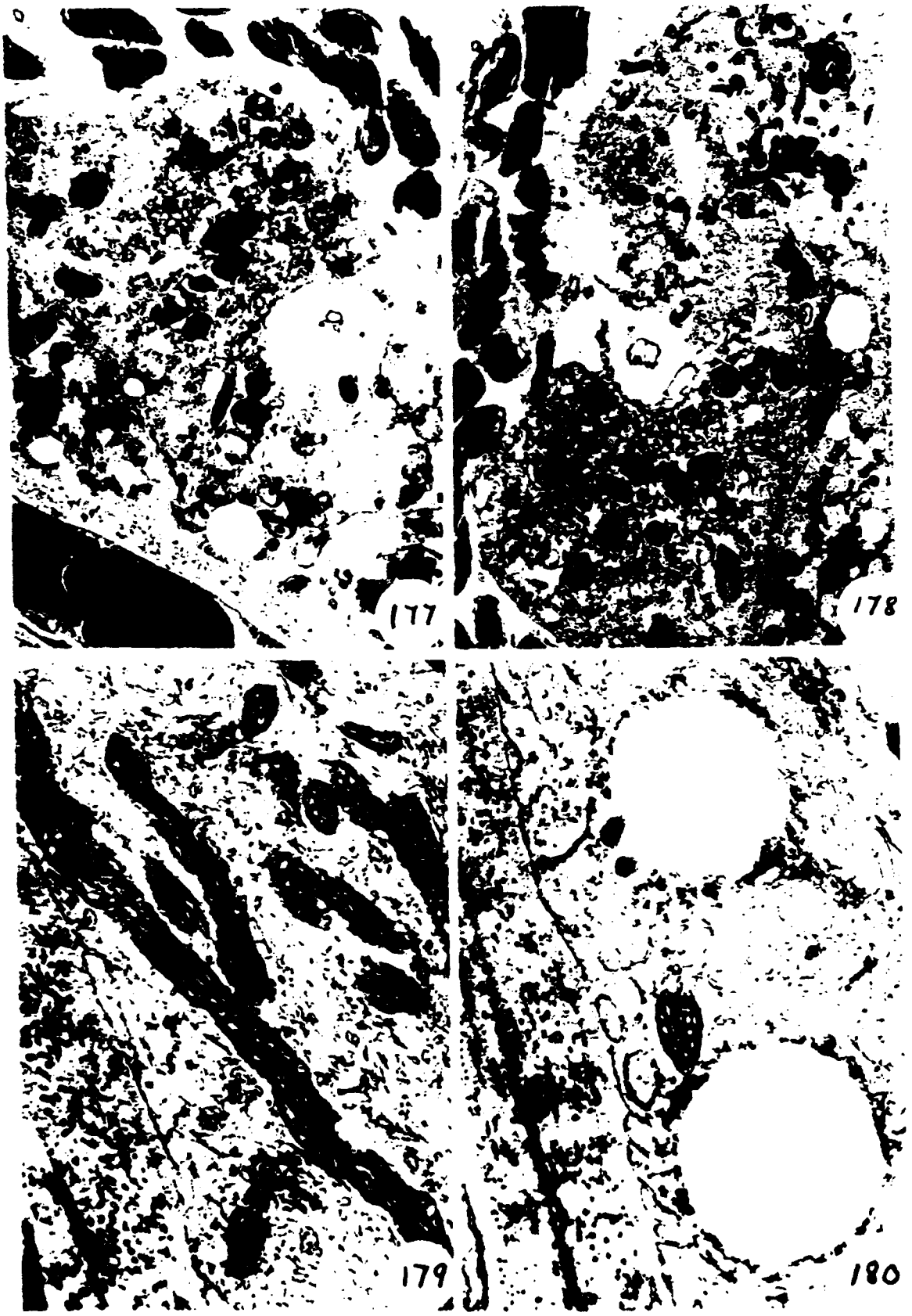

Plate 4

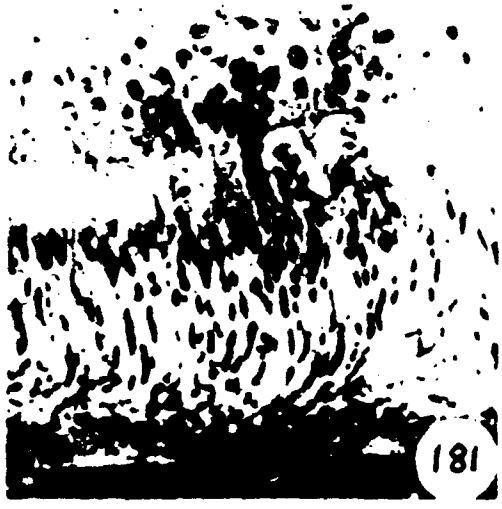

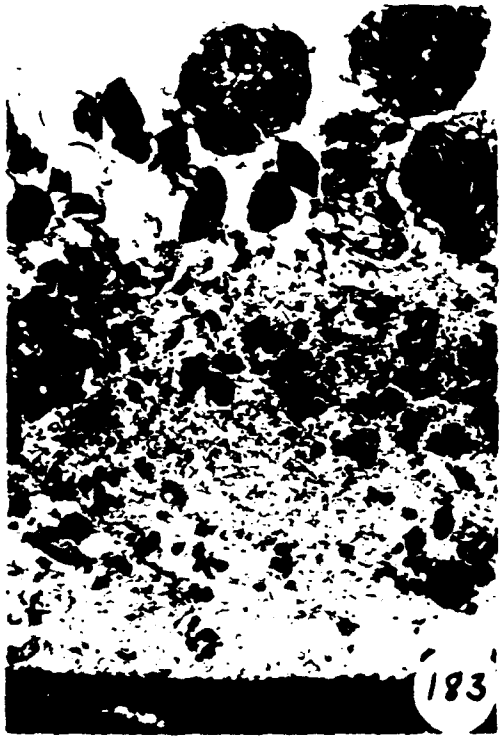

Plate 65

LITERATURE REVIEW

There has been considerable interest in the capacity of light to damage, or cause alterations to, retinal structures ever since Noell et al.[45] showed in albino and hooded rats than even short duration intense fluorescent light could damage the retina; that continuous light was damaging even at levels lower than that of normal daylight. The outer segments were shown to exhibit early changes[21]. Lanum's[24] comprehensive review made clear that retinal damage can result from intensities of light below those which cause thermal burns, but that 'recovery' can occur if the inner segments and nuclei are not extensively damaged.

The normal primate retinal pigment epithelium and its many pathological states are well described[58].

The advent of the laser brought into use a powerful and versatile tool with which to explore many aspects of effects of light upon the retina[7,16-20,25,34,39-43,52]. Since the eye is constructed to concentrate light upon the retina, the retina was early recognized as being especially vulnerable to damage by laser irradiation[57].

Ham et al.[20] introduced the term "retinal thermal threshold lesion" to describe an ophthalmoscopically observable lesion barely visible five minutes after exposure, and the concept of "threshold lesions" has been widely used. The threshold of damage, indeed the extent of the damage depends upon a number of factors: the characteristics of the laser (e.g. wavelength, pulse duration), the optical and pigmentary properties of the eye; the local conditions within the retina (pigmentation of the pigment epithelium especially); the properties of the choroid and the presence of capillaries[34,42,43].

Examination of some of the ultrastructural changes in retinas for subthreshold lesions specifically were undertaken early for a variety of lasers: Helium-Neon[25], argon[7], ruby[29], gallium arsenide[30].

The present study concentrates on subthreshold lesions from a Neodymium-YAG laser, invisible to the eye (1064 nm), by which alterations to the retina can be created without exceeding the corneal damage threshold[31].

Goldman et al.[13,14] found that 1064 nm wavelength laser light damage was restricted to the area of the retina between the retinal pigment epithelium and the outer nuclear layer, at 43 μJ, but that at 62 μJ the inner nuclear layer was also affected. In the present study, no two lesions were identical, no doubt in large part due to local variations within the retina and its pigmented epithelium. The alterations in most subthreshold lesions was not only limited to the area between the retinal pigment epithelium (RPE) and outer nuclear layer (ONL) it was limited mainly to the RPE and outer segments, and inner segments were less severely and not always affected, and the photoreceptor nuclei were usually not altered morphologically. In essence, the subthreshold lesion is limited to the RPE and OS[4], but the choroid is also involved. Since some of the changes seen in the choroid in Rhesus monkey were also seen identically in the controls they are probably attributable to ageing. However, there were changes in the endothelium of the choriocapillaris, and in the degree of patency of the lumens.

There is a very sparse literature on the effects of Neodymium-YAG subthreshold or threshold lesions on the outer choroid.

Some authors[28,48] have claimed with other lasers that it is the outer segments and not the RPE which is first damaged, but in the present study and in others[4,16] subtle first changes seen in the smallest lesions were in the RPE, and almost entirely limited to the RPE.

The distinct and abrupt margins in the PRE of the laser-induced spots of damage was dramatically demonstrated by scanning electron microscopy in rabbit retinas[6], and is well shown in the electron micrographs in this study. It is the loss of apical RPE microvilli which shows so clearly by SEM[6].

The hypopigmentation of the RPE, most significantly by loss of melanin granules (which do not get replaced) which results from even low level laser irradiation may be the essential factor contributing to irreversible damage even when there is little general damage to the retina and restricted to relatively few cells[16-19]. To what extent this impairs visual acuity or function, or renders the retina more vulnerable to later light damage is not definitively known, but there are indicators that this occurs. Zwick et al.[59-64] found that in certain circumstances there was long-term suppression of photopic spectral sensitivity and very little recovery of this over two years. They caution that repetitive low level laser viewing or prolonged viewing of laser display systems, albeit at very low levels, presumed safe by existing laser safety standards, may depress photopic function, especially for the highest acuity criteria.

Visual acuity changes, in unpredictable ways, were reported in human eyes after Nd-YAG exposure in the macula, with outer retinal layers being affected sooner and inner retinal damage developing later[8].

Repeated light exposures of the same retinal site may increase the extent of the damage even when the total irradiation received equals that delivered in one dose[10,15,23,29,45].

Noell et al.[45] first showed that there can be a cumulative light damage effect.

Griess and Blankenstein[15] conclude that "the maximum permissible exposure to light should be reduced ... when exposures are repeated". However, Ham et al.[17] found that repetitive "minimal" lesions in Rhesus 48 hours apart showed that there were repair mechanisms which can cope with the damaging effects of short wavelength light for intermittent exposures at low levels of irradiance. This may well depend on sufficient time (24 hrs) elapsing between successive exposures to allow repair processes to work[23].

Photic insult over a long period has been implicated in the development of senile macular degeneration, a leading cause of visual impairment in the older population of Americans and Canadians.

Although the photoreceptor nuclei did not often display necrotic or pyknotic changes, some Henle fibres showed pyknosis in response to the Nd-YAG irradiations in the present study. Similar degenerative changes were noted after foveal irradiations with argon and krypton lasers[30,51]. This also warns of subtle damage.

It is the fovea and macula that has the highest concentration of cones, although rods are present[5], and any impairment of these, not fully repaired, may be long-lasting in subtle ways. The greater sensitivity of the macula (compared to extra-macular regions) to the damaging effects of laser irradiation has been documented[29,30,39]. There is seemingly a paradox in that cone outer segment discs are more affected by photic stress while cone nuclei are more resistant than rod

nuclei to pyknotic and necrotic changes. The cone outer segment greater vulnerability seems to be independent of wavelength of light[18,59,61] and they do not recover as readily as rods[40,50,52]. The cone outer segments appear to have a more limited renewal capacity than do rods[3,36]. Aging primate cone outer segments contain disoriented disks[41] and have nodular excrescences[3]. While disordered cone outer segments were seen in this study in both control and lased areas, the degree and type of disorder differs.

Except for hypopigmentation of the RPE, and perhaps ongoing disarray of the outer segment discs, low-level damage may well be generally repairable in the RPE and photoreceptors as long as the original laser damage did not extend to the rod and cone nuclei and the proximal inner segments. The RPE has considerable and speedy reparative capacity. To what extent the choroid repairs, especially if the melanocytes are injured, is not known, but choroidal repair in general is known to be slower than retinal repair[46,55], although the choriocapillaris can repair itself. Novack et al.[46] found in the avascular retina of rabbit that laser treatment damaged the endothelium and choroidal capillaries and that these took longer to recover than did the RPE. The superabundance of photoreceptors may enable the retina to maintain adequate visual acuity even when some are lost, unless the damage rate and extent exceeds the repair capacity[49-54]. Bruch's membrane retained debris-derived inclusions after laser injury to the retina, although it itself did not appear to be breached in the small lesions. The retention of debris might reduce the efficiency of the choriocapillaris and RPE to transfer essential elements. It has been suggested[8] that as Bruch's membrane provides a selective filtration barrier for nutrients from the choriocapillaris to the outer retina, ageing or pathological changes can create abnormal function, and lead to reduced efficiency of maintenance of the outer retina[21]. Long-term follow-up of subthreshold lesions is needed to provide reassurance that visual acuity in all its aspects and outer retinal function remain intact. Again, one cannot assume that there is no persistent subtle damage changes from small and circumscribed subthreshold lesions especially in the macula. The choriocapillaris is occluded in Nd-YAG exposure of human retinas[8], as it was in this study.

The retraction into the RPE cell, the thickening, fragmentation and loss of the RPE apical microvilli as a very early response to laser irradiation is consistently seen in this study and has been reported in rabbits[6] and monkeys[49].

Another very early and consistent response to laser irradiation is in the RPE basal infolds, which widen and disappear, in a gradient from the centre to the periphery of the lesion. While ageing RPE also has basal infold reductions[41], there is a remarkable difference in the basal infolds in the lased and control areas.

Clusters of cells, laden with RPE-like melanin granules, resembling macrophage, are frequently seen in this study in the sub-retinal space, and these are almost certainly of RPE origin. The gradations of their formation from the RPE are most clearly seen in the rabbit. Blood derived macrophage may also play a role. Spencer and Leaffer (San Francisco)[personal communication] have seen by electron microscopy one such cell (in primate) traversing the RPE, and Eckmiller and Steinberg[9] concluded that the many macrophage seen in the bullfrog subretinal space were monocyte-derived, as did LaVail in rodents[26]. In hundreds of sections examined by LM and TEM, one hour to one day post-exposure, no monocyte or macrophage was ever seen in passage from the retinal vessels or choriocapillaris. Macrophage of RPE origin have been described after retinal detachment[10,32,33], in argon exposed monkey retinas[7]. There are many reports of phagocytes, filled with pigment granules, near the RPE border following laser or light exposure[12,29,37,38,44,52,55] and after poisoning with drugs.

An increase in phagosomes soon after laser irradiation has been reported in mice[47] and rabbits[55], and this was frequently the case in this study as were shed packets of outer segment discs which often lined the RPE apical border.

In rats previous dark-adaptation produced greater sensitivity to light[1,56]. In the monkeys in this study there was only a slightly increased effect of dark-adaptation. Rodents are nocturnal animals; their retinas may well react very differently from cone-rich diurnal retinas.

The migration of RPE cells along Bruch's membrane to fill in the denuded area left after argon laser damage to the RPE has been reported in human eyes[44].

There were in this study no measurable differences in the lesions inserted in the morning or afternoon unlike that reported in albino rats[65] where there was greater damage in the morning, leading to the conclusion that longer light-adaptation is protective.

There were only very slight (and uncertain) differences in lesions inserted in the dark-adapted compared to the light-adapted state compared to rat studies[54].

The types of damage created by the various monochromatic lights of equivalent "bleaching power" are very similar[48] and the superior region (of the rat retina) was more severely damaged by constant light than the inferior region. There appears to be generally a greater vulnerability in the superior retina[54].

Light damage injury thresholds are higher in primates than in rats[28] and this is generally known now. The greater damage seen after prior dark-adaptation may be restricted to nocturnal animals.

The laser is a very effective tool for studying low level subthreshold light effects of different wavelengths on the retinal cells and their organelles, but long-term follow up studies are required to ascertain if reductions in visual performance result.

LITERATURE CITED

1. Birch, D.G. and G.H. Jacobs (1980) Light induced damage to photopic and scotopic mechanisms in the rat depends on rearing conditions. Exp. Neurology 68: 269-283.
2. Bok, D. and R.W. Young (1979) Metabolism of the retinal pigment epithelium. In: The Retinal Pigment Epithelium. K.M. Zinn and M.F. Marmor, eds., Harvard University Press, pp. 103-123.
3. Borwein, B. (1981) The retinal receptor: A description. In: Vertebrate Photoreceptor Optics. J.M. Enoch, F.L. Tobey, eds. Springer Series in Optical Science. Vol. 23, pp. 11-81.
4. Borwein, B. (1982) Neodymium laser lesions in Rhesus monkey retina. ARVO Suppl. to Invest. Ophthal. Visual Sci. p. 52.
5. Borwein, B., D. Borwein, J. Medeiros and J. Wm. McGowan (1980) The ultrastructure of monkey foveal photoreceptors with special reference to the structure shape size and spacing of foveal cones. Am. J. Anat. 159: 125-146.
6. Borwein, B., M. Sanwal, J.A. Medeiros and J. Wm. McGowan (1977) Scanning electron microscopy of normal and lased rabbit pigment epithelium. Invest. Ophthalmol. Vis. Sci. 16: 700-710.
7. Bresnick, G.H., G.D. Frisch, J.O. Powell, M.B. Landers, G.C. Holst and A.G. Dallas (1970) Ocular effects of argon laser radiation. I. Retinal damage threshold studies. Invest. Ophthalmol. 9: 901-910.
8. deJong, P.T., G.F. Vrensen, B.L. Willekens and C.M. Mooy (1989) Free-running neodymium-YAG laser coagulation of the human fovea. A light and electron microscope study. Retina. 9: 312-318.
9. Eckmiller, M.S. and R.H. Steinberg (1981) Localised depigmentation of the retinal pigment epithelium and macrophage invasion of the retina in the bullfrog. Invest. Ophthalmol. Visual Sci. 21: 369-394.
10. Feeney, L., R.P. Burns, and R.M. Mixon (1975) Human subretinal fluid. Archivs. Ophthalmol. 93: 62-69.
11. Gibbons, W.D. (1973) Retinal burn thresholds for exposure to a frequency-doubled neodymium laser. Report SAM-TR-73-45, pp. 1-13.
12. Gloor, B.P. (1969) Phagocytic activity of the pigment epithelium after photocoagulation. Albrecht v. Graefes. Arch Klin Exp. Ophthal. 179: 105-117.
13. Goldman, A.I., W.T. Ham, Jr. and H.W. Mueller (1975) Mechanisms of retinal damage resulting from the exposure of Rhesus monkeys to ultrashort laser pulses. Exp. Eye Res. 21: 457-469.
14. Goldman, A.I., W.T. Ham, Jr. and H.W. Mueller (1977) Ocular damage thresholds and mechanisms for ultrashort pulses of both visible and infrared laser radiation in the Rhesus monkey. Exp. Eye Res. 24: 45-56.
15. Griess, G.A. and M.F. Blankenstein (1981) Additivity and repair of actinic retinal lesions. Invest. Ophthalmol. Visual Sci. 20: 803-806.
16. Ham, W.T. Jr., H.A. Mueller, A.I. Goldman, B.E. Newman, L.M. Holland and T. Kuwabara (1974) Ocular hazard from picosecond pulses of Nd:YAG radiation. Science 185: 362-363.
17. Ham, W.T. Jr., H.A. Mueller, J.J. Ruffolo and A.M. Clarke (1979) Sensitivity of the retina to radiation damage as a function of wavelength. Photochem. Photobiol. 29: 735-742.
18. Ham, W.T., H. Mueller and D. Sliney (1976) Retinal sensitivity to damage from short wavelength light. Nature 260: 153-155.
19. Ham, W.T. Jr., J.J. Ruffolo, M.A. Mueller, A.M. Clarke and M.E. Moon (1978) Histologic analysis of photochemical lesions produced in Rhesus retina by short wavelength light. Invest. Ophthalmol. Visual Sci. 117: 1029-1035.

20. Ham, W.T., H. Wiesinger, F.M. Schmidt, R.C. Williams, R.S. Ruffen, M.C. Schaeffer and D. Guerry, III (1958) Flashburns in the rabbit retina. Am. J. Ophthalmology 46: 700-723.
21. Hewitt, A.T., K. Nakazawa and D.A. Newsome (1989) Analysis of newly synthesised Bruch's membrane proteoglycans. Invest. Ophthalmol. Visual Sci. 30: 478-486.
22. Kuwabara, T. and R.A. Gorn (1968) Retinal damage by visible light. Arch. Ophthal. 79: 69-78.
23. Kuwabara, T. and S. Okisaka (1976) Effect of electronic strobe flashlight on the monkey retina. Jap. J. Ophthalmol. 20: 9-18.
24. Lanum, J. (1978) The damaging effects of light on the retina. Empirical findings, theoretical and practical implications. Survey of Ophthalmology 22: 221-249.
25. Lappin, P.W. and P.S. Coogan (1970) Histologic evaluation of ophthalmoscopically subvisible retinal laser exposures. Invest. Ophthalmol. 9: 537-542.
26. LaVail, M.M. (1979) The retinal pigment epithelium in mice and rats with inherited retinal degeneration. pp. 357-380. In: The Retinal Pigment Epithelium. K.M. Zinn and M.F. Marmor, eds., Harvard University Press.
27. Lawwill, T. (1973) Effects of prolonged exposure of rabbit retina to low intensity light. Invest. Ophthalmol. 12: 45-51.
28. Lawwill, T., S. Crockett and G. Currier (1977) Retinal damage secondary to chronic light exposure; thresholds and mechanisms. Doc. Ophthalmologica. 442: 379-0402.
29. Leibowitz, H.M., G.R. Peacock and E. Friedman (1969) The retinal pigment epithelium radiation thresholds associated with the Q-switched ruby laser. Arch. Ophthalmol. 82: 332-338.
30. Lund, D.J., D.O. Adams and C. Carver (1976) Ocular hazard of the gallium arsenide laser. LAIR Institute Report No. 30.
31. Lund, D.J., B.E. Stuck and E.E. Beatrice (1981) Biological Research in Support of Project Miles. Institute Report # 96.
32. Machemer, R. (1988) Proliferative vitreoretinopathy PVR. A personal account of its pathogenesis and treatment. Proctor Lecture. Invest. Ophthalmol. Vis. Sci. 29: 1771-1783.
33. Machemer, R. and H. Laqua (1975) Pigment epithelial proliferation in retinal detachment (massive periretinal proliferation). Am. J. Ophthalmol. 80: 1-23.
34. Marshall, J. (1973) Laser damage to ocular tissues. Proc. Roy. Soc. Med. 66: 842-844.
35. Marshall, J. (1978) Eye hazards associcated with lasers. Am. Occup. Hyg. J. 21: 69-77.
36. Marshall, J. (1978) Ageing changes in human cones. Ophthalmology. Vol. 1, Excerpta Medica pp. 375-378.
37. Marshall, J. (1981) Interactions between sensory cells, glial cells and the retinal pigment epithelium and their responses to photocoagulation. Dev.Ophthalmol. 2: 308-317.
38. Marshall, J. and A.C. Bird (1979) A comparative histopathological study of argon and krypton laser irradiation of the human retina. Brit. J. Ophthalmol. 63: 657-668.
39. Marshall, J., A.M. Hamilton and A.C. Bird (1974) Intra-retinal absorption of argon laser irradiation in human and monkey retina. Experientia 30: 1335-1337.
40. Marshall, J., A.M. Hamilton and A.C. Bird (1975) Histopathology of ruby-argon laser lesions in monkey and human retina - a comparative study. Brit. J. Ophthalmol. 59: 610-630.
41. Marshall, J. and Laties (1985) The special pathology of the aging Macula. pp. 389-400. In: Retinal Degeneration. Eds. M.M. LaVail, J.C. Hollyfield, R.E. Andersons. Alan R. Liss.
42. Marshall, J. and J. Mellerio (1967) Histology of the formation of retinal laser lesion. Exp. Eye Res. 6: 4-9.
43. Marshall, J. and J. Mellerio (1970) Laser radiation of retinal tissue. Brit. Med. Bull. 26: 156-160.

44. Nicolaissen, B. Jr., R.J. Ulshafer, E.S. Clausnitzer, A. Nicolaisseen and M.L. Ruben (1990) Electron microscopy of laser lesions in human RPE. Invest. Ophthalmol. Visual Sci. (ARVO Suppl.) 31: 69.
45. Noell, W.K, B.S. Walker, B.S. Kang and S. Berman (1966) Retinal damage by light in rats. Invest. Ophthalmol. 5: 540-573.
46. Novack, R.L., E. Stefansson and D.L. Hatchell (1990) The effect of photocoagulation on the oxygenation and ultrastructure of avascular retina. Exp. Eye Res. 50: 289-296.
47. Poon, A.M.L. and D.T. Yew (1980) The effect of low dose laser on the functional activities of the mice retina. Anat. Anz. Jena 148: 236-244.
48. Rapp, L.M. and T.P. Williams (1980) A parametric study of retinal light damage in albino and pigmented rats. pp. 135-159. In: The Effects of Constant Light on Visual Processes: T.P. Williams and B.N. Baker, eds. Plenum Press.
49. Schmidt, R.E., J. Taboada and W.I. Butcher (1979) Suprathreshold retinal damage due to single and picosecond 1060 nm laser light pulses. Aviat. Space Environ. Med. 50: 788-791.
50. Tso, M.O. (1973) Photic maculopathy in Rhesus monkey. Invest. Ophthalmol. 12: 17-34.
51. Tso, M.O.M. and B.S. Fine (1979) Repair and late degeneration of the primate foveola after injury by argon laser. Invest. Ophthalmol. Visual Sci. 18: 447-461.
52. Tso. M.O.M., I.H.L. Wallow and J.O. Powell (1973) Differential susceptibility of rod and cone cells to argon laser. Arch. Ophthalmology 89: 228-234.
53. Tso. M.O.M., I.H.L. Wallow, J.O. Powell, and L.E. Zimmerman (1972) Recovery of the rod and cone cells after photic injury. Tr. Am. Acad. Ophthol. Otolaryng. 76: 1247-1262.
54. Tso, M.O.M. and B.J. Woodford (1983) Effect of photic injury on the retinal tissues. Ophthal. 90: 952-963.
55. Van der Zypen, E., F. Fankhauser, K. Raess and C. England (1986) Morphologic findings in the rabbit retina following irradiation with the free-running neodymium-YAG laser. Archiv. Ophthalmol. 104: 1070-1077.
56. Yew, D.T. and Y.-W. Chan (1978) Comparison of the effects of laser on the light- and dark-adapted rodent retinas. Acta Anatomica 102: 90-93.
57. Zaret, M.M., G.M. Breinen, H. Schmidt, M. Ripps, I.M. Seigel and L.R. Solon (1961) Ocular lesions produced by an optical Maser (laser). Science 134: 1525-1526.
58. Zinn, K.M. and M.F. Marmor (1979) The Retinal Pigment Epithelium. Eds. K.M. Zinn and M.F. Marmor. Harvard University Press.
59. Zwick, H. (1978) Low level laser light effects. SPIE Visual Simulation and Image Realism. 162: 112-118.
60. Zwick, H. and E.S. Beatrice (1978) Long-term changes in spectral sensitivity after low level laser (514 nm) exposure. Mod. Probl. Ophthalmol. 19: 319-325.
61. Zwick, H., E.S. Beatrice and J.E. Canham. (1978) Laser bioeffects: low level effects: Impact on Army laser systems. Proceedings 10th Army Science Conference.
62. Zwick, H., E.S. Beatrice and T.A. Garcia (1980) Long-term and progressive changes in Rhesus spectral sensitivity after low-level coherent light (514 nm) exposure. Colour Vision Deficiencies V: Chapter 1: 52-60.
63. Zwick, H., B.E. Stuck and E.S. Beatrice (1980) Low level laser effects on Rhesus visual function. Publ. Soc. Photo Optical Instru. Engineers. Seminar on non-ionizing Radiation Effects. page 8.
64. Zwick, H., B.E. Stuck, J. Molchany, V.C. Parmley, J. Lund, J.J. Kearney and M. Belkin (1990) Two informative cases of Q-switched laser retinal injury. Invest. Ophthalmol. Vis. Sci. ARVO Suppl. 31: 282.
65. White, M.P. and L.J. Fisher (1979) A comparison of retinal light damage produced in the morning and afternoon in albino rats. Invest. Ophthalmol. Visual Sci. April ARVO Suppl.